

Record 2014/03 | GeoCat 78873

Coastal inundation modelling for Busselton, Western Australia, under current and future climate

S. Martin, D. Moore and M. Hazelwood

Coastal inundation modelling for Busselton, Western Australia, under current and future climate

GEOSCIENCE AUSTRALIA
RECORD 2014/03

S. Martin, D. Moore and M. Hazelwood.



Australian Government
Geoscience Australia

Department of Industry

Minister for Industry: The Hon Ian Macfarlane MP
Parliamentary Secretary: The Hon Bob Baldwin MP
Secretary: Ms Glenys Beauchamp PSM

Geoscience Australia

Chief Executive Officer: Dr Chris Pigram
This paper is published with the permission of the CEO, Geoscience Australia



© Commonwealth of Australia (Geoscience Australia) and Government of Western Australia (Dept. of Planning and Planning Commission) 2014

With the exception of the Commonwealth Coat of Arms and where otherwise noted, all material in this publication is provided under a Creative Commons Attribution 3.0 Australia Licence.
(<http://www.creativecommons.org/licenses/by/3.0/au/deed.en>)

Geoscience Australia has tried to make the information in this product as accurate as possible. However, it does not guarantee that the information is totally accurate or complete. Therefore, you should not solely rely on this information when making a commercial decision.

Geoscience Australia is committed to providing web accessible content wherever possible. If you are having difficulties with accessing this document please email clientservices@ga.gov.au.

ISSN 2201-702X (PDF)

ISBN 978-1-922201-89-8 (PDF)

GeoCat 78873

Bibliographic reference: Martin, S., Moore, D. & Hazelwood, M. 2014. *Coastal inundation modelling for Busselton, Western Australia, under current and future climate*. Record 2014/03. Geoscience Australia: Canberra. <http://dx.doi.org/10.11636/Record.2014.003>

Version: 1302

Contents

| | |
|--|-----|
| Figures..... | vii |
| Tables..... | x |
| Modelling Assumptions | 1 |
| Executive Summary | 3 |
| Key observations | 5 |
| Conclusions | 6 |
| 1. Introduction..... | 7 |
| 1.1. Background..... | 7 |
| 1.2. Aim..... | 7 |
| 1.3. Outputs | 9 |
| 2. Methodology..... | 11 |
| 2.1. Busselton case study..... | 12 |
| 2.1.1. Step 1 – Modelling inputs..... | 13 |
| 2.1.1.1. Digital elevation model | 13 |
| 2.1.1.2. Riverine hydrographs | 16 |
| 2.1.1.3. Estuary depth..... | 19 |
| 2.1.2. Step 2 – Regional storm modelling | 19 |
| 2.1.2.1. GCOM2D output data | 21 |
| 2.1.3. Step 3 – ANUGA storm modelling..... | 21 |
| 2.1.3.1. Set the boundary conditions | 24 |
| 2.1.4. Step 4 – Investigation of climate change impacts..... | 24 |
| 2.1.4.1. Combined storm and flood inputs..... | 26 |
| 2.2. Coastal erosion modelling | 27 |
| 2.2.1. Modelling extent | 28 |
| 2.2.2. Output data..... | 29 |
| 3. Modelling results and analysis | 31 |
| 3.1. Map series | 31 |
| 3.2. Storm tide and riverine flood inundation | 32 |
| 3.2.1. Current SLR scenarios..... | 33 |
| 3.2.1.1. B0 - TC Alby validation | 33 |
| 3.2.1.2. B1 - Worst case (TC Alby track and time shift) | 39 |
| 3.2.1.3. B5 - Worst-case TC Alby + 25 year ARI flood..... | 44 |
| 3.2.1.4. B6 - Worst-case TC Alby + 100 year ARI flood..... | 47 |
| 3.2.2. 0.4 m SLR scenarios..... | 51 |
| 3.2.2.1. B2 - Worst-case TC Alby + 0.4 m SLR..... | 51 |
| 3.2.2.2. B8 - Worst-case TC Alby + 0.4 m SLR + 100 year ARI flood..... | 55 |
| 3.2.3. 0.9 m SLR scenarios..... | 59 |
| 3.2.3.1. B3 - Worst-case TC Alby + 0.9 m SLR..... | 59 |
| 3.2.3.2. B7 - Worst-case TC Alby + 0.9 m SLR + 25 year ARI flood..... | 61 |
| 3.2.3.3. B9 - Worst-case TC Alby + 0.9 m SLR + 100 year ARI flood..... | 63 |
| 3.2.4. 1.1 m SLR scenarios..... | 65 |

| | |
|--|----|
| 3.2.4.1. B4 - Worst-case TC Alby + 1.1 m SLR | 65 |
| 3.2.4.2. B10 - Worst-case TC Alby + 1.1 m SLR + 100 year ARI flood | 68 |
| 3.3. Coastal erosion | 71 |
| 4. Summary and discussion..... | 73 |
| 4.1. Results summary | 73 |
| 4.1.1. SLR scenarios | 74 |
| 4.1.1.1. Scenario B2 – TC Alby worst case + 0.4 m SLR..... | 74 |
| 4.1.1.2. Scenario B3 – TC Alby worst case + 0.9 m of SLR | 75 |
| 4.1.1.3. Scenario B4 – TC Alby worst case + 1.1 m SLR | 76 |
| 4.1.2. Riverine flooding scenarios | 77 |
| 4.1.3. Coastal erosion modelling | 78 |
| 4.1.3.1. Coastal erosion estimates for Busselton | 78 |
| 4.2. Modelling issues and limitations | 79 |
| 4.2.1. Surface roughness coefficient | 79 |
| 4.2.2. Treatment of estuary storm-tide gates | 79 |
| 4.2.3. Wave setup and wind shear | 80 |
| 4.2.4. Recorded hydrographs | 80 |
| 4.3. Further work | 81 |
| 4.3.1. Improvements to this study..... | 81 |
| 4.3.1.1. Validation | 81 |
| 4.3.1.2. Flood modelling..... | 81 |
| 4.3.1.3. Include flood management measures..... | 81 |
| 4.3.1.4. Undertake sensitivity testing | 81 |
| 4.3.2. Expansion of this study..... | 82 |
| 5. Conclusions | 83 |
| 6. References | 85 |

Glossary

This table defines technical terms and abbreviations used in this document.

| | |
|-------------------|---|
| AHD | Australian Height Datum. Vertical height datum defined as a surface that passed through mean sea level between 1966-1968 at 30 tide gauges. See http://www.ga.gov.au/earth-monitoring/geodesy/geodetic-datums/australian-height-datum-ahd.html for further information. |
| AMSA | Australian Maritime Safety Authority |
| ANUGA | ANUGA is a Free and Open Source Software (FOSS) mathematical model that simulates fluid flow (hydrodynamics), including wetting and drying phases. ANUGA has been used to model the impact of hydrological disasters such as dam breaks, riverine flooding, storm surge and tsunamis. ANUGA is developed by the Australian National University (ANU) and Geoscience Australia (GA). http://anuga.anu.edu.au/ |
| ARI | Average Recurrence Interval The average or expected value of the periods between exceedance values of a given event magnitude. It is implicit in this definition that the periods between exceedances are generally random ¹ |
| ASCII Grid | American Standard Code for Information Interchange. A spatial grid data format. |
| Bathymetric LiDAR | Offshore LiDAR derived elevation data or digital elevation model |
| BoM | Bureau of Meteorology |
| DEM | Digital Elevation Model. A data grid where each grid value is the surface elevation above, or below a vertical datum. Within this study the Australian Height Datum (AHD71) is the vertical datum. |
| Flooding | Riverine flood inundation |
| GCOM2D | GEMS 2D Coastal Ocean Model |
| GEMS | Global Environmental Modelling Systems Pty Ltd |
| GEMSURGE | GEMS storm-tide modelling software |
| Grid | Regular square mesh spatial data |
| HSD | Horizontal Setback Datum: 'the line, determined with regard to physical or biological factors of the coast, from which setback will be applied' ² |
| Hydrograph(s) | A flood hydrograph is graph showing the rate of flow or discharge of floodwater over time measured at a specific location. It can also show the volume of floodwater that passes a specific location. |
| Inundation | Land under water where normally dry. This applies equally to storm tide and riverine flood inundation. |
| IPCC AR4 | Intergovernmental Panel on Climate Change Fourth Assessment Report |
| LiDAR | Light Distance and Ranging. An airborne sensor used to capture high-resolution elevation data. |
| LSCB | Large-Scale Coastal Behaviour |
| MHWS | Mean High Water Spring |

¹ <http://www.bom.gov.au/water/awid/id-704.shtml>

² http://www.planning.wa.gov.au/dop_pub_pdf/pcps_a3_report_08_glossary_acronyms.pdf

| | |
|--------------------------|---|
| MSL | Mean sea-level |
| NCI | National Computational Infrastructure |
| Peak momentum | A resulting data grid showing the maximum momentum magnitudes for each grid cell |
| Raster | Regular square mesh spatial data |
| RMW | Radius of Maximum Winds |
| Rock ASL | Rock Above Sea-level |
| SLR | Sea-Level Rise |
| STM | Shoreface Translation Model(ling) |
| Storm surge | Elevated water level above astronomical tide caused by the storm as a function of wind and low atmospheric pressure. The storm surge height does not include astronomical tide. |
| Storm tide | The combined water height of astronomical tide and the elevated water level caused by the storm (storm surge). |
| TC | Tropical Cyclone |
| Topographic LiDAR | Onshore LiDAR derived elevation data or digital elevation model |
| WA | Western Australia |
| WA DoP | Western Australian Department of Planning |
| WA DoT | Western Australian Department of Transport |
| Worst case scenario (B1) | The 1978 TC Alby storm track was changed to direct maximum winds over Busselton and coincide with a spring tide. |

Figures

| | |
|---|----|
| Figure 1. An overview of the river channels in the Busselton-Dunsborough area. | 4 |
| Figure 2. Validation (B0), TC Alby worst case (B1) and worst case plus sea-level rise (B2 to B4) scenario inundation extents. | 6 |
| Figure 3. Busselton location. | 8 |
| Figure 4. General modelling framework. | 11 |
| Figure 5. Busselton 1m DEM. | 13 |
| Figure 6. DEM constituent dataset coverage. | 15 |
| Figure 7. An overview of the river channels in the Busselton-Dunsborough area. | 16 |
| Figure 8. Location of the Busselton Hydrographs. | 16 |
| Figure 9. Vasse River Diversion Drain hydrograph (25 and 100 year ARI events). | 17 |
| Figure 10. Abba River – Vasse Estuary Inlet hydrograph (25 and 100 year ARI events). | 18 |
| Figure 11. Sabina River – Vasse Estuary Inlet hydrograph (25 and 100 year ARI events). | 18 |
| Figure 12. ‘Actual case’ (black) and ‘worst case’ (pink) tracks for TC Alby used for verification and prediction of extreme outcomes respectively (Hubbert et al., 2012). | 20 |
| Figure 13. Inundation modelling domain. | 22 |
| Figure 14 (a). Small scale ANUGA mesh refinement for Busselton inundation model. (b). ANUGA mesh refinement for Busselton inundation model. The larger triangles have a maximum area of 350 m ² and the smaller triangles were restricted to an area less than 5 m ² | 23 |
| Figure 15. Location of GEMS boundary condition data points. | 24 |
| Figure 16. Storm tide and riverine hydrograph input timing. | 26 |
| Figure 17. The coastal erosion modelling extent. | 29 |
| Figure 18. Example map sheet. | 31 |
| Figure 19. Busselton estuaries, watercourses and Moore St. floodgates. | 32 |
| Figure 20. B0 inundation depth (TC Alby scenario). | 34 |
| Figure 21. TC Alby observations at the Busselton Jetty and the GEMS modelling results (Hubbert et al., 2012). | 34 |
| Figure 22. TC Alby validation focus areas. | 35 |
| Figure 23. Busselton Jetty validation site showing both the observed TC Alby and modelled B0 inundation extents. | 36 |
| Figure 24. Siesta Park Groyne, near Lennox Drain validation site and B0 inundation extent. The 1975 maps have not been shown for ease of interpretation. | 37 |
| Figure 25. Busselton Townsite validation and B0 inundation extent. | 38 |
| Figure 26. B1 inundation depth (TC Alby - worst case). | 39 |
| Figure 27. Difference in the inundation depth; B1 - B0. | 40 |
| Figure 28. Difference in the inundation depth; B1 - B0 where the difference is greater than 1 m. | 40 |
| Figure 29. B1 peak momentum. | 41 |
| Figure 30. Dunsborough drain breakouts - B1 Scenario. | 42 |

| | |
|---|----|
| Figure 31. Modelling flow within the Toby Inlet. | 43 |
| Figure 32. B5 inundation depth (TC Alby Worst case + 25 year ARI flood). | 44 |
| Figure 33. B5 and B1 inundation extents. | 45 |
| Figure 34. Difference in the inundation depth; B5 - B1 where greater than 0.1 m. | 46 |
| Figure 35. B6 inundation depth (TC Alby Worst case + 100 year ARI flood). | 47 |
| Figure 36. B1, B5 and B6 inundation extents. | 48 |
| Figure 37. Difference in the inundation depth; B6 - B1 where the difference is greater than 0.1 m. | 49 |
| Figure 38. Inundation depth difference - B6 - B5. | 50 |
| Figure 39. B2 inundation depth (TC Alby - Worst case + 0.4 m SLR). | 51 |
| Figure 40. B1 and B2 inundation extents. | 52 |
| Figure 41. Difference in the inundation depth; B2 - B1. | 52 |
| Figure 42. Difference in the inundation depth; B2 - B1 (revised symbol range). | 53 |
| Figure 43. B2 peak momentum. | 54 |
| Figure 44. B8 inundation depth (TC Alby - Worst case + 0.4 m SLR + 100 year ARI flood). | 55 |
| Figure 45. B8 and B2 inundation extents. | 56 |
| Figure 46. Difference in the inundation depth; B8 - B2. | 57 |
| Figure 47. B8 peak momentum. | 58 |
| Figure 48. B3 inundation depth (TC Alby - Worst case + 0.9 m SLR). | 59 |
| Figure 49. B1 and B3 inundation extents. | 60 |
| Figure 50. Difference in the inundation depth; B1 - B3. | 60 |
| Figure 51. B3 peak momentum. | 61 |
| Figure 52. B7 inundation depth (TC Alby - Worst case + 0.9 m SLR + 25 year ARI Flood). | 62 |
| Figure 53. B3 and B7 inundation extents. | 62 |
| Figure 54. B9 inundation depth (TC Alby – worst case + 0.9 m SLR + 100 year ARI Flood). | 63 |
| Figure 55. B3 and B9 inundation extents. | 64 |
| Figure 56. B9 peak momentum. | 64 |
| Figure 57. B4 inundation depth (TC Alby - worst case + 1.1 m SLR). | 65 |
| Figure 58. B4 and B1 inundation extents. | 66 |
| Figure 59. Difference in the inundation depth; B4 - B1. | 66 |
| Figure 60. B4 peak momentum. | 67 |
| Figure 61. B10 inundation depth (TC Alby - worst case + 1.1 m SLR + 100 year ARI Flood). | 68 |
| Figure 62. B10 and B4 inundation extents. | 69 |
| Figure 63. Difference in the inundation depth; B10 - B4 where greater than 0.1 m. | 70 |
| Figure 64. Spatial extent of coastal erosion forecast by the STM for 2030. | 71 |
| Figure 65. Spatial extent of coastal erosion forecast by the STM for 2070. | 72 |
| Figure 66. Spatial extent of coastal erosion forecast by the STM for 2100. | 72 |
| Figure 67. Busselton, including rivers, diversion drain, estuaries and the Moore St floodgate. | 73 |
| Figure 68. B2 inundation (TC Alby worst case + 0.4 m SLR). | 74 |
| Figure 69. B3 inundation (TC Alby worst case + 0.9 m SLR). | 75 |

| | |
|--|----|
| Figure 70. B4 inundation (TC Alby worst case + 1.1 m SLR). | 76 |
| Figure 71. Comparison of the inundation extents for all SLR scenarios with the TC Alby validation (B0) and worst case (B1) scenarios. | 77 |

Tables

| | |
|--|----|
| Table 1. Storm tide and flood modelling scenarios. | 4 |
| Table 2. Storm tide and flood modelling scenarios. | 25 |
| Table 3. Shoreface translation modelling SLR scenarios (in metres; from Cowell and Barry, 2012). .. | 28 |
| Table 4. Comparison of the setback allowances and coastal erosion distance (in metres) for Busselton. | 78 |

Modelling Assumptions

The information within this document has been prepared with the purpose of identifying the ANUGA³ hydrodynamic inundation model's capacity to model coincident riverine and storm-tide inundation by testing scenarios at Busselton, south-western Western Australia. The scenarios include variations on storm track, sea level and river flow.

The results are based on several regional-scale models (hydrodynamic and data models) and therefore the results are indicative at the regional scale. The results should not be solely relied upon for making any related decisions. Key limitations/approximations include the following:

- **This report describes outputs derived from models.** All care has been taken to validate the results. However, due to the bathymetric and topographic changes that have occurred since Tropical Cyclone (TC) Alby occurred in 1978, and the anomalies in the inundation extent records, the validation is at best indicative.
- **Elevation data is a critical input into the model.** The elevation data (bathymetric and topographic) used in this model was the best available at the time of modelling and consists of both high- and low-resolution data. The predicted inundation extent is sensitive to variations in the quality, resolution and coverage of elevation data and should therefore be used with this understanding.
- **'Bare earth' elevation was used in this study.** The onshore elevation data does not include structures (including the Busselton Jetty) or vegetation and therefore the model does not account for the wave and inundation flow interactions with such structures. A single value for surface roughness was also used.
- **The topography does not change over the course of the model.** Long-term coastal change, as driven by sea-level rise, and the resulting effect on the topography and bathymetry was initially considered for inclusion in the future climate scenarios. However, the future climate elevation surfaces generated for this purpose were found to be physically flawed and, therefore, the future climate scenarios were modelled over the current elevation surface. Given the changes in the topography identified since TC Alby, the elevation surface remaining stable over the next 100 years is highly unlikely.
- **The boundary between the regional storm model (GCOM2D) and the local storm model (ANUGA) was not varied.** The regional model includes tidal modelling whereas the local storm model does not. Varying the boundary location between the regional and local storm models would test the inundation extent sensitivity to this variation. This has not been considered within this study.
- **A limited selection of storm, sea-level rise and riverine flood scenarios have been modelled for this study.** Therefore the results do not necessarily represent all possible scenarios in which a storm may occur. TC Alby is the worst tropical cyclone on record to impact south-western Western Australia and the track change modelled increases the inundation.

³ ANUGA is a Free and Open Source Software (FOSS) package capable of modelling the impact of hydrological disasters such as dam breaks, riverine flooding, storm surge or tsunamis. ANUGA is developed by the Australian National University (ANU) and Geoscience Australia (GA). <http://anuga.anu.edu.au/>

- **Climate change was only considered through the addition of sea-level rise to the current climate sea-level height.** For example, there was no consideration of the possible increase in storm or flood intensity caused by climate change within the future climate scenarios.
- **Riverine flood water management responses were assumed and remained static within the models.** Infrastructure is in place to divert riverine water flows and its use is driven by human decision-making processes or reliance on guidelines. These were assumed and not varied within the individual scenarios or between the current and future climate scenarios.

This document is the professional opinion of Geoscience Australia and has been based on the best modelling efforts and the most current data available. This process and the subsequent models are continually under development and review.

Executive Summary

Geoscience Australia, the Western Australian Department of Planning and the Western Australian Planning Commission have collaborated within this study to develop a regional-scale inundation model capable of simulating combined storm tide and riverine flood scenarios within current and future climate conditions (sea-level rise influences).

ANUGA is a hydrodynamic inundation model developed by the Australian National University and Geoscience Australia. ANUGA is a mathematical model that simulates water flow (hydrodynamics) over the land surface and includes wetting and drying phases. ANUGA has been used by Geoscience Australia since 2005 to model tsunami waves and storm tide (e.g. Fountain *et al.*, 2010). ANUGA has also been used to model riverine flooding from rainfall events in Wollongong, NSW (e.g. Van Drie *et al.*, 2010). This is the first time that ANUGA has been applied to model coincident storm-tide and riverine flood inundation.

Within this study, inputs used to model inundation with ANUGA included:

- regional storm-tide modelling results
- riverine flood hydrographs
- coastal erosion modelling results (modified 3D land and sea floor surfaces).

The regional storm-tide modelling was completed by Global Environmental Modelling Systems (GEMS) and they used a two-dimensional coastal ocean model (GCOM2D) to model two storm scenarios. The first scenario (B0 - [Table 1](#)) was based on Tropical Cyclone (TC) Alby, a storm which occurred in 1978 and impacted south-western Western Australia, including Busselton. The second scenario, was a 'worst case' TC Alby scenario (B1 - [Table 1](#)), where the storm track and timing were changed to direct maximum winds over Busselton with a coincident spring tide. The inundation of the land surface by the storm-tide was modelled using ANUGA. The remaining scenarios modelled were based on the *worst case* scenario (B1) with the inclusion of sea-level rise and/or coincident flooding. Three sea-level rise scenarios were considered: 0.4 m, 0.9 m (WAPC, 2003 and Bicknell, 2010) and 1.1 m. The 1.1 m sea-level rise scenario is a high-end scenario based on the Intergovernmental Panel on Climate Change (IPCC) Fourth Assessment Report (AR4) and subsequent research (DCCEE, 2009). Within the Busselton to Dunsborough region there are a number of rivers and creeks. However, hydrographs were only available for the: Vasse River Diversion Drain, Sabina River and Abba River ([Figure 1](#)). Storm tide, however, was considered for the complete extent of the Busselton to Dunsborough region.

In order to accurately model the flow of water in Busselton's man-made channels, a high-resolution Digital Elevation Model (DEM) was required to resolve the flow of water in and around these features. Inclusion of these sharp-relief features, combined with the large modelling extent, significantly increased the computational demands. For this reason ANUGA was modified to run on the National Computational Infrastructure, a high-performance computing initiative of the Australian Government hosted at the Australian National University.

The coastal erosion modelling was undertaken by the University of Sydney (Cowell and Barry, 2012). This study was a regional scale quantitative assessment of coastal-erosion risk from Busselton to Rockingham. Coastal erosion modified coastlines and modified DEMs were created through the

application of a sediment transport model, the Shoreface Translation Model, over four time horizons (2030, 2070, 2100 and 2300) and a range of sea-level rise scenarios. The objective was then to use ANUGA to simulate water flow over the modified DEMs for the future climate scenarios (B2-B4 and B7-B10, [Table 1](#)).

Table 1. Storm tide and flood modelling scenarios.

| ID | Type | Sea Level | Riverine Flood |
|-----|--|-----------|----------------|
| B0 | Base Case (Validation against TC Alby) | Current | None |
| B1 | Worst Case (TC Alby, track and time shift) | Current | None |
| B2 | Worst Case + Sea-Level Rise (SLR) | + 0.4 m | None |
| B3 | Worst Case + SLR | + 0.9 m | None |
| B4 | Worst Case + SLR | + 1.1 m | None |
| B5 | Worst Case + Coincident Flooding | Current | 25 year ARI |
| B6 | Worst Case + Coincident Flooding | Current | 100 year ARI |
| B7 | Worst Case + Coincident Flooding + SLR | + 0.9 m | 25 year ARI |
| B8 | Worst Case + Coincident Flooding + SLR | + 0.4 m | 100 year ARI |
| B9 | Worst Case + Coincident Flooding + SLR | + 0.9 m | 100 year ARI |
| B10 | Worst Case + Coincident Flooding + SLR | + 1.1 m | 100 year ARI |

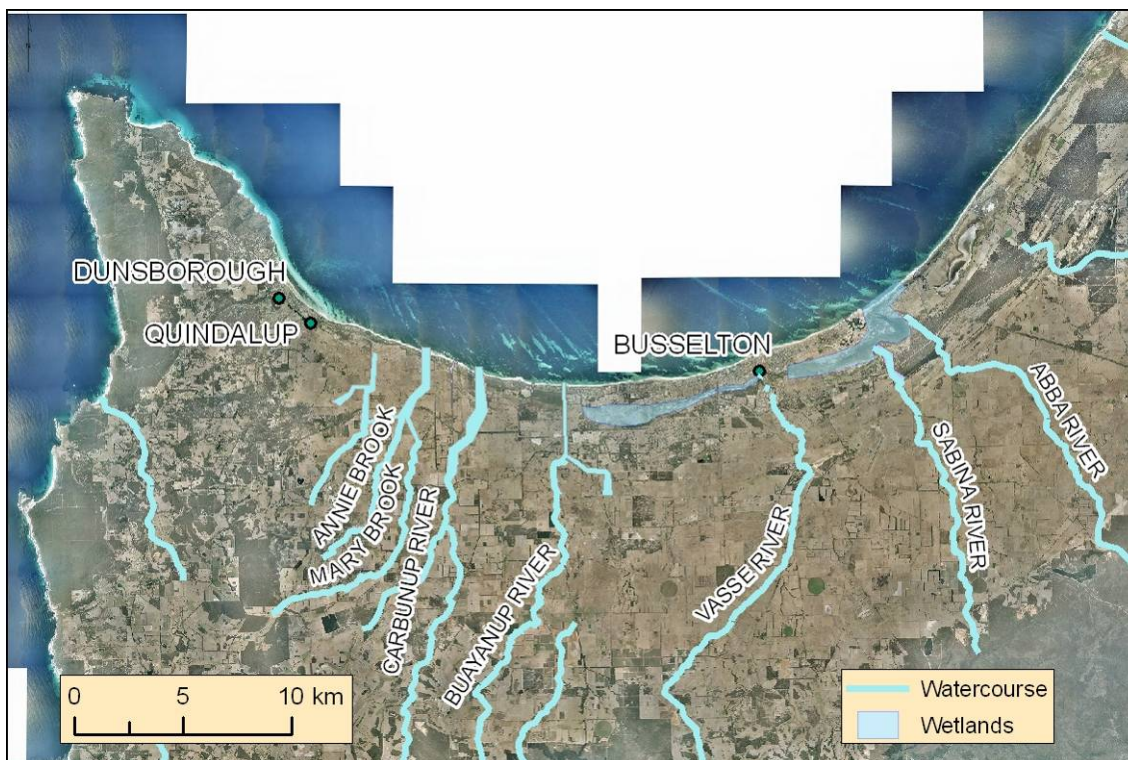


Figure 1. An overview of the river channels in the Busselton-Dunsborough area.

Key observations

- Geoscience Australia was able to successfully model coincident riverine flooding and storm-tide inundation using the ANUGA model.
- The ANUGA *Base Case* (B0) simulated inundation was compared with TC Alby observations. Due to sea floor (bathymetric) and land surface (topographic) changes since 1978, a direct model validation was not possible. However, the regional storm model (GCOM2D) results showed a good match to the Busselton Jetty tide-gauge recordings of the TC Alby storm-tide water levels.
- A significant increase to the inundation extent was due to the track and tide change applied to TC Alby to produce the *Worst Case* scenario (B1). This highlights the importance of storm trajectory and tidal state in these scenarios.
- Following the significant increase in inundation extent from the *Base Case* scenario (B0) to the *Worst Case* scenario (B1), the *Worst Case + 0.9 m* sea-level rise *scenario* (B3) was the next significant increase with larger areas of Dunsborough being inundated (Figure 2).
- Increases in sea-level rise increase the inundation extent (Figure 2). Areas inundated by earlier scenarios, e.g. Busselton Jetty, experience higher water velocities and therefore an increase in the destructive potential of the storm event with further sea-level rise.
- The combination of riverine flooding with storm-tide inundation was found to have little impact on the inundation extent as compared to the equivalent storm-tide only scenarios (e.g. B5 vs. B1 scenario)(Figure 33).
- The Shoreface Translation Model produces the greatest recession distances of any coastal erosion modelling completed for Busselton to date (Cowell and Barry, 2012). Within the context of sea-level rise, Andrews (2003) and Damara (2007) predict 38 m and 59 m recession distances respectively for the response to sea-level rise over the next 100 years; although they use differing sea-level rise scenarios, 0.38 m and 0.9 m respectively. Cowell and Barry (2012) identify coastal erosion to be within the range of 263 m and 537 m respectively for a 50% and 10% probability of exceedance under a 1.1 m sea-level rise scenario.
- The Shoreface Translation Model coastal erosion modified DEMs were initially considered for inclusion within the ANUGA sea-level rise scenarios, however, the modified DEMs did not reflect a physically credible future surface and therefore these were not included in the study. The coastal erosion modelling has been independently reviewed by the Western Australian and Australian Government.
- The general practice of maintaining the Vasse estuary level at 0.4 m Australian Height Datum (AHD) (Davis *et al.*, 1998) is very important. The impact of an event similar to Tropical Cyclone Alby on Busselton when the estuary levels are significantly higher than 0.4 m would be far more severe than the sea level rise scenarios presented in this report.
- The effects of coincident riverine flood are largely confined to an increase in the water levels within the estuaries. However, additional inundation occurs when the Vasse Diversion Drain spills out. In the event of coincident storm tide, sea-level rise and riverine flooding, the effect of the riverine flooding will be greatly reduced if the Vasse Diversion Drain can be prevented from spilling out above the Busselton Bypass.

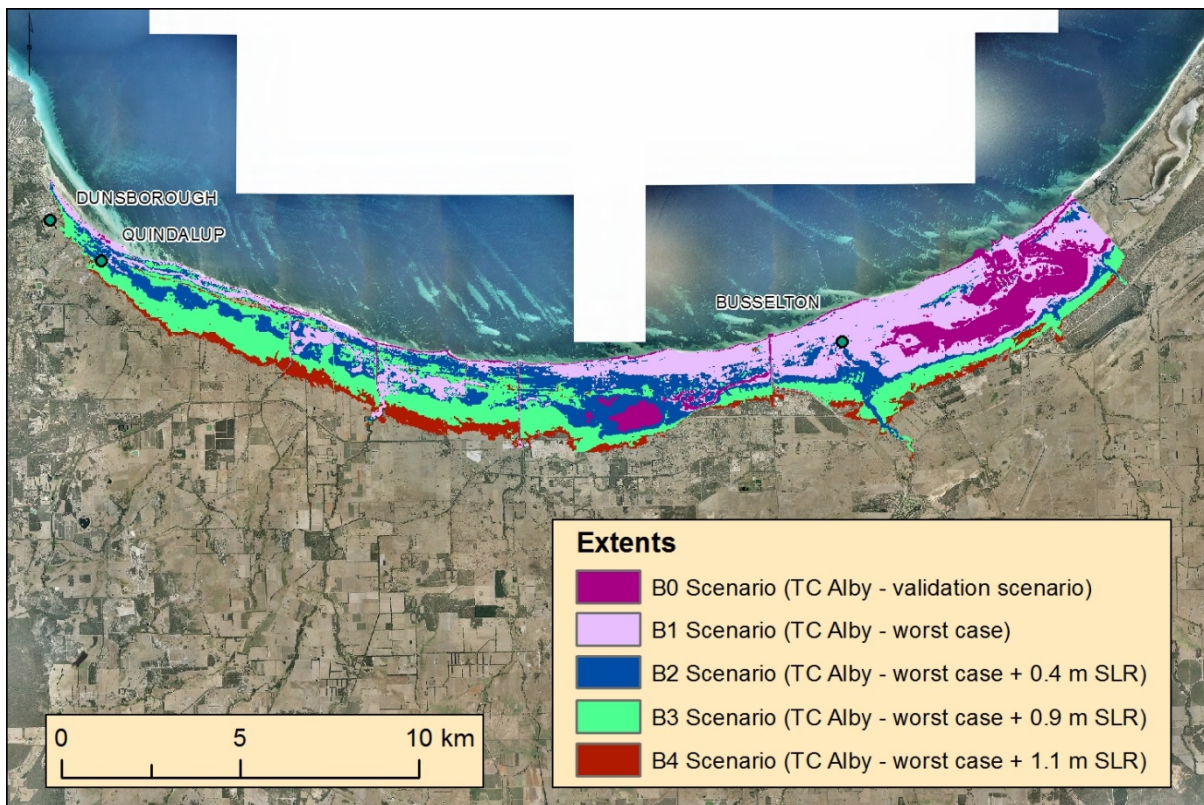


Figure 2. Validation (B0), TC Alby worst case (B1) and worst case plus sea-level rise (B2 to B4) scenario inundation extents⁴.

Conclusions

Geoscience Australia has demonstrated the capability of the ANUGA model to simulate coincident storm tide and riverine flooding for Busselton, within current and future climate environments, and simulated water flow over a high resolution (1 m)⁵ DEM. Eleven scenarios were modelled over the Busselton to Dunsborough region. Riverine flooding was found to have a relatively minimal impact on the inundation areas as compared with the storm-tide inundation. Within current-climate conditions the TC Alby track change and coinciding spring tide scenario (B1) was found to have the greatest impact to the inundation extent. Within the future-climate scenarios the increase of sea level by 0.9 m was found to have the largest impact to the inundation extent.

Outputs from this study include this report, hazard maps for each ANUGA scenario and each equivalent time period considered in the Shoreface Translation Model (2030, 2070 and 2100), and animations for each ANUGA scenario.

A complete understanding of the content of this report, as well as the contributing reports by GEMS and the University of Sydney, is required before considering the application of the results of this study. The results are based on several-regional scale models (hydrodynamic and data models) and therefore the results are indicative at the regional scale. Further work is required before the results are used for more than a qualitative understanding of riverine flooding, storm-tide and coastal erosion inundation.

⁴ The white background offshore is where imagery was unavailable.

⁵ The vertical accuracy varies across the modelling domain due to the varied input data. See the digital elevation model section on [p19](#) for details.

1. Introduction

1.1. Background

The Western Australia (WA) coastline is particularly vulnerable to the impacts of storm tide. This is predominantly due to the close proximity of the urban environment to the coast and, generally, the low relief of the Swan Coastal Plain. Numerous historical storm-tide events have been recorded in WA (Hubbert *et al.*, 2012). The effects of climate change, in particular sea-level rise (SLR), and the changing behaviour of cyclones may lead to increased vulnerability to storm-tide inundation. This has been recognised nationally (DCC, 2009).

Geoscience Australia has been developing and applying a tsunami modelling methodology since 2005 largely based on the ANUGA⁶ hydrodynamic inundation model. Recently, ANUGA has also been trialled (e.g. Van Drie *et al.*, 2010.) and further developed by local councils to work as a tool for the simulation of riverine flooding from rainfall events.

Geoscience Australia has developed and demonstrated the application of ANUGA to model storm-tide inundation at Bunbury with the inclusion of SLR scenarios (Fountain *et al.*, 2010). The ANUGA model used the near-shore outputs from the GCOM2D (GEMS Coastal Ocean Model) developed by Global Environmental Modelling Systems (GEMS). The ANUGA inundation results compared well with those of the GCOM2D model which was validated against the sea level heights recorded for Tropical Cyclone (TC) Alby. This study included coastal erosion, driven by SLR, and this was modelled by the University of Sydney.

1.2. Aim

The WA Government is seeking to better understand the present and future vulnerability of this area of the coast with the view to determining the needs for future modelling and analysis. This future work will ultimately provide a set of tools that can be used to influence and inform planning decisions for the region. As a coastal hazard affected by SLR, coastal erosion modelling is also within scope of this project.

Geoscience Australia, in partnership with the WA Department of Planning (WA DoP), aims to:

- investigate the capacity of ANUGA to model coincident storm tide and riverine flood inundation
- model coastal erosion and include the resulting changed sea/land surface in the ANUGA modelling.

In addition, the aim includes attempting to validate the methodology and to provide a case study to the WA DoP in the form of storm tide and coincident flood scenarios for Busselton, WA (Figure 3).

There are more appropriate models than ANUGA for a full riverine flood study. However, ANUGA can include both storm tide and flood in one dynamic numerical model. Previous studies have also

⁶ ANUGA is a Free and Open Source Software (FOSS) package capable of modelling the impact of hydrological disasters such as dam breaks, riverine flooding, storm-surge or tsunamis. ANUGA is developed by the Australian National University (ANU) and Geoscience Australia (GA). <http://anuga.anu.edu.au/>

identified ANUGA as the best free and open-source software that can include an accurate estimation of the maximum elevation reached by the inundation (e.g. Baldock *et al.*, 2007) and is capable of hydrodynamic riverine flooding.

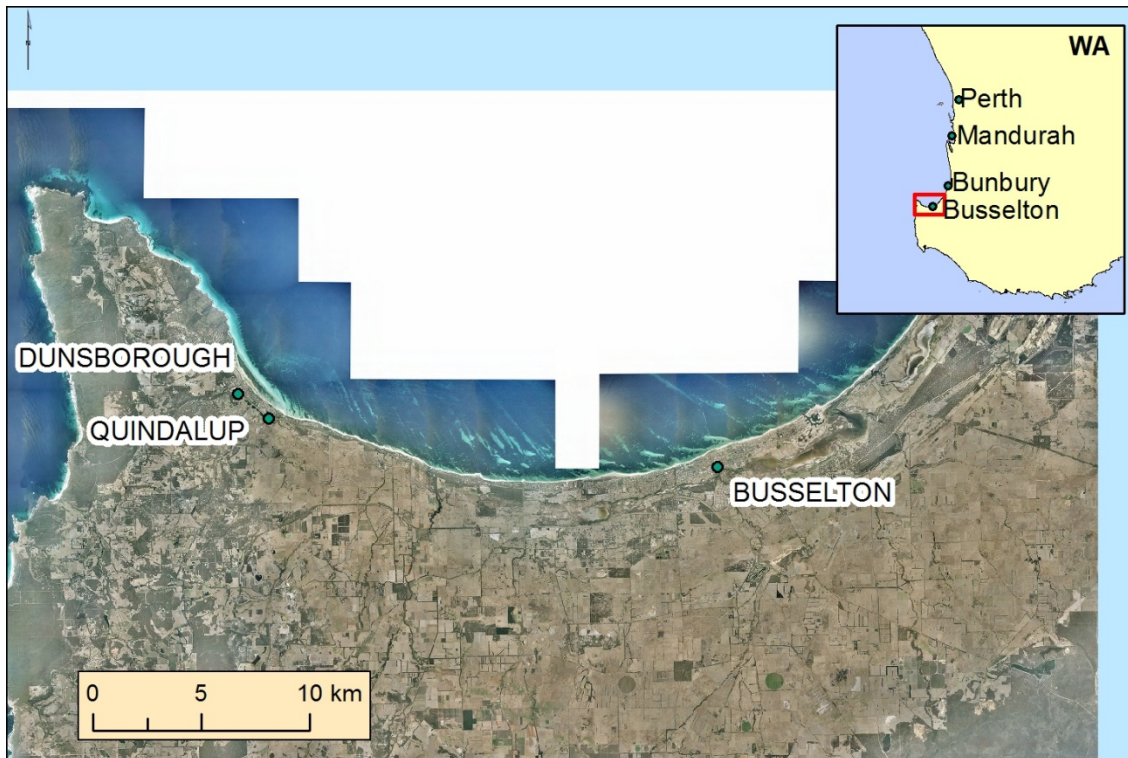


Figure 3. Busselton location.

The benefits of the Busselton case study include:

- Demonstrating the capacity of ANUGA to model storm and flood under current and future sea levels.
- Providing the WA DoP with an understanding of the potential impact of a TC Alby-sized storm-tide event on the Busselton coastline under current and future climate conditions.
- Increasing the understanding of the potential impacts of coincident cyclonic storm-tide and rainfall events.
- Providing indicative coastal hazard impact maps to the Busselton Shire Council to consider during planning for future growth.

1.3. Outputs

The outputs include:

- This summary report.
- The GEMS regional storm modelling report.
- The University of Sydney coastal erosion modelling report.
- Maps showing the results of the modelling.
- Digital product delivery (DVD) including report and maps.
- Attendance at a workshop with WA DoP and other stakeholders to discuss the project.

This page is intentionally blank

2. Methodology

This section introduces the modelling methodology employed by Geoscience Australia to model the storm tide and riverine flooding at Busselton. The general outline of the methodology is illustrated in Figure 4.

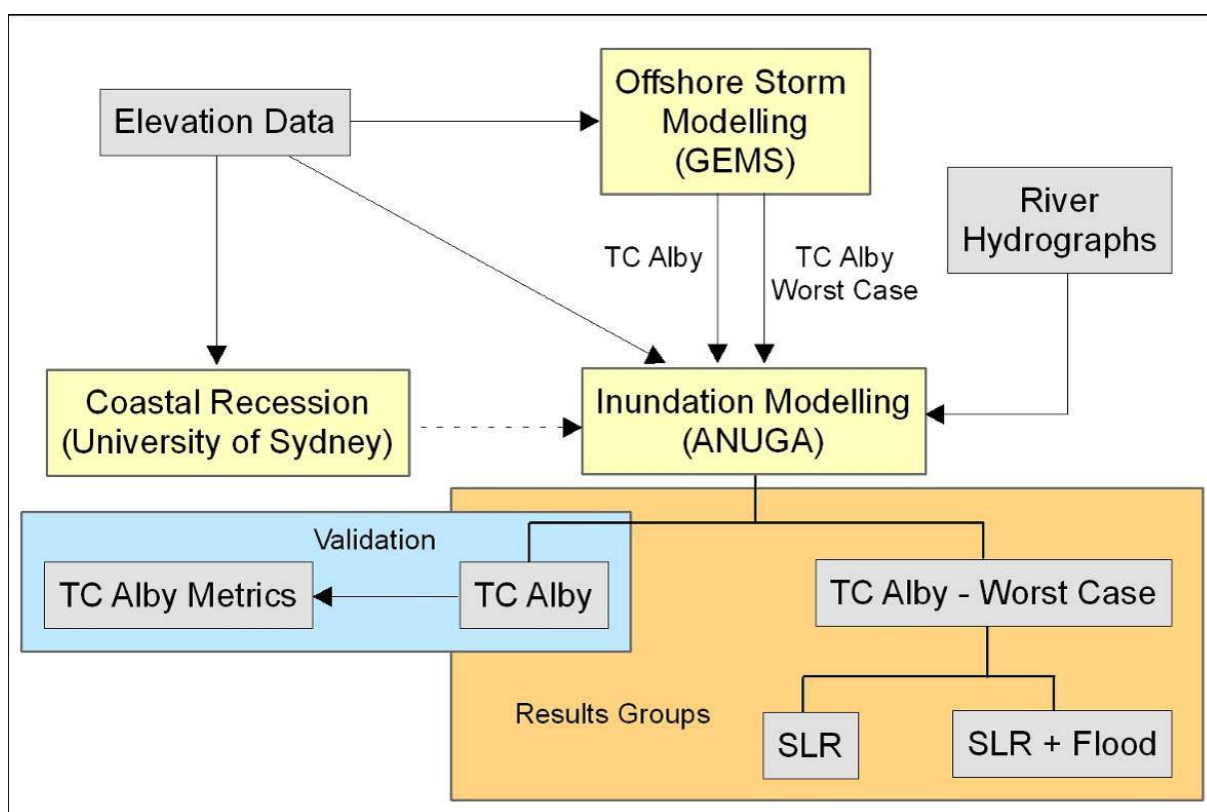


Figure 4. General modelling framework.

This methodology followed a number of distinct stages. First, bathymetric and topographic elevation data and the river hydrographs were prepared. The elevation data underpins construction of the offshore storm tide and the onshore inundation models. Second, the regional offshore storm modelling was completed by GEMS using the GCOM2D model. Third, the local storm and riverine inundation modelling was completed by Geoscience Australia utilising the ANUGA inundation model.

Finally, when investigating the potential effects of climate change on the coast, an appropriate model is required to estimate the extent of coastal erosion (or accretion) due to changes in the long-term climatic processes. This study used the coastal erosion modelling outputs from a study undertaken by the University of Sydney for the Commonwealth in 2011 (Cowell and Barry, 2012). This study undertook a regional-scale quantitative assessment of coastal-recession risk due to future climate change impacts on the coast between Busselton and Rockingham. The coastal erosion was computed using a sediment budget model, the Shoreface Translation Model (STM). For some general limitations imposed on the model see the Modelling issues and limitations Section (p79).

2.1. Busselton case study

The storm-tide modelling method is generally similar to that used within the Bunbury storm-tide modelling (Fountain *et al.*, 2010), although without the inclusion of the storm gate function. The procedure is described in the following steps.

1. Preparation of the input datasets.
 - a. Elevation data – bathymetry and topography.
 - b. River hydrographs.
2. Build a storm model for TC Alby using GCOM2D.
 - a. Generate storm events for TC Alby (actual and worse case track) using a vortex model.
 - i. Set the original storm parameters; path central pressure, radius of maximum wind and the shape parameter “B”.
 - b. Model the storm tide.
 - i. Determine locations of interest where the model is refined.
 - ii. Set the initial conditions (time of day, initial sea-level, Vasse Estuary water level).
 - iii. Set the boundary conditions within the nested model extents (e.g. tide).
 - iv. Run the model for a specified time.
 - v. Calibrate the model by comparing the modelling results to the Busselton Jetty tide gauge observations during TC Alby..
 - c. Alter the storm track for maximum impact at Busselton.
3. Build an inundation model (ANUGA).
 - a. Model the storm tide.
 - i. Determine locations of interest where model is refined (model domain).
 - ii. Set the initial conditions (initial sea-level, elevation).
 - iii. Set the boundary conditions (in this case the outputs from GCOM2D).
 - iv. Simulate the scenario for a specified time.
 - v. Determine the maximum inundation extents (including depths and momentum) reached during the simulation.
 - b. Model the riverine flood.
 - i. Determine the hydrographs for the rivers and drains of interest.
 - ii. Simulate the riverine flooding.
 - iii. Alter the time the riverine flooding is initiated to coincide with storm tide.
4. Investigate the impact of various climate change scenarios.
 - a. Change initial sea-level in step 3.a.ii and rerun.
 - b. Use outputs from coastal erosion model to predict the changes to the shoreline due to climate change induced SLR in step 3.a.ii and rerun.

2.1.1. Step 1 – Modelling inputs

2.1.1.1. Digital elevation model

The creation of a high resolution and hydrologically enforced⁷ DEM was of paramount importance to accurately model the flow of water. Specifically, sections of the Vasse Diversion Drain needed to be very high resolution for the model to correctly resolve the sharp relief levee banks to accurately channel the water. Other areas were not required to be resolved in such a detailed manner and therefore lower resolution spatial data was suitable. To obtain the flexibility that this process required, while still maintaining a consistent elevation dataset, a 1 m (horizontal resolution) DEM of the inundation modelling extent was created (Figure 5). The high- and low-resolution data was then derived from the 1 m DEM during the elevation data setup within ANUGA (ANUGA mesh generation, see p22)

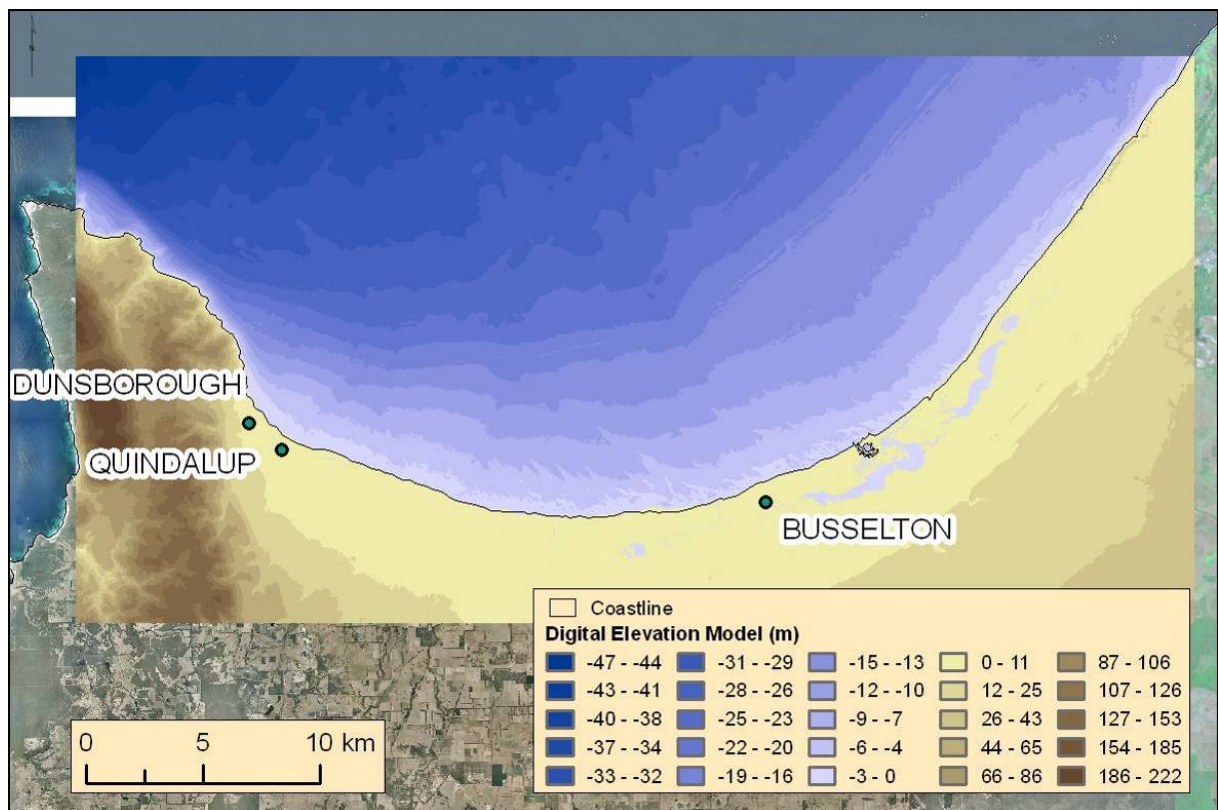


Figure 5. Busselton 1m DEM.

⁷ That is, an elevation surface that accurately allows modelling the flow of water without the modelled flow being impeded by elevation features overpassing the channel, i.e. bridges.

The following elevation datasets were obtained for this study and their extents can be seen in [Figure 6](#).

- Topographic LiDAR: Armadal-Dunsborough North Metro and 3 Towns LiDAR Survey.
 - Date of Capture: February 2008.
 - Captured By: Fugro Spatial Solutions.
 - Client: Department of Water – WA Government.
- Bathymetric LiDAR: Two Rocks to Cape Naturaliste Bathymetry and Seabed Survey.
 - Date of Capture: April/May 2009.
 - Captured By: Fugro LADS Corporation.
 - Client: WA DoP and Department of Transport (DoT).
- Offshore Bathymetry: Royal Australian Navy Fairsheet Survey data (points) digitised by Geoscience Australia in 2000.
- One Second SRTM derived DEM-H Version 1.0: Sourced from Geoscience Australia.
 - Horizontal accuracy: 90% of tested locations within +/- 9.8 m (Rodriguez *et al.*, 2006).
- Port Geographe Bathymetry: As used in the study “Port Geographe Sand and Seagrass Wrack Modelling Study, Western Australia” by the University of Western Australia.

In order to retain the higher resolution LiDAR derived inputs, it was necessary to interpolate the coarser resolution datasets, the one-second SRTM⁸ data and the Navy data, to match the 1 m grid resolution of the LiDAR derived data. The method selected to accomplish this was the exponential kriging functionality available in ArcGIS10. The Kriging interpolation method was selected over other methods because the most irregularly spaced and sparse Navy data resembled the data used in the analysis carried out by Bello-Pineda *et al.* (2007) in their comparative study of spatial interpolation methods. In that study, exponential kriging was identified as producing the most accurate results when constructing a digital bathymetric model of the Yucatan submerged platform.

After applying the Kriging interpolation method to the individual input datasets, the resulting 1 m resolution datasets were combined into a mosaic to form the base DEM ([Figure 5](#)).

The onshore LiDAR derived DEM did not have complete coverage; dams and a small section in the Vasse Estuary were not covered. These sections were small enough to be filled with the exponential kriging method.

This data represents the bare earth surface, that is, without any surface structure such as buildings. However, surface structures will change the flow characteristics and, therefore, it is likely that the inundation extents shown here are overestimates. This, and the vulnerability of such structures, could be the basis for further studies (see the Expansion of this study section, [p82](#)).

GEMS sought the inclusion of the spur to the west of Dunsborough to yield the most accurate results through the inclusion of wave reflection occurring within this zone. The final extent of the base DEM, taking into consideration these factors, is shown in [Figure 6](#).

⁸ Shuttle Radar Topography Mission

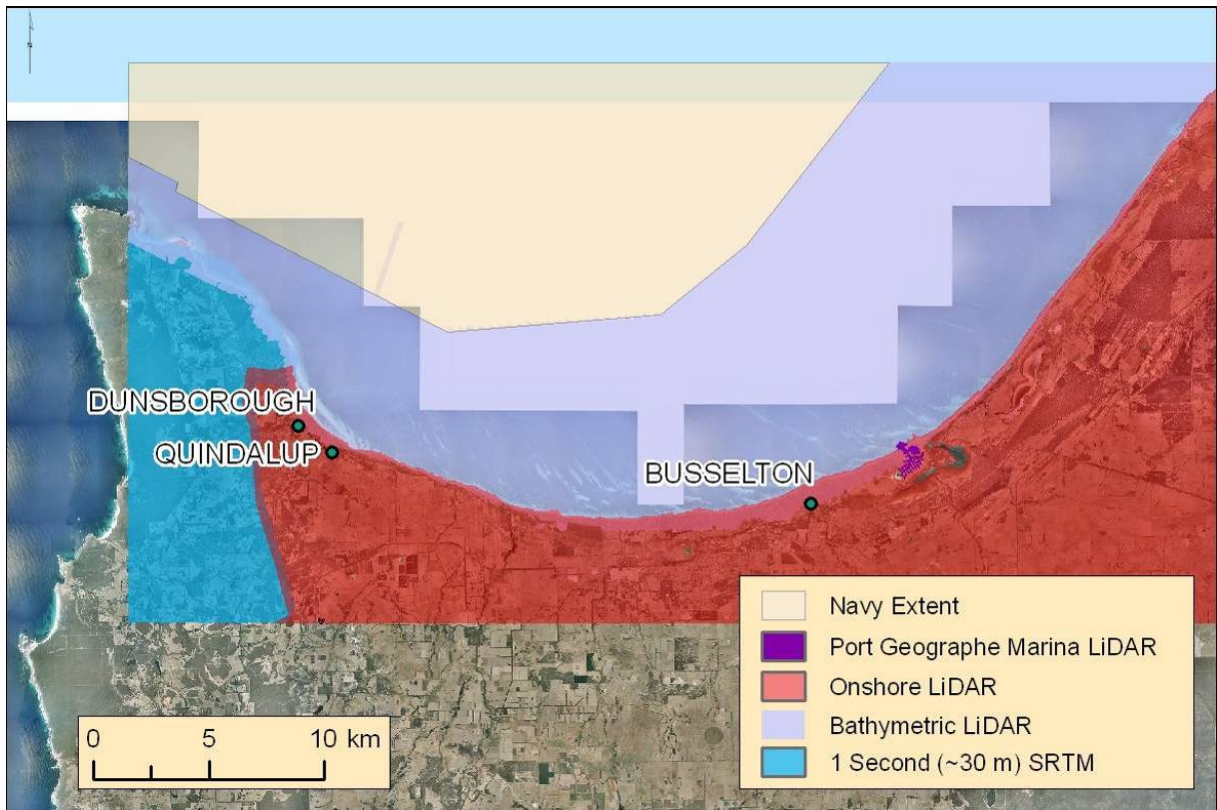


Figure 6. DEM constituent dataset coverage.

Other modelling details that formed part of the DEM creation process can be found in the modelling issues and limitations section (p79).

2.1.1.2. Riverine hydrographs

The regional drainage into Geographe Bay is shown in Figure 7.

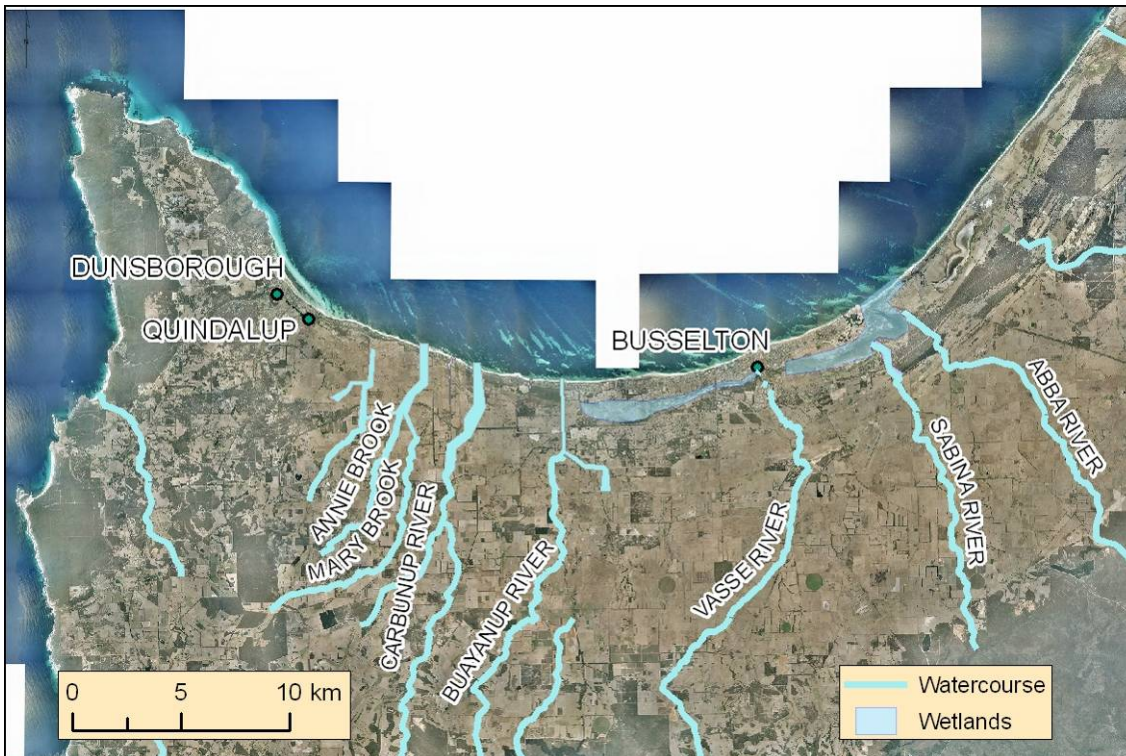


Figure 7. An overview of the river channels in the Busselton-Dunsborough area.

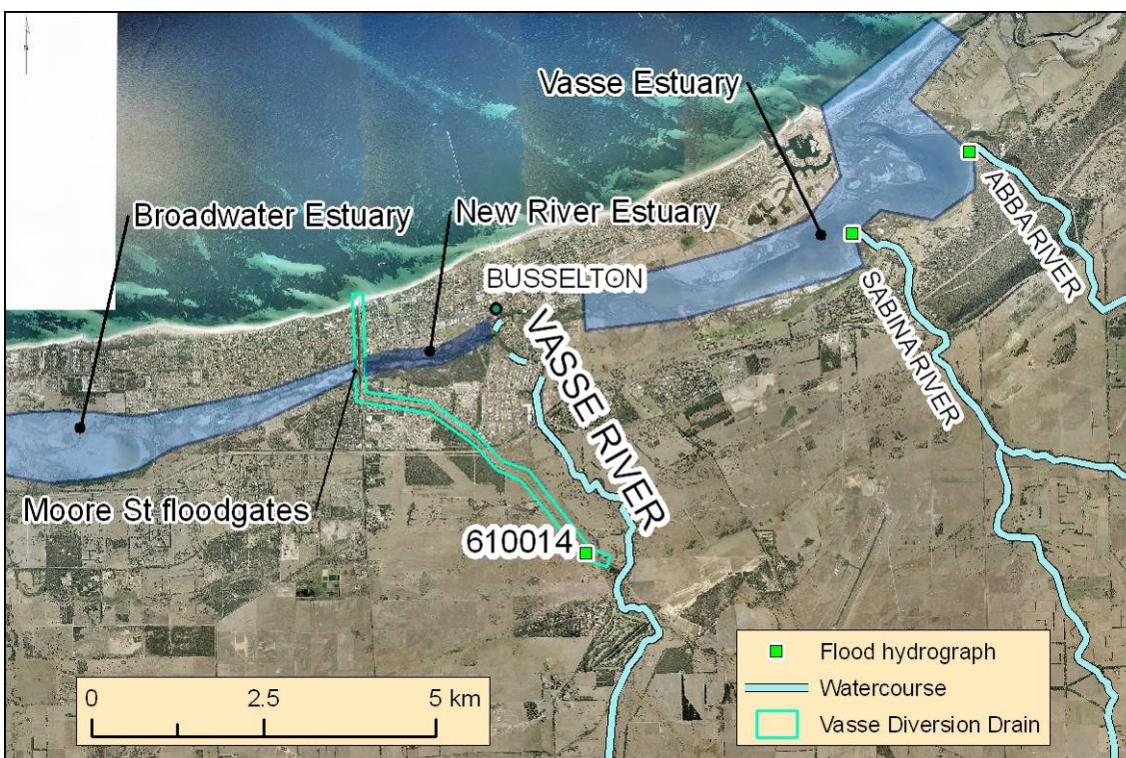


Figure 8. Location of the Busselton Hydrographs.

Within the Busselton region there are a number rivers and creeks; however, recorded hydrographs were only available for the Vasse River Diversion Drain, Sabina River and Abba River (Figure 8).

The flood modelling of the Busselton area involved the flooding of three waterways at the positions marked in Figure 8 (Flood hydrograph locations). The hydrographs used for the Vasse River Diversion Drain were sourced from an unpublished report by the Waters and Rivers Commission detailing the August 1997 flood event, deemed in the report to be a 25 year ARI event at gauging station 610014 (Figure 8). Using the 25 year ARI hydrograph and the recommended interim design flow for the Vasse Diversion Drain at gauging station 610014, $190 \text{ m}^3\text{s}^{-1}$ at 100 year ARI, a 100 year ARI hydrograph was constructed. In constructing the hydrograph it was a priority to maintain a similar shape to the 25 year ARI graph recorded in 1997. These two hydrographs are shown in Figure 9 and were used as dynamic inputs into the model at gauging station 610014. This method was discussed with, and the resulting hydrograph provided to, the WA DoW (Rodgers pers. comm., 2012).

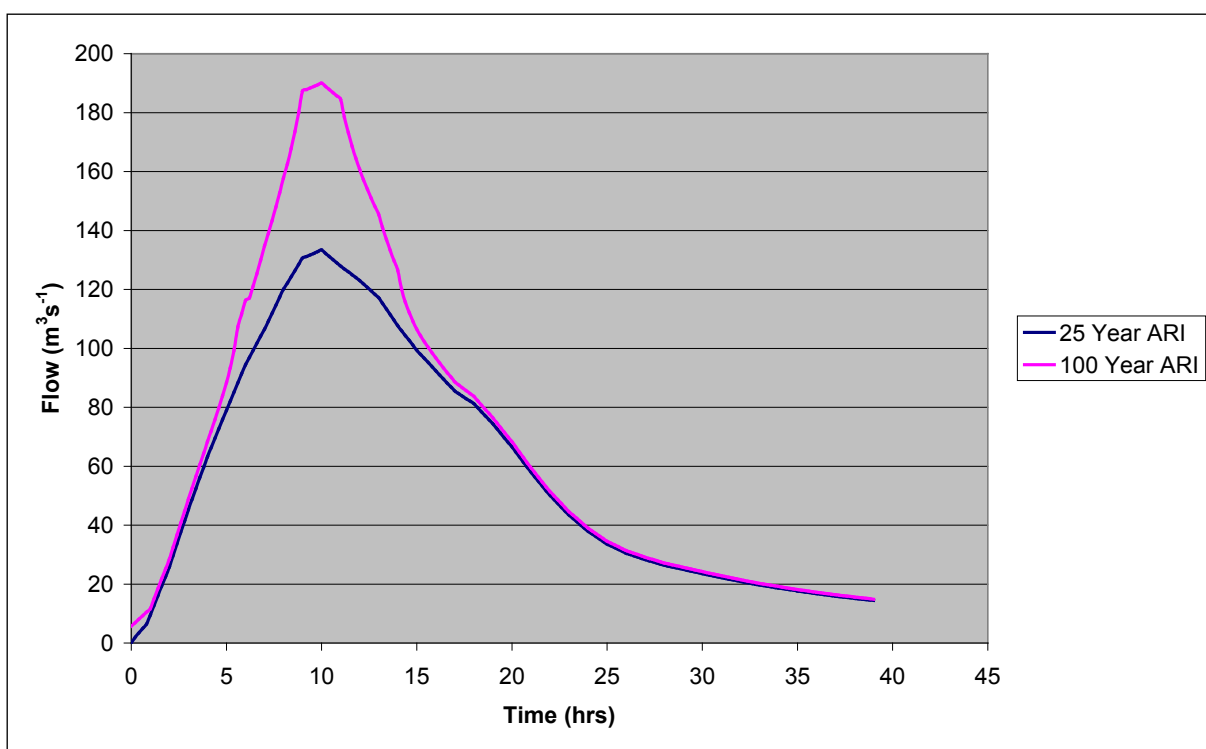


Figure 9. Vasse River Diversion Drain hydrograph (25 and 100 year ARI events).

The two other rivers included in the study, Sabina and Abba, have their input hydrographs to the simulation located at their respective inlets into the Vasse estuary (Figure 8). The two hydrographs for these rivers (Figure 10 and Figure 11) were sourced from Appendix B of the JDA Consultants Busselton Regional Flood Study Review (Davies *et al.*, 1998) and were created using HEC-RAS⁹. These hydrographs were used to simulate the additional water entering into the Vasse Estuary during the flooding scenarios.

⁹ <http://www.hec.usace.army.mil/software/hec-ras/>

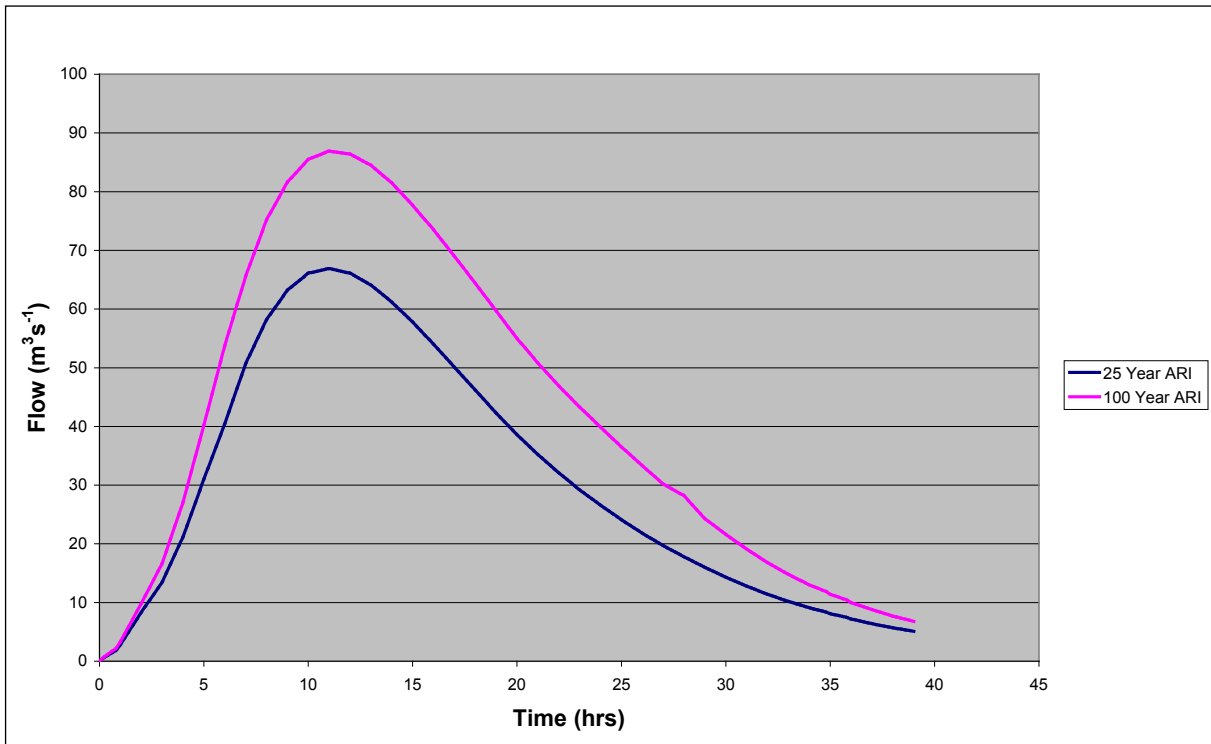


Figure 10. Abba River – Vasse Estuary Inlet hydrograph (25 and 100 year ARI events).

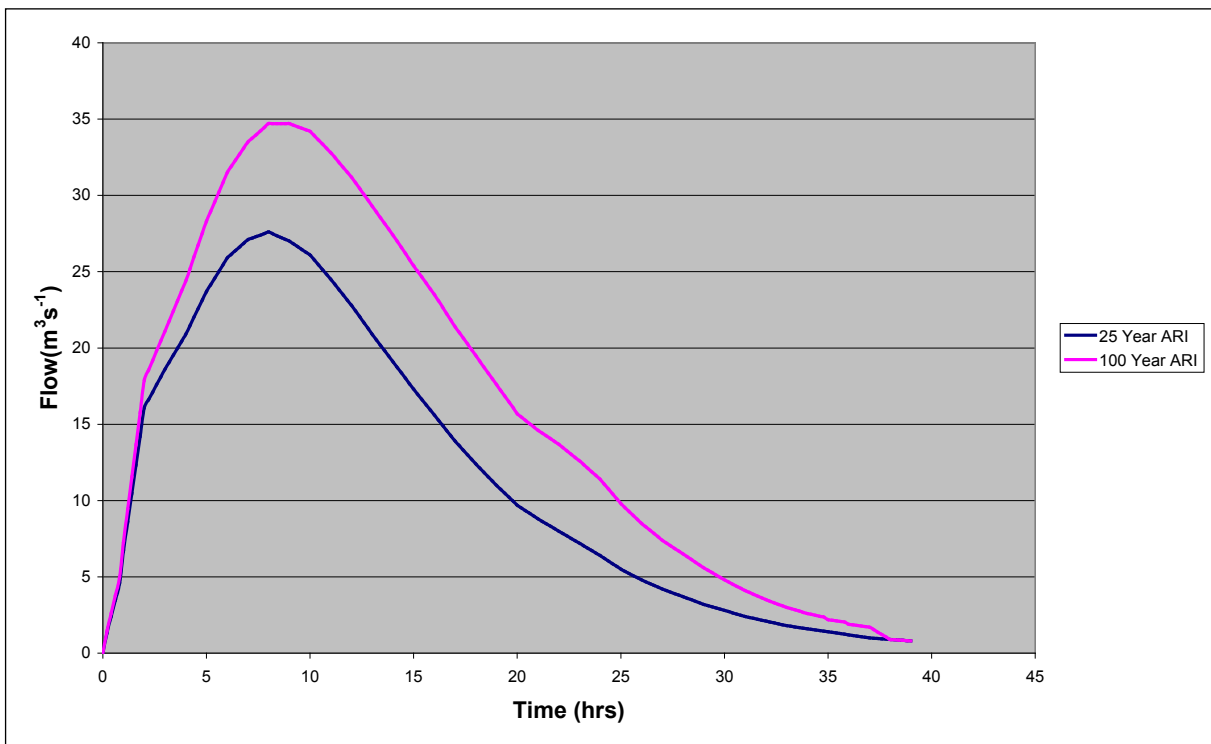


Figure 11. Sabina River – Vasse Estuary Inlet hydrograph (25 and 100 year ARI events).

The use of a constructed 100 year ARI hydrograph based on the results of other simulations is not ideal. The true behaviour of the watercourses in a flooding event will be different than the simulated hydrographs; however, that does not detract from the simulations usefulness in:

- giving an indication of any differences that coincident 100 year ARI riverine flooding introduces when combined with storm tide
- demonstrating that the ANUGA modelling methodology can be adapted to include coincident riverine flooding.

2.1.1.3. Estuary depth

Within this study the initial height of the estuaries was set to 0.4 m AHD as the WA DoW maintain the estuaries at this level (Davis *et al.*, 1998). The initial estuary water height was set for all scenarios and varying this value was not considered, e.g. maintaining the estuary at a higher level under SLR conditions or in the case of recent floods.

2.1.2. Step 2 – Regional storm modelling

Below is an adapted excerpt from the regional storm modelling report. The full report (Hubbert *et al.*, 2012) , was included in the digital product accompanying the final submission of this document..

TC Alby occurred in 1978 and, was one of the most intense cyclones on record to impact the southern reaches of the west coast of WA. Therefore it has been used as the baseline event for this project. Modelling a recent historical event has the benefit of the impacts being remembered by the community. This is very important when the model results are being communicated as the community can more easily relate to the scenario and can compare the model outputs with what they may have experienced or heard. If the results match people's experiences, then the community may have a greater trust in model results for future hypothetical events.

TC Alby was the fifth tropical cyclone of the 1977/78 cyclone season in the north-western Australian region. A detailed description of the life cycle and impact of TC Alby is contained in the Bureau of Meteorology report of TC Alby (BOM, 2012).

An estimation of an ARI for TC Alby is problematic because of the relatively small number of cyclonic events that have had a major impact on the west coast of WA. The regional storm modelling report (Hubbert *et al.*, 2012) provides an analysis of the history of these events for the period 1950-2008 to estimate the ARI for TC Alby to be in the order of 150 to 200 years for the region and an approximate ARI of 2000 to 10 000 years for direct impact on Busselton.

The TC Alby scenario (B0) results were used to validate the model. In order to investigate the impact of a 'worst case' strike, this track was shifted in space and time so that the maximum storm winds impacted more directly on Busselton in combination with a peak tide. The shift of the TC track in time in the modelling ensured the cyclone exhibited maximum wind speeds at Busselton and coincided with a spring tide (mean high water springs) of 1.5 m. The timing of the cyclone to strike Busselton coinciding with a spring tide further increases the rarity of the event. The shifted track is shown in [Figure 12](#) along with the actual track used for verification purposes.

A large number of alternative tracks were investigated in order to determine the worst cyclone track using the same cyclone intensity and dimension parameters exhibited by TC Alby. It emerged from these studies that the same 'worst case' storm track also applied to both Mandurah and Bunbury due to the nature of the sea-level response to TC Alby in the region. To understand this it is important to

note that the data from the tide gauges at Mandurah, Bunbury and Busselton showed that the peak sea-levels at each location occurred at all three locations within an hour of each other. This is due to the fact that TC Alby was moving very quickly as it passed along this region producing a sea-level response along the coast which was almost concurrent at each of the three locations.

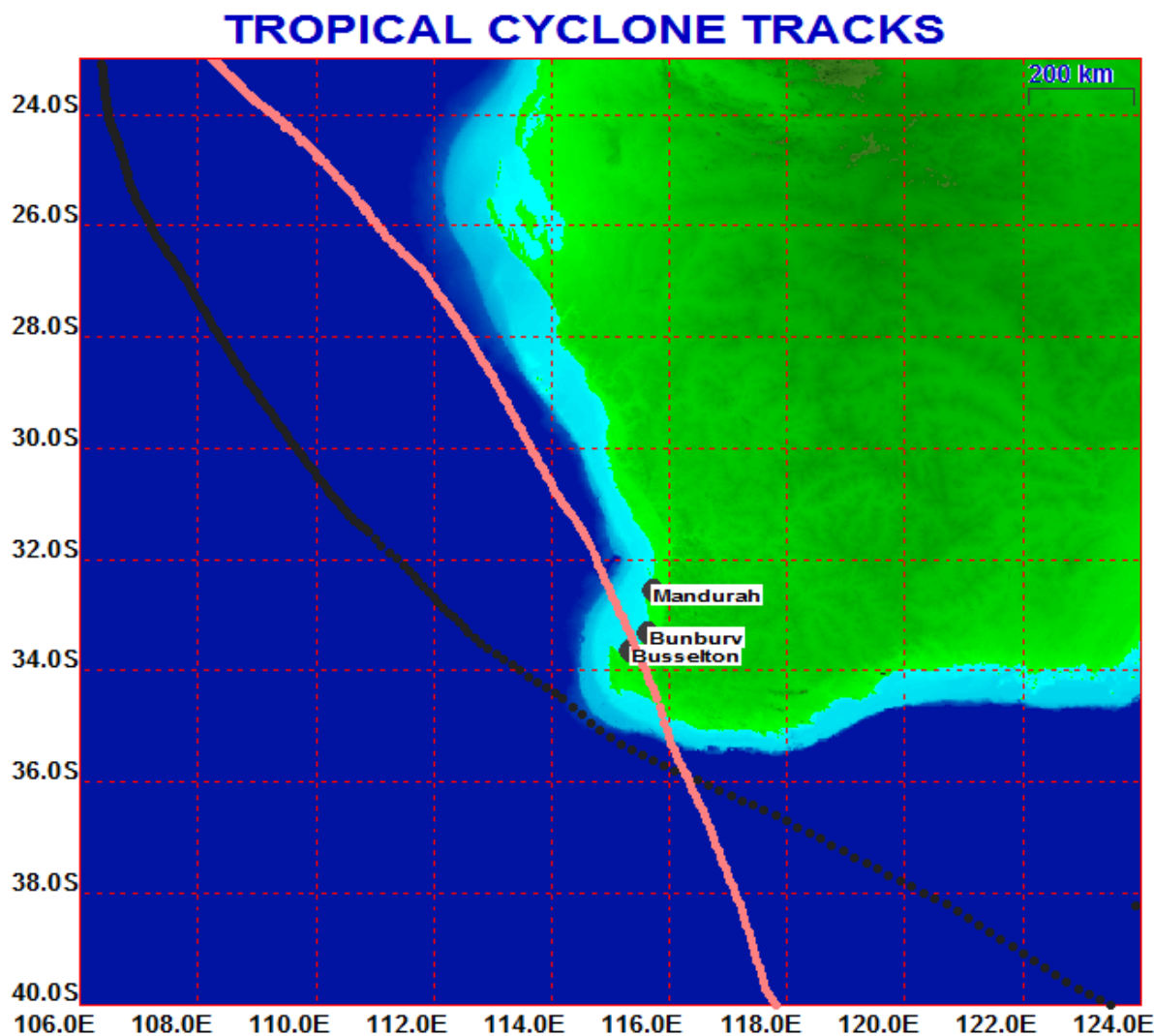


Figure 12. 'Actual case' (black) and 'worst case' (pink) tracks for TC Alby used for verification and prediction of extreme outcomes respectively (Hubbert et al., 2012).

The model simulations were carried out with the GEMS Coastal Ocean Model (GCOM2D). This model simulates the atmospheric pressures, winds and tides resulting from tropical cyclones. The atmospheric pressures and the wind fields were predicted from the cyclone track information with a cyclone model based on the Holland vortex model (1980 and 2008).

The tidal forcing for the studies was generated from the GEMS tidal constituent database which was initially developed for the WA coast for the Australian Maritime Safety Authority (AMSA) to support the AMSA Search and Rescue Ocean prediction system which is based on the GEMS ocean model. The tidal constituent data was derived from a long term modelling study on a 1.8 km grid around Australia which involved multiple iterations of model predictions, comparison with tide gauge data and

adjustment of boundary conditions based on error analyses. The model iterations were continued until errors reached a minimum status.

The official track for TC Alby provided by the Bureau of Meteorology was given in decimal degrees of latitude and longitude quoted to one decimal place. The potential numerical error in this track is therefore approximately +/-5 km. The initial simulation with the precise official track did not produce a good verification at Bunbury and Mandurah with the errors being higher at Mandurah. Adjustment of the track within the +/-5 km error margin resulted in a much better verification.

GEMS completed validation of the regional modelling results through comparing these results to the TC Alby tide gauge data recorded at the Busselton Jetty which recorded a maximum height of 2.58 m. Detail of this validation is provided in the GEMS regional storm-modelling report (Hubbert *et al.*, 2012) which was included in the digital product accompanying the final submission of this document..

2.1.2.1. GCOM2D output data

The outputs of the storm modelling were an array of rasters with a storm characteristic value in each of the 25 m by 25 m grid cells for each scenario. GEMS modelled two scenarios: a base case simulation of TC Alby (B0) and the TC Alby event with a modified track (B1) to focus peak winds over Busselton.

Six rasters, one for each storm characteristic, were produced at 12 minute intervals within each simulation. The six storm characteristics include:

- wind speed
- wind direction
- atmospheric pressure
- sea surface height
- current velocity east
- current velocity north.

This data was then visualised for quality assurance checks and then processed at Geoscience Australia to extract the required sea surface heights and momentum required to run the inundation simulations with ANUGA. There is scope in future work to include more of the GEMS data, such as wind velocity, into ANUGA simulations as well as general analysis of the GCOM2D outputs that may be of interest to local communities (see the expansion of the study section on [p82](#)).

2.1.3. Step 3 – ANUGA storm modelling

Any model should be set up according to end user requirements and it should also consider what may have been inundated in the past. The modelling extent was discussed with officers from the Busselton Council and representatives from the WA DoP and the WA DoT at a meeting in Busselton in September 2011. The agreed extent is shown in [Figure 13](#).

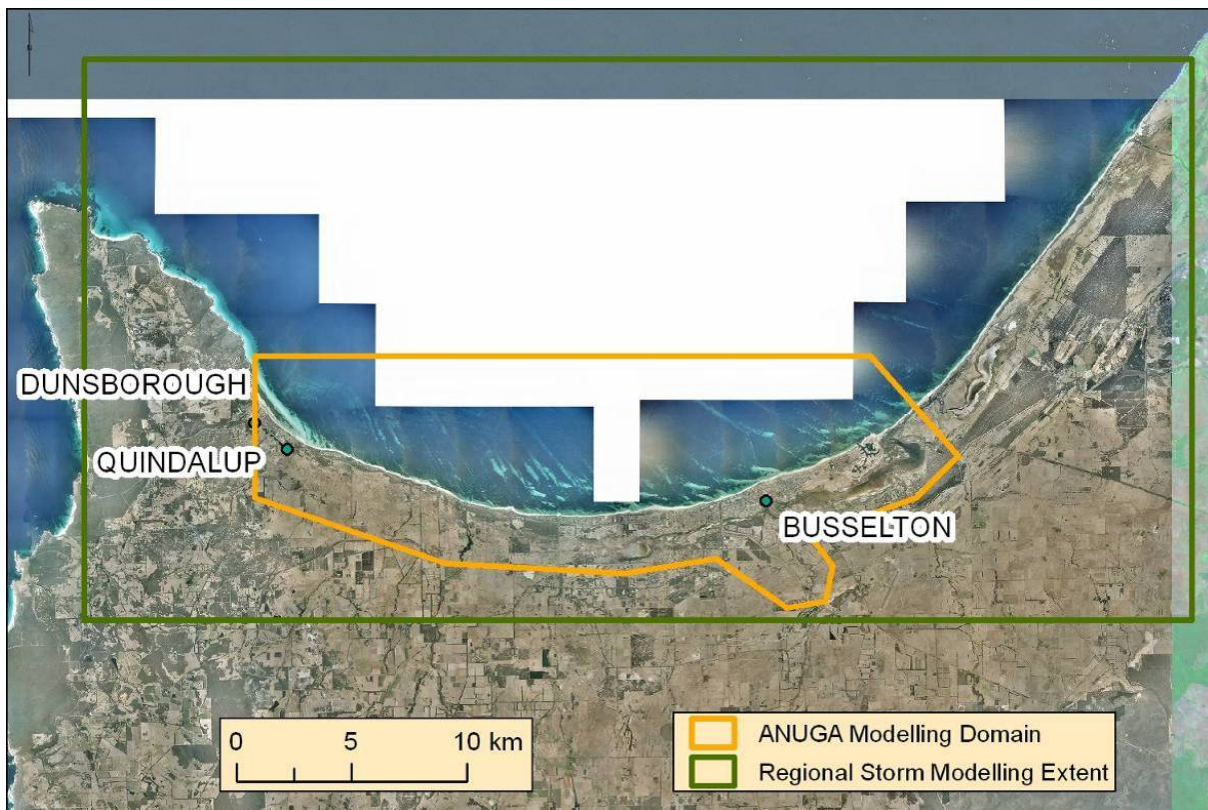


Figure 13. Inundation modelling domain.

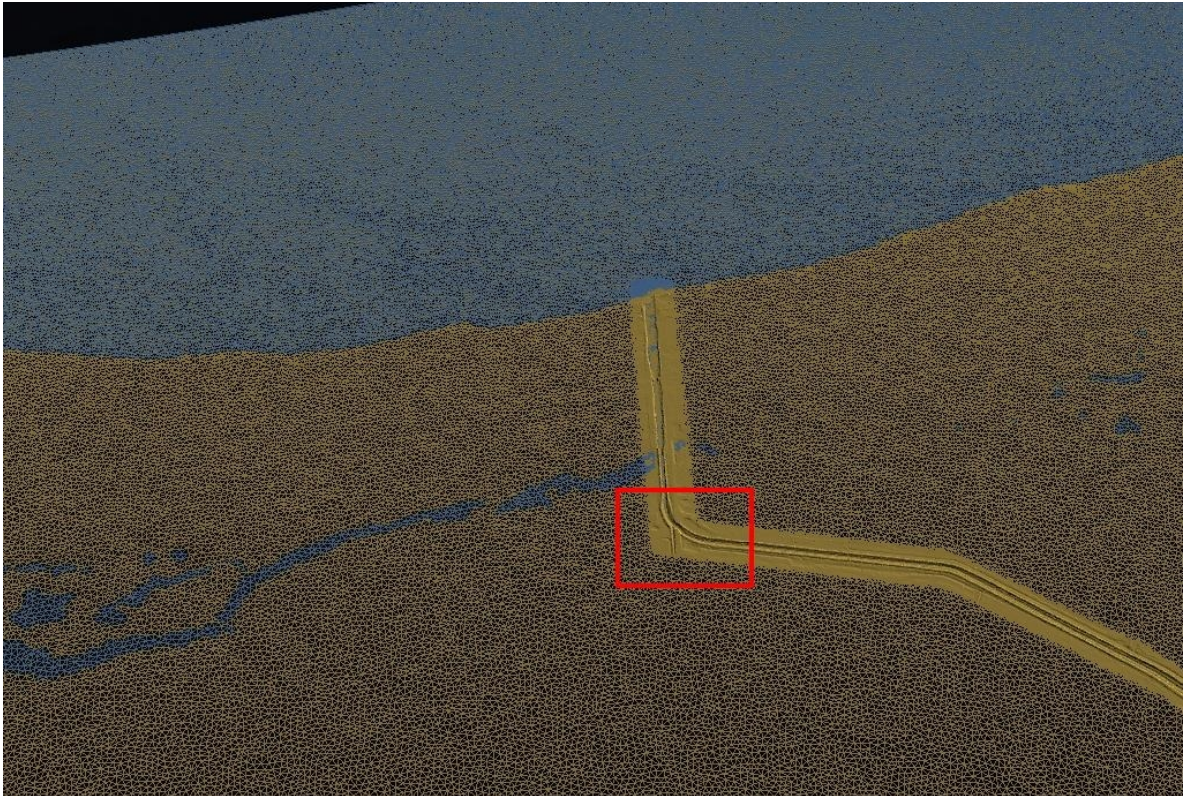
ANUGA interpolates the elevation data to an unstructured triangular mesh to underpin the computations (Jakeman, 2006). In order to accurately capture the dynamics, the mesh was built with embedded internal polygons that identify fine mesh resolutions over the watercourses and coarser resolutions where the surface is less variable. Figure 14 shows an example of the two mesh resolutions used in building the ANUGA inundation model.

The model configuration specifies the maximum allowable triangle area, in this case 350 m^2 (Figure 14(a)). A zoomed view of the modelling mesh is shown in Figure 14 (b) to highlight the smallest triangles, maximum area of 5 m^2 , used in the simulation that were needed to accurately model the flow in the Vasse Diversion Drain.

A minimum estimate of the triangle count for this simulation is approximately 1.5 million triangles. It was therefore necessary to run the ANUGA code on the National Computational Infrastructure (NCI¹⁰) to achieve the completion of the modelling over a mesh of this size in a reasonable timeframe. Further, the parallel version of the ANUGA code was used which distributes components of the simulation simultaneously across a number of processors.

¹⁰ The NCI is a supercomputer facility hosted by the Australian National University for use in scientific research. It is an initiative of the Australian Government. <http://nf.nci.org.au/>

(a)



(b)

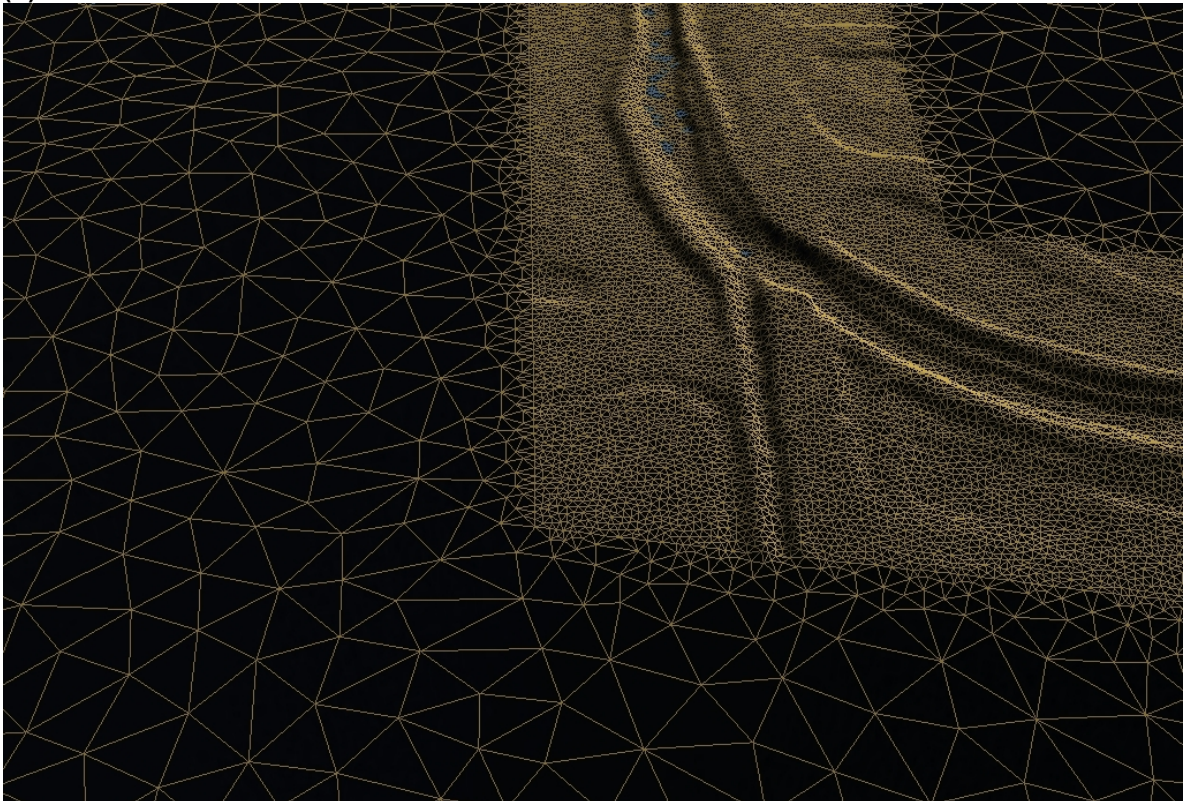


Figure 14 (a). Small scale ANUGA mesh refinement for Busselton inundation model. (b). ANUGA mesh refinement for Busselton inundation model. The larger triangles have a maximum area of 350 m^2 and the smaller triangles were restricted to an area less than 5 m^2 .

The regional model simulation was initiated at 0600 on the 4 March, 1978 with the initial sea level at mean sea level. The total model simulation time for the GCOM model was two days. This time was selected to allow the full dynamics of the storm-tide event to reach the area of interest and cover the major effects of the complex interaction with the near-shore environment. The ANUGA simulation uses this input data, input at a 12 minute time interval, for the 56 hours around the peak storm tide from 0900 on the 3 March 1978 to 1700 on the 5 March 1978. The ANUGA simulation uses the flood hydrograph data, input at a 12 minute time interval, for the 39 hours around the peak storm tide from 1500 on the 3 March 1978 to 0600 on the 5 March 1978.

2.1.3.1. Set the boundary conditions

Astronomical tidal forces were implicitly captured by the ANUGA simulation via the coupling with the GEMS model. The time varying boundary condition, derived from the GCOM2D results, captures the change in ocean momentum and water-surface elevation due to the cumulative effect of the astronomical tide and the storm related processes. The GCOM2D data was applied at the boundary of the ANUGA model at 200 boundary points (Figure 15).

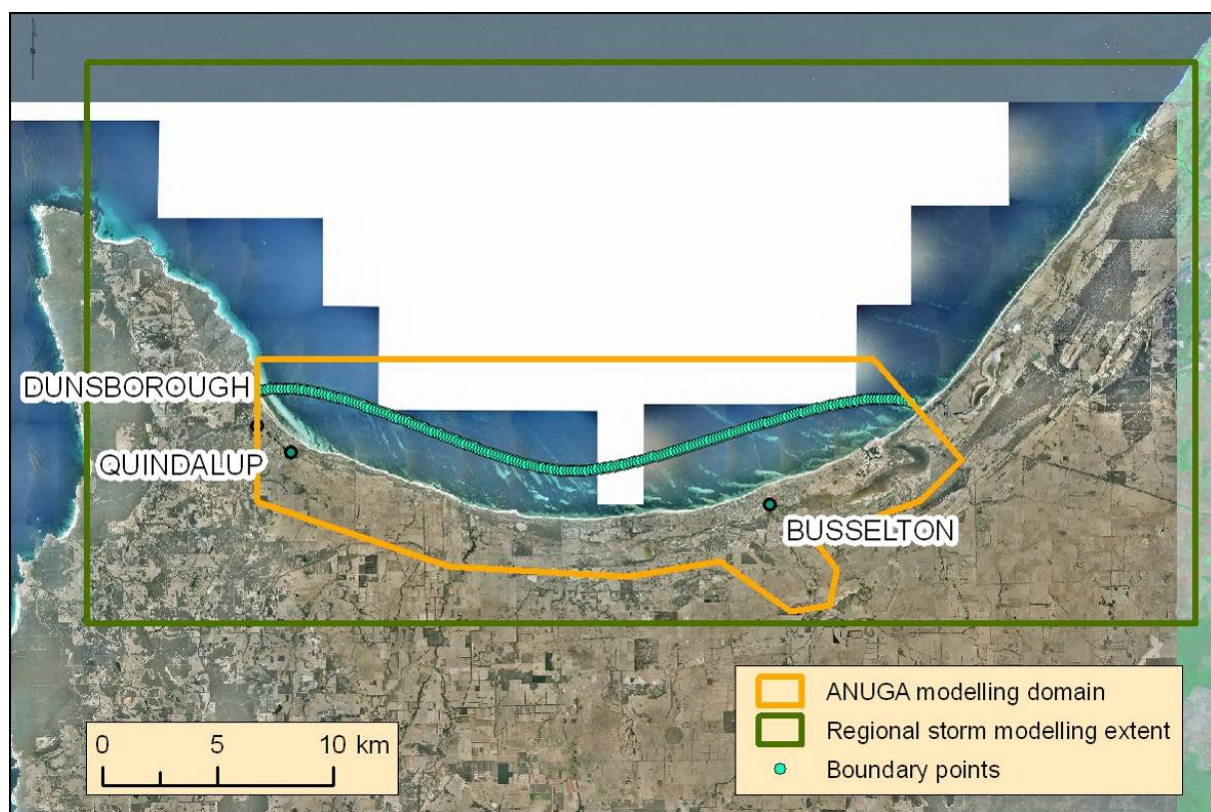


Figure 15. Location of GEMS boundary condition data points.

2.1.4. Step 4 – Investigation of climate change impacts

The effects of climate change have been incorporated in two ways:

- A range of SLR values were applied as changes to the initial still water level in ANUGA.
- Examination of the changes in elevation caused by erosion in the coastal zone in response to SLR and increased storminess.

The SLR and flood scenarios considered within the modelling are shown in [Table 2](#). The 0.4 m and 0.9 m SLR scenarios were sourced from the WA Government (WAPC, 2003 and Bicknell, 2010). The 1.1 m SLR scenario is a high-end scenario based on the IPCC AR4 and subsequent research (DCCEE, 2009)

Table 2. Storm tide and flood modelling scenarios.

| ID | Type | Sea-Level | Riverine Flood |
|-----|--|-----------|----------------|
| B0 | Base Case (Validation against TC Alby) | Current | None |
| B1 | Worst Case (TC Alby, track and time shift) | Current | None |
| B2 | Worst Case + SLR | + 0.4 m | None |
| B3 | Worst Case + SLR | + 0.9 m | None |
| B4 | Worst Case + SLR | + 1.1 m | None |
| B5 | Worst Case + Coincident Flooding | Current | 25 year ARI |
| B6 | Worst Case + Coincident Flooding | Current | 100 year ARI |
| B7 | Worst Case + Coincident Flooding + SLR | + 0.9 m | 25 year ARI |
| B8 | Worst Case + Coincident Flooding + SLR | + 0.4 m | 100 year ARI |
| B9 | Worst Case + Coincident Flooding + SLR | + 0.9 m | 100 year ARI |
| B10 | Worst Case + Coincident Flooding + SLR | + 1.1 m | 100 year ARI |

2.1.4.1. Combined storm and flood inputs

Figure 16 shows the riverine hydrographs and the observed TC Alby inundation heights from the Busselton Jetty tide gauge. The peaks seen in Figure 16 represent different locations, i.e. the jetty and the riverine hydrograph inlet point (Figure 8). The location of riverine and storm-tide inundation coincidence within the Vasse Diversion Drain has been generally observed to be between the Moore St. flood gates and the first bend in the Vasse Diversion Drain.

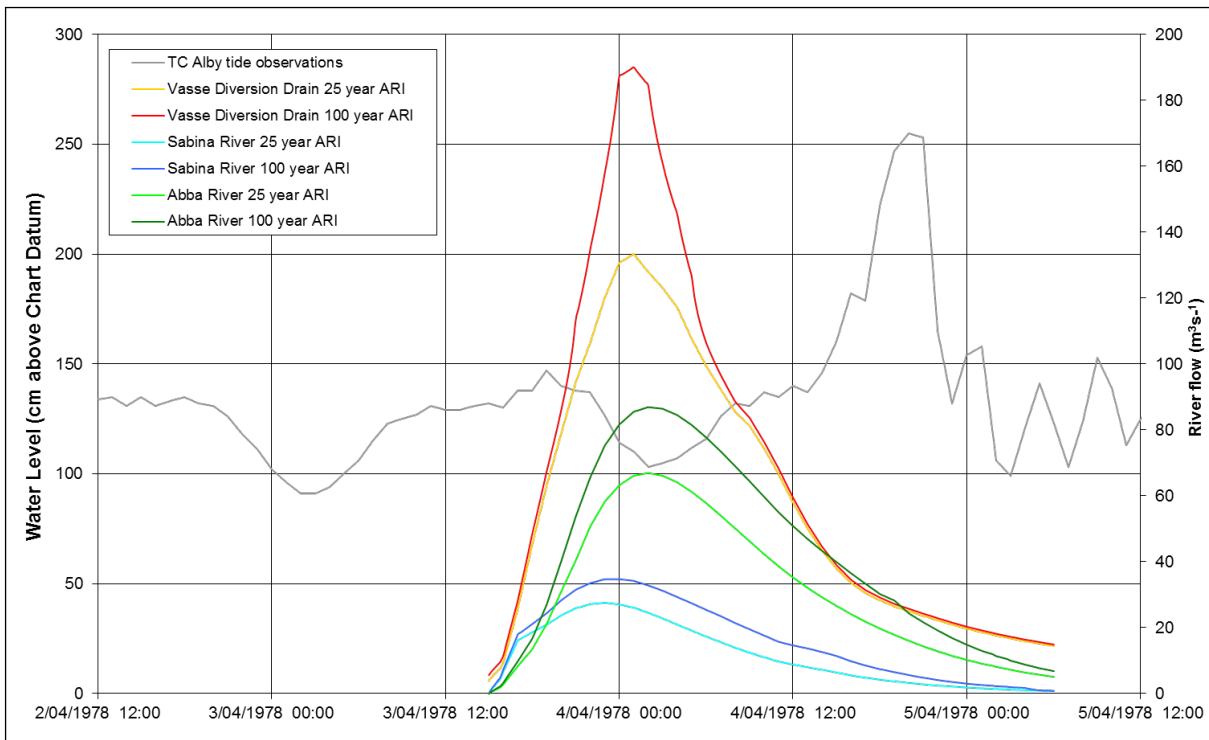


Figure 16. Storm tide and riverine hydrograph input timing.

2.2. Coastal erosion modelling

A number of studies have been undertaken in order to qualitatively assess the potential for coastal erosion along the Busselton coastline. The first, undertaken for the WA DoP and Infrastructure in 1997 and updated by Andrews (2003), developed an erosion setback line for the sandy shorelines of Geographe Bay. This erosion set back line represented the location behind which residential, commercial and transport infrastructure can be defended against beach erosion for the planning period of 50 to 100 years. This assessment was based on the requirements set out in the West Australian Planning Commission's (WAPC) State Planning Policy No. 2.6 (State Coastal Planning Policy; WAPC, 2001) which stipulates that the following factors must be taken into account when calculating the setback distances from the horizontal setback datum (HSD – defined as the landward limit of active coastal processes).

- (S1) Distance for absorbing acute erosion due to the impact of a sequence of extreme storm events on the shoreline. The default value is 40 metres.
- (S2) Distance to allow for historical trend based on the present longer term annual rate of erosion. The assessment should be based on a least a 40 year record of shoreline movement. Stable shorelines are allocated a "safety" allowance of at least 20 m and where there is evidence of the shoreline accreting a value of 0 m is applied.
- (S3) Distance to allow for sea-level change based on the median model from the IPCC 3rd assessment report which predicts vertical change in SLR of 0.38 metres by 2100. Based on the Bruun Rule (Bruun, 1962) a multiplier of 100 is applied to sandy shores to give S3 a value of 38 metres¹¹.

The second study was undertaken by Damara WA Pty Ltd (Damara, 2011), who adopted a different approach by considering the behaviour of the Geographe Bay coastline over the next 100 years rather than simply applying the calculation within the WAPC State Planning Policy 2.6 (WAPC, 2001). This was accomplished by incorporating the effects of localised processes; inter alia, ongoing coastal accretion and erosion patterns, the cumulative lag effect on downdrift sediment transport from multiple protection structures and the natural variations in alongshore sediment transport. Damara also considered the meteorological and ocean conditions (wind, waves and tides) and morphology of the Geographe Bay when considering likely impacts of sea-level change. Importantly, they undertook cross-shore modelling using SBEACH12 rather than applying the Bruun Rule multiplier to the SLR. This resulted in a number of changes to the way in which the erosion set back components were calculated:

- S1 including the effect of beach rotation and the downdrift lag response from the protection structures along the coast
- S2 is now considered in terms of the net sediment budget and localised variations thereof
- S3 has been derived by considering sediment movement from the coastal barrier to the beach.

The most recent study was undertaken by the University of Sydney (Cowell and Barry, 2012) for the Australian Government. This study was a regional scale quantitative assessment of coastal-recession risk from Busselton to Rockingham. Coastal erosion risk forecasts were derived through the application of a sediment transport model, the STM, over four time horizons (2030, 2070, 2100 and

¹¹ This policy was revised in 2009 following a review of the IPCC AR4 to a 0.9 m SLR by 2110, with the multiplier of 100 still applied for sandy shores (90 metres).

¹² Storm-induced Beach Change Model <http://www.veritechinc.com/products/cedas/sbeach.php>

2300) and a range of SLR scenarios. When forecasting coastal erosion risk, the STM considered not only the changes in sea level, but also considered the various sediment sources and sinks for beach and dune sand, and the effects of the erosion resistant rock substrate outcropping in the coastal zone. The STM simulates the effects of SLR, disturbance to sediment budgets, erosion resistant substrate and time-dependent morphological behaviour to forecast possible future locations of the shoreline. Forecasts differ from previous single estimate predictions (deterministic) as they provide a range of possible erosion magnitudes each with a measure of likelihood.

The STM is able to model the coastal response to the effects of SLR, disturbances to sediment budgets, effects of mixed sediment-sizes (including sand and mud), variable resistance to erosion for material comprising strata in the substrate (which can include bedrock and reefs), and complex topography. The STM considered the SLR scenarios shown in [Table 3](#) and produced coastline probabilities for each scenario¹³.

Table 3. Shoreface translation modelling SLR scenarios (in metres; from Cowell and Barry, 2012).

| Year | Lower Limit | Mode | Upper Limit |
|------|-------------|-------|-------------|
| 2030 | 0.132 | 0.146 | 0.200 |
| 2070 | 0.333 | 0.460 | 0.700 |
| 2100 | 0.500 | 0.800 | 1.100 |
| 2300 | 2.500 | 3.750 | 5.000 |

The STM applies stochastic or Monte Carlo simulations to manage the predictive uncertainty in cases involving complications resulting from open sediment budgets, rock reefs and seawalls (all commonly occurring along the WA coastline). Stochastic simulation makes it possible to establish confidence limits and determine the statistical significance of differences caused by varying effects, e.g. substrate resistance and shoreface geometry. It also enables the likelihood of critical impacts to be specified in terms of probability.

2.2.1. Modelling extent

This study used the coastal erosion modelling outputs from a study undertaken by the University of Sydney for the Australian Government in 2012 (Hazelwood and Moore, 2012). The storm tide and coastal erosion modelling extents differ. Whilst the extent of the storm-tide modelling was able to be extended to include Dunsborough, due to interest in this area from the WA DoP, the coastal erosion modelling had been completed prior to the Dunsborough inclusion. [Figure 17](#) shows the coastal erosion modelling extent.

¹³ This is shown in the STM outputs as future coastlines. Each coastline represents the probability of exceedance that the coastline will be in that location within the SLR scenario.

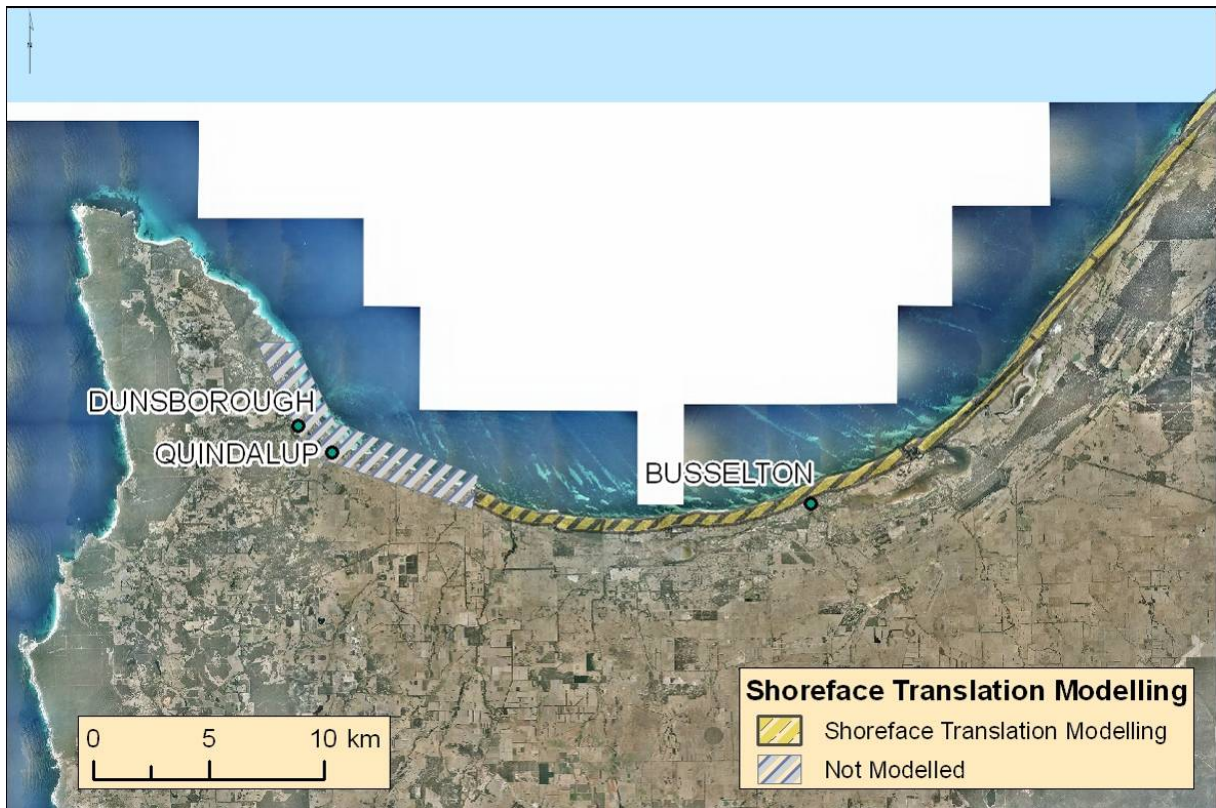


Figure 17. The coastal erosion modelling extent.

2.2.2. Output data

The STM spatial data outputs were expressed as possible future coastlines (linear spatial data) with each possible coastline given a probability based on the number of Monte Carlo simulations forecasting an extent of recession less than or greater than that location. The probabilities for each SLR scenario year considered (2030, 2070, 2100 and 2300) were: 0.001, 0.01, 0.1, 0.2, 0.3, 0.4, 0.5, 0.6, 0.7, 0.8, 0.9, and 0.99. For the purposes of establishing the underlying recession range, the coastal erosion distances defined by the 0.5 (or 50%) and the 0.1 (or 10%) probability values were selected. The 10% value represents the risk averse scenario, in which there is 10% probability that the location of the future shoreline will be translated landward equal to or greater than the distance reported.

Coastal erosion footprints were visualised through mapping the location of the future coastline for each probability of exceedance. Beach recession results were derived from the simulations as recession risk contours. There were 48 risk contours, considering each of the four SLR scenarios with twelve probabilities per scenario.

Although the STM coastal erosion modified DEMs were initially considered for inclusion within the ANUGA SLR scenarios, the modified DEMs did not reflect a realistic future surface and therefore these were not included in the ANUGA modelling.

For a more detailed explanation of the STM modelling and results, see the report included in the digital product accompanying the final submission of this document.

This page is intentionally blank

3. Modelling results and analysis

The results are presented as a collection of maps for each scenario in a map series provided in the digital product accompanying the final submission of this document. The map series can be reviewed in conjunction with the information presented later in this section.

3.1. Map series

The maximum inundation depth maps show the maximum depth above the elevation recorded over the entire simulation time. A map series presenting this peak storm tide and riverine flood inundation and coastal erosion per scenario has been produced. The map sheet is presented at a scale of 1:50 000 and has been designed to be printed to an A3 paper size. Figure 18 shows an example map sheet. For each map series there is a cover map showing the extent of the larger scale maps included in the map series. In the B0 example shown in Figure 18 the larger scale maps that follow in this map series are indicated by the extent of squares 1, 2 and 3 with the larger scale maps labelled accordingly in the lower right label which for the overview map references “Map A3/1 to 3”. Within the following results, maps are also included but for greater detail refer to the provided map series for each simulation.

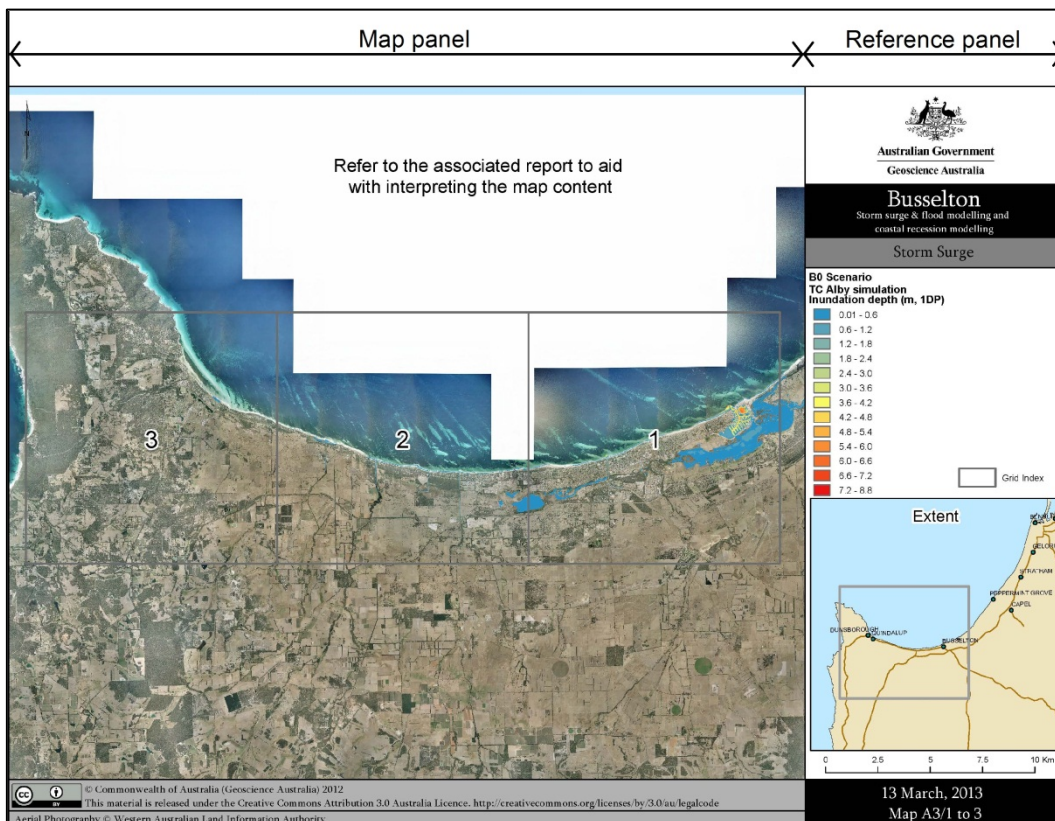


Figure 18. Example map sheet.

3.2. Storm tide and riverine flood inundation

All references to the riverine flooding scenarios in the following analysis of the Vasse and New River Estuaries and the Broadwater refer to those water bodies as they are identified in Figure 19. That is, the Vasse Estuary is defined as the water body east of the mouth of the Vasse River, the Broadwater as the water body west of the Vasse Diversion Drain and the New River Estuary as the water body in-between.



Figure 19. Busselton estuaries, watercourses and Moore St. floodgates.

The following sections show a more detailed analysis of the modelling undertaken grouped by SLR:

- Current SLR Scenarios (p33).
 - a. TC Alby validation (B0).
 - b. Worst-case TC Alby (B1).
 - c. Worst-case TC Alby + 25 year ARI Flood (B5).
 - d. Worst-case TC Alby + 100 year ARI Flood (B6).
- 0.4 m SLR Scenarios (p51).
 - e. Worst-case TC Alby + 0.4 m SLR (B2).
 - f. Worst-case TC Alby + 0.4 m SLR + 100 year ARI Flood (B8).
- 0.9 m SLR Scenarios (p59).
 - g. Worst-case TC Alby + 0.9 m SLR (B3).
 - h. Worst-case TC Alby + 0.9 m SLR + 25 year ARI Flood (B7).
 - i. Worst-case TC Alby + 0.9 m SLR + 100 year ARI Flood (B9).
- 1.1 m SLR Scenarios (p65).
 - j. Worst-case TC Alby + 1.1 m SLR (B4).
 - k. Worst-case TC Alby + 1.1 m SLR + 100 year ARI Flood (B10).

3.2.1. Current SLR scenarios

3.2.1.1. B0 - TC Alby validation

The base case (B0 - [Figure 20](#)) was generated from the TC Alby track data from the BOM as input into the GCOM2D model. The resulting storm-tide water levels (combined astronomical tide and storm surge) were taken from approximately 150 m from the coast ([Figure 15](#)) and input to ANUGA (as a boundary condition) which models inundation over the ANUGA modelling domain ([Figure 15](#)).

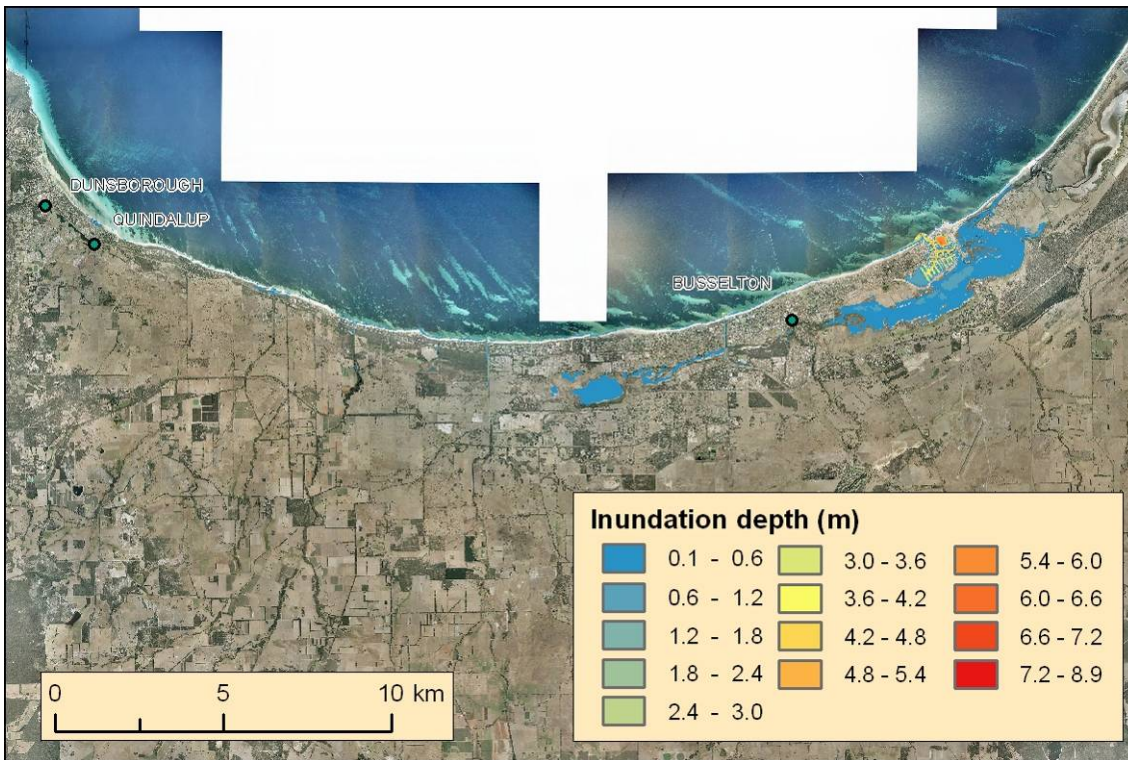


Figure 20. B0 inundation depth (TC Alby scenario).

As part of the regional storm modelling (Hubbert *et al.*, 2012), GEMS completed validation of the TC Alby scenario (BO) regional modelling through comparing these results to the TC Alby tide gauge data recorded at the Busselton Jetty. Although the tidal regime did not appear to be a good match between the model results and the observations, the peak inundation was a much closer match (Figure 21). This is discussed in detail within the GEMS report (Hubbert *et al.*, 2012).

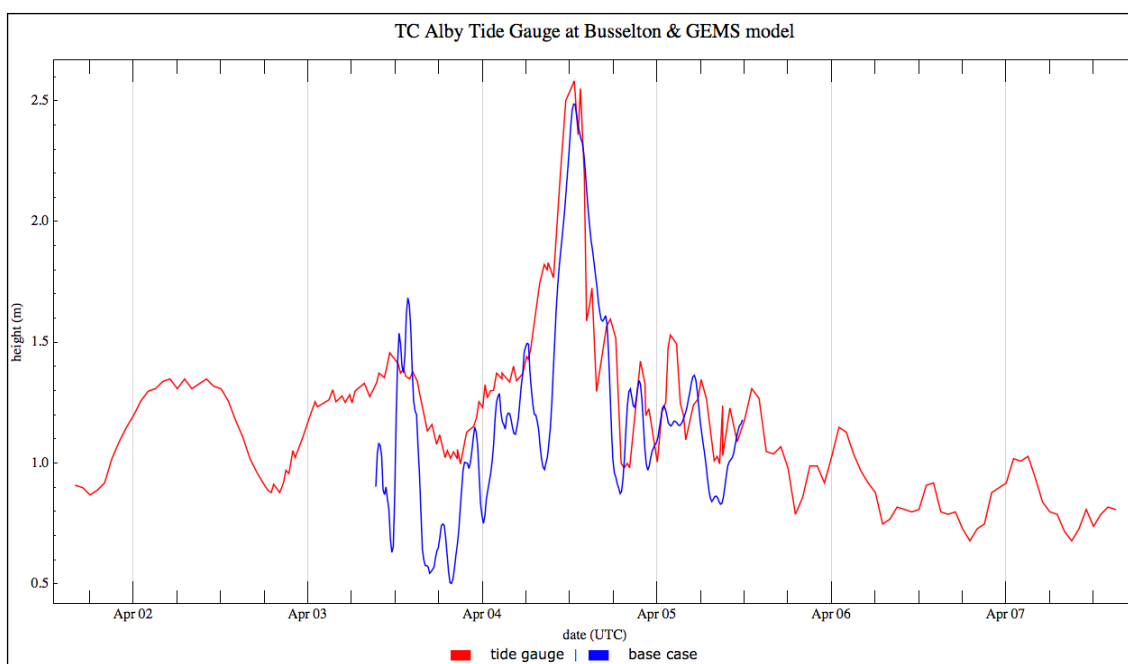


Figure 21. TC Alby observations at the Busselton Jetty and the GEMS modelling results (Hubbert *et al.*, 2012).

Following the regional modelling validation, the local inundation modelling was also compared to TC Alby observations. The ANUGA modelled TC Alby inundation extents were compared to the observed TC Alby inundation extent. In the aftermath of TC Alby, the inundation extent was marked on WA Department of Lands and Survey maps. To compare the ANUGA model results, the observed inundation maps were georeferenced and a transparency applied; their extents can be seen within [Figure 22](#). [Figure 22](#) shows three validation locations which were from west to east, referred to as: Siesta Groyne near Lennox Drain (west), Busselton Jetty (centre) and Busselton Townsite (east).

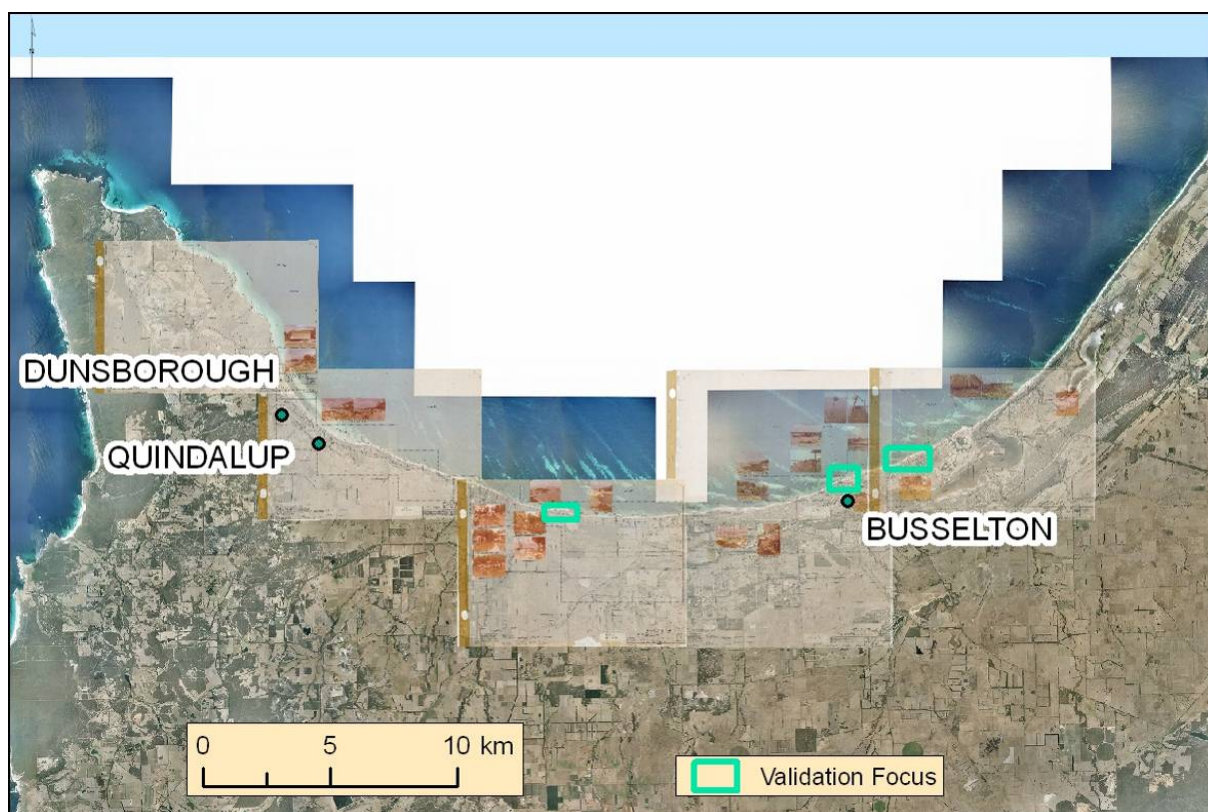


Figure 22. TC Alby validation focus areas.

The black dashed line in [Figure 23](#) to [Figure 25](#) was digitised from the 1975 mapped coastline. Following TC Alby the maximum extent of inundation was mapped and is represented by the red line, again digitised from the hand drawn line on the maps. The maps also appear to include recorded storm-tide high water marks at certain locations. Due to the uncertainty in these recordings these observations were not used in the local inundation validation.

In the 35 years between TC Alby occurring (1978) and this study being completed there has been significant natural adjustment to the shoreline of Geographe Bay. The changes in bathymetry, due to sandbar migration, as well as the effects of coastal defences (not resolved in the base DEM) could also be significant (Damara, 2011) and may have a large effect on the model validation. This reduced the ability to properly validate inundation footprints generated by ANUGA. To undertake a thorough validation of the model for TC Alby far more work would need to be done to modify the base DEM to reflect the surface as it was in 1978 preceding the storm. This was outside the scope of the study. In light of these factors, a full model validation was not possible, therefore only an indicative validation is presented here.

Following is a discussion of the three validation sites and comparison with the B0 scenario inundation extent.

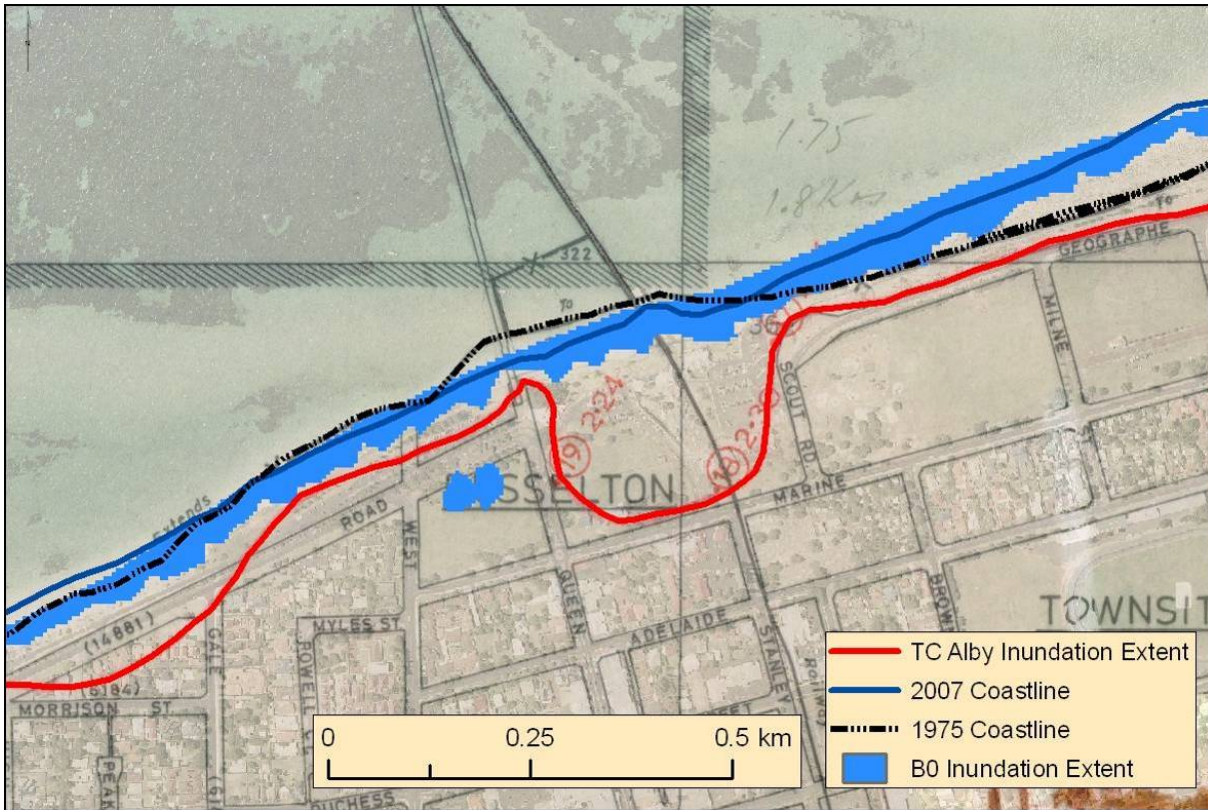


Figure 23. Busselton Jetty validation site showing both the observed TC Alby and modelled B0 inundation extents.

The first validation site was the Busselton Jetty validation site (Figure 23). The extent of inundation recorded in 1978 indicates an incursion on the eastern side of the old jetty position. This indicates the effect of the generally west to east surge (Fig 26, Hubbert *et al.*, 2012) diffracting around and propagating down the jetty to inundate the area marked by the red line. As the old jetty was not included in the base DEM these effects were not present in the simulation and areas immediately to the east of the jetty should be treated with caution. However, the area of inundation modelled west of the jetty is broadly consistent with the extent of inundation (area between the black and red line) observed during TC Alby. As this particular area of coastline is at a similar position to that in 1978¹⁴ it is expected, in the absence of bathymetric changes nearby, that these extents would be similar. Also of note here is the isolated inland area of inundation. This is due to the ANUGA setup threshold value below where transient depths of less than 10 cm were not recorded. The dry section between the areas of inundation is where the storm tide is less than 10cm deep and not recorded in the modelling output file.

¹⁴ The imagery capture in 2008 shows the coastline to be a visual match to the 1975 mapped coastline.

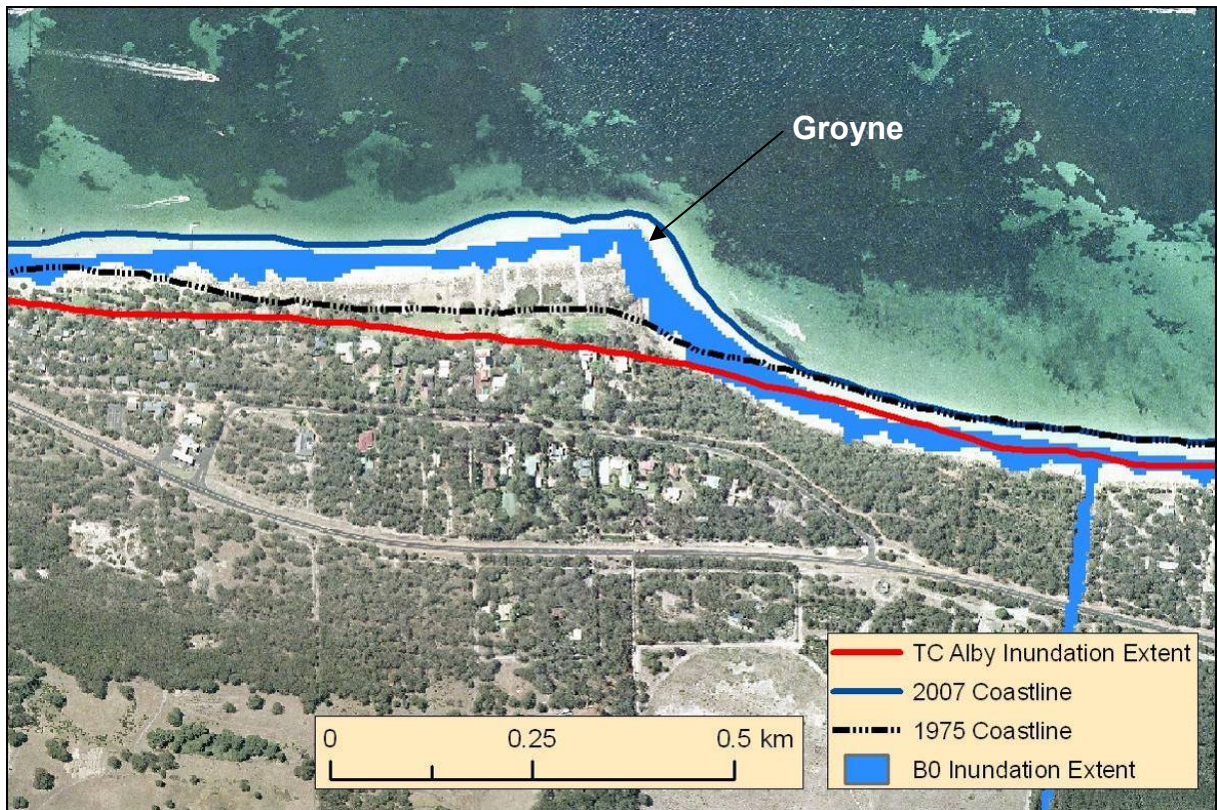


Figure 24. Siesta Park Groyne, near Lennox Drain validation site and B0 inundation extent. The 1975 maps have not been shown for ease of interpretation.

The addition of the Siesta Park groyne has significantly altered the coast by trapping sediment on the western side of the groyne and creating 100 m of new beach (Figure 24). On the eastern side of the groyne, this has resulted in the shoreline retreating from its 1975 position. This demonstrates how the current topography can differ from that recorded in 1975 and adversely affect validation attempts.

3.2.1.2. B1 - Worst case (TC Alby track and time shift)

The maximum inundation depth recorded due to a shifting of the track of TC Alby, is shown in [Figure 26](#) and in the provided B1 map series (see the Map series section on p31).

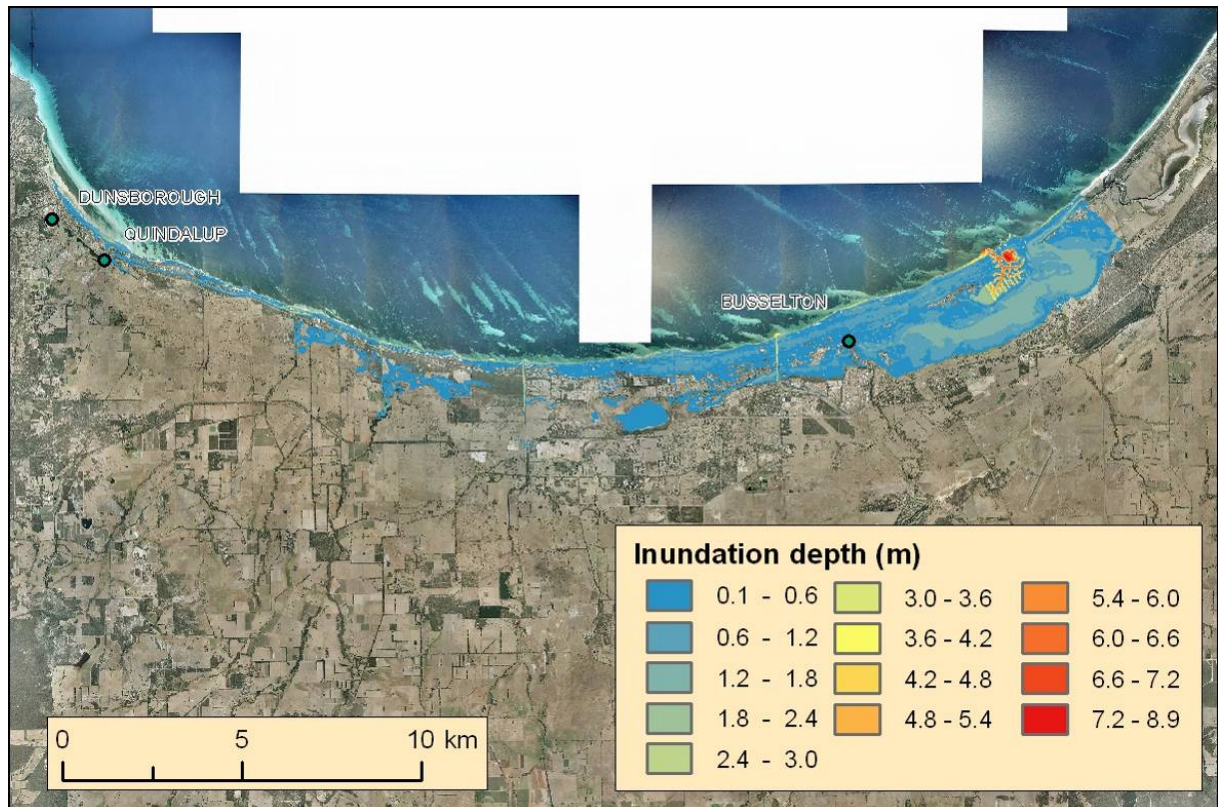


Figure 26. B1 inundation depth (TC Alby - worst case).

[Figure 26](#) shows that the majority of the inundation occurs in the Vasse Estuary and in the areas of low elevation between the coast and estuary. Despite the Moore St floodgates ([Figure 28](#)) being closed, there was overtopping into the Broadwater. The drainage channels between Busselton and Dunsborough were overtopping in places and delivering water to the southern side of Caves Road.

The change of track of TC Alby has significantly increased the extent of the inundation. This is shown graphically by subtracting the inundation of the base case scenario, B0, from B1 ([Figure 27](#)).

[Figure 28](#) shows where the inundation difference is greater than 1 m. The largest increase in inundation occurs in the entrances to the estuaries and along areas of lower elevation between the Vasse Estuary and the coast. The localised build-up of water at the end of the marina is a result of the state of construction at the time of LiDAR data capture.



Figure 27. Difference in the inundation depth; B1 - B0.

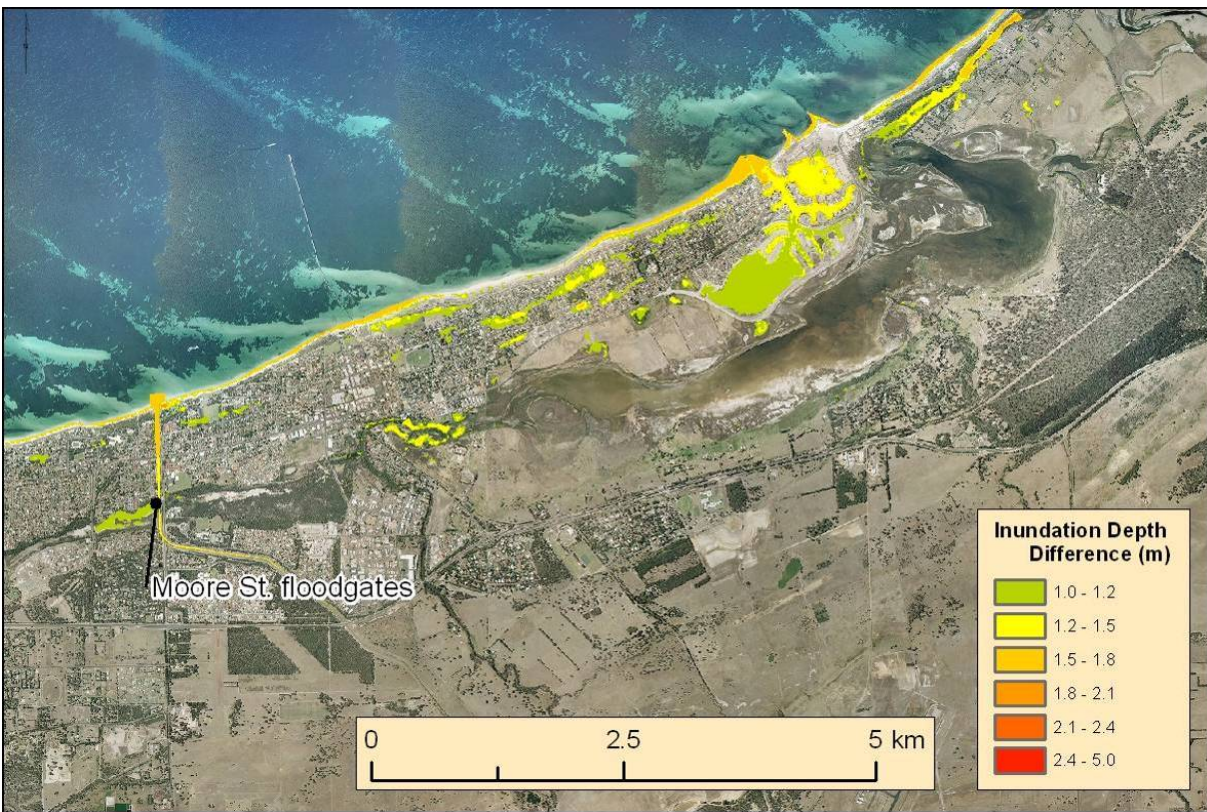


Figure 28. Difference in the inundation depth; B1 - B0 where the difference is greater than 1 m.

One of the mechanisms to infer the source or flow direction of the inundation is to investigate the maximum momentum¹⁶ parameter. Figure 29 shows the maximum momentum reached during the ANUGA simulation of the B1 scenario. This provides a way to differentiate between inundation due to the overtopping of the coastal dunes and inundation from the Vasse Estuary.

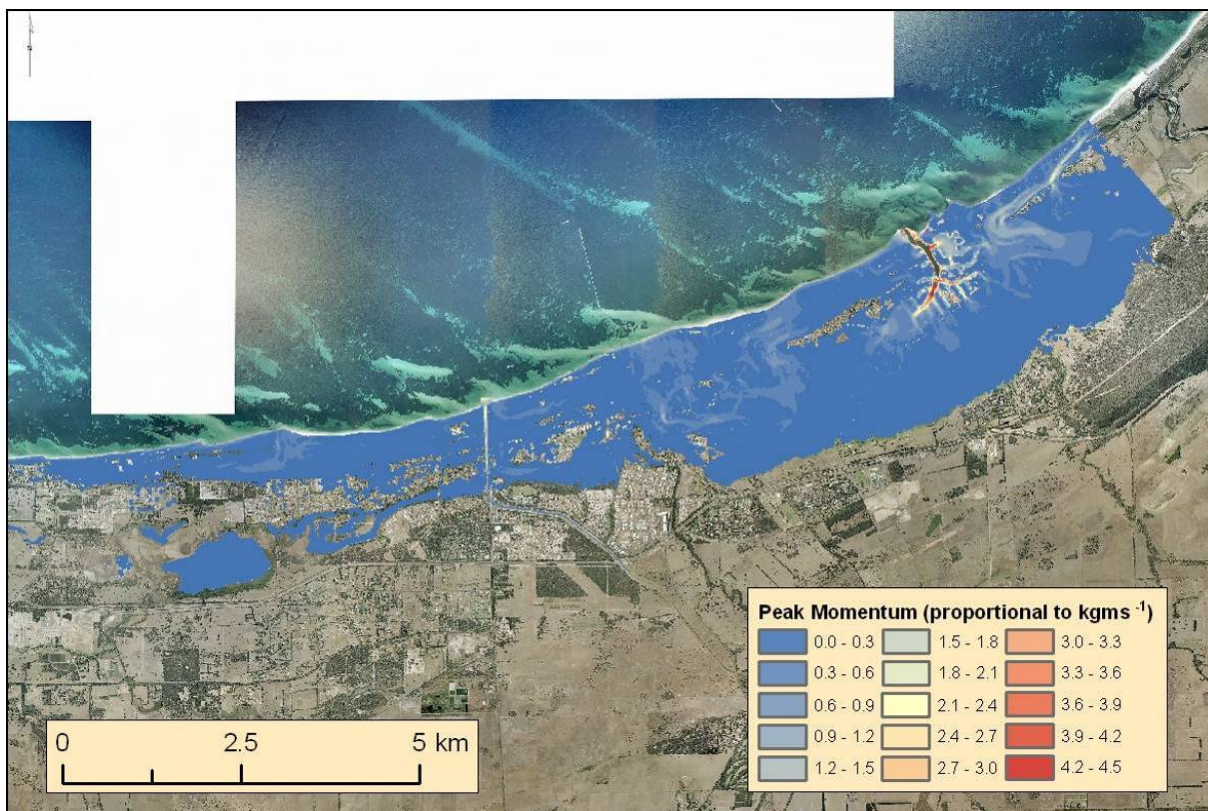


Figure 29. B1 peak momentum.

The majority of the inundation between the coast and the Vasse Estuary was caused by the oceanic storm tide, i.e. not from storm tide into the mouth of the estuary. The marina inlet experiences the highest momentum during the B1 scenario. The east side of the marina does show water leaving the marina and flowing into the estuary. This was confirmed through visually inspecting the scenario results throughout the simulation time.

From examining the structure of the maximum momentum recorded around the Moore St. floodgates, it was clear that they were being overtopped and that the inundation in the Broadwater estuary does not flow overland in this scenario.

¹⁶ The parameter that is referred to as momentum here, and in the remainder of the report, is calculated as the depth integrated velocity which, while proportional to momentum, is not numerically equal to momentum.

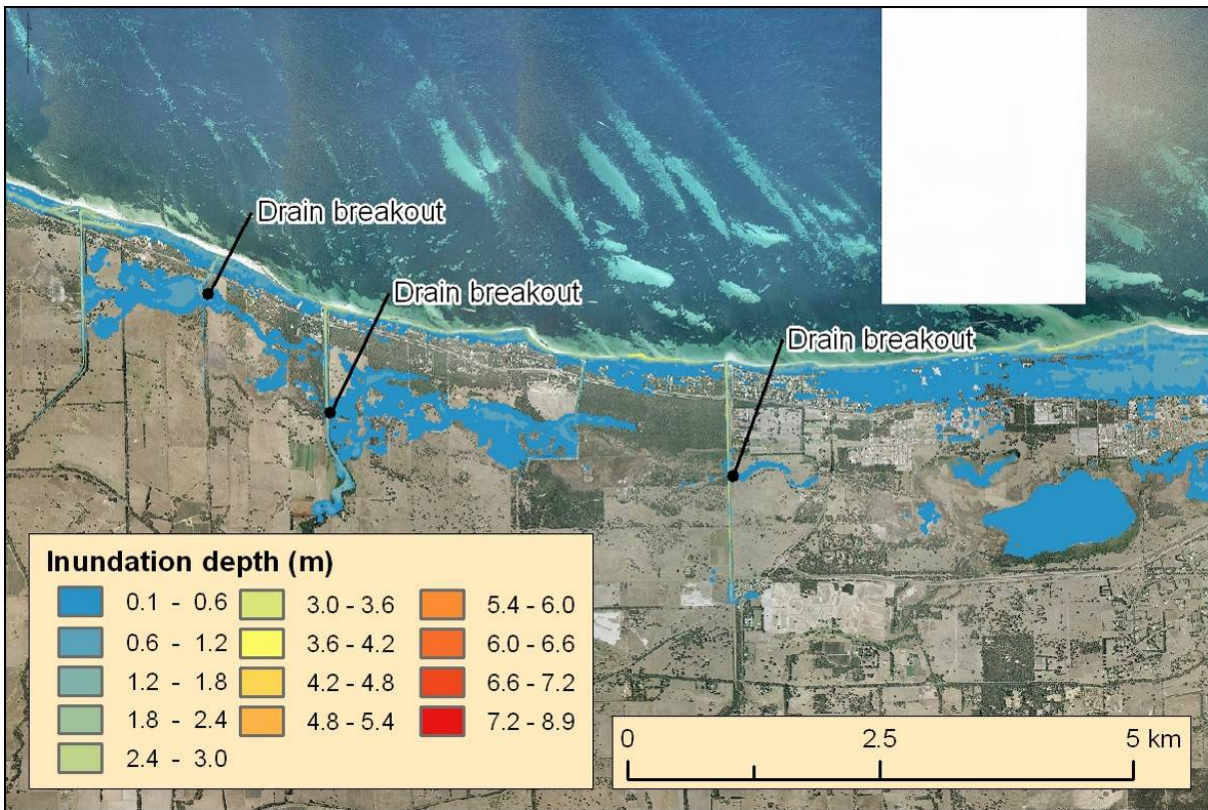


Figure 30. Dunsborough drain breakouts - B1 Scenario.

Figure 30 shows the areas in Dunsborough where the breakout of water from the drains has been recorded. As the SLR value increases in the later scenarios these breakouts become indistinguishable from overland storm-tide inundation and. Inundation depth in these areas would be magnified in the event of riverine flood waters also flowing in these channels.

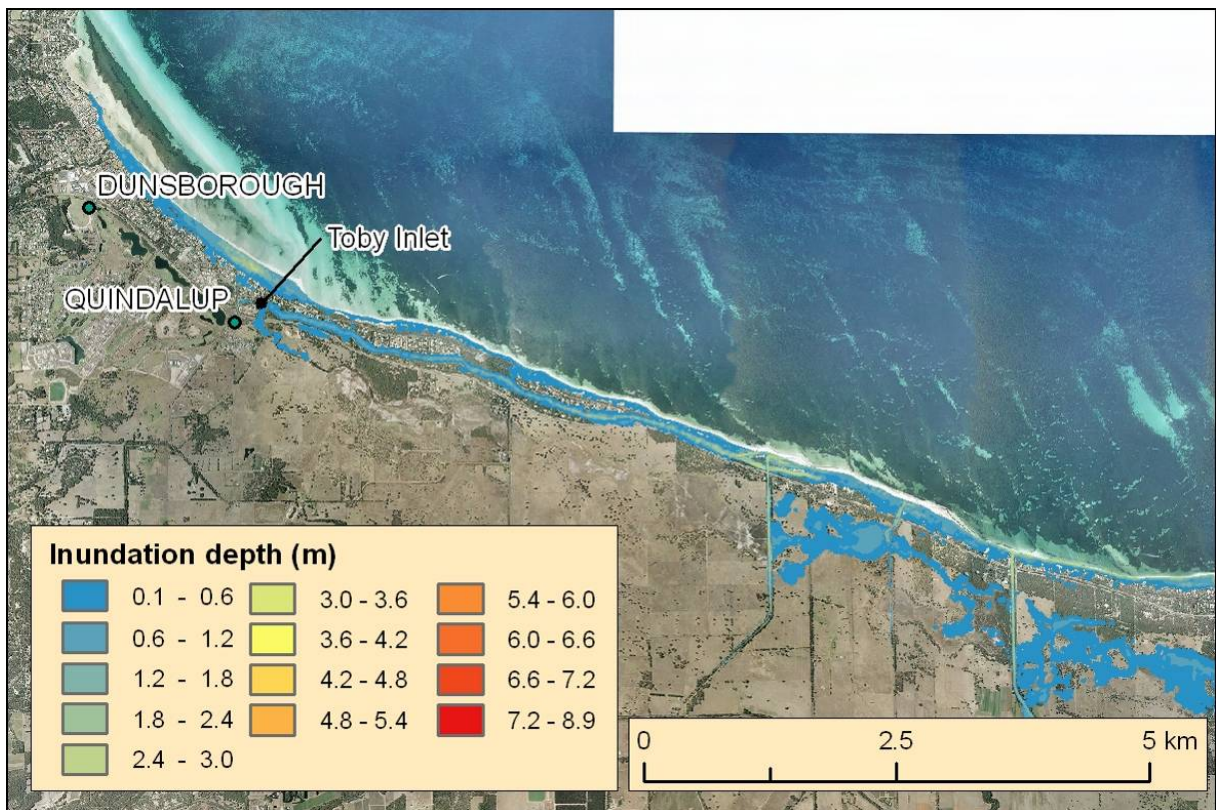


Figure 31. Modelling flow within the Toby Inlet.

The resolution of the modelling mesh was selected to be sufficiently high to simulate natural waterways as can be seen in Figure 31 where the storm tide in Toby Inlet is shown accurately following a 180° bend in the inlet.

All remaining scenarios, B2-B10, in the results section are organised under the appropriate SLR headings for ease of comparison and all will share the basic characteristics of B1 that have been discussed above. In this context B1 can be considered as the base scenario upon which the remaining scenarios have had SLR and/or riverine flooding added.

3.2.1.3. B5 - Worst-case TC Alby + 25 year ARI flood

The peak inundation depth results of the B5 scenario around the Busselton area are shown in Figure 32. As riverine flooding was not included in the Dunsborough watercourses the B5 results for Dunsborough are identical to B1, as can be seen in the B5 map series (see Map series section on p31). Therefore the Dunsborough results are not further presented or discussed. For similar reasons the Dunsborough results for B6 to B10 are also omitted from the report.

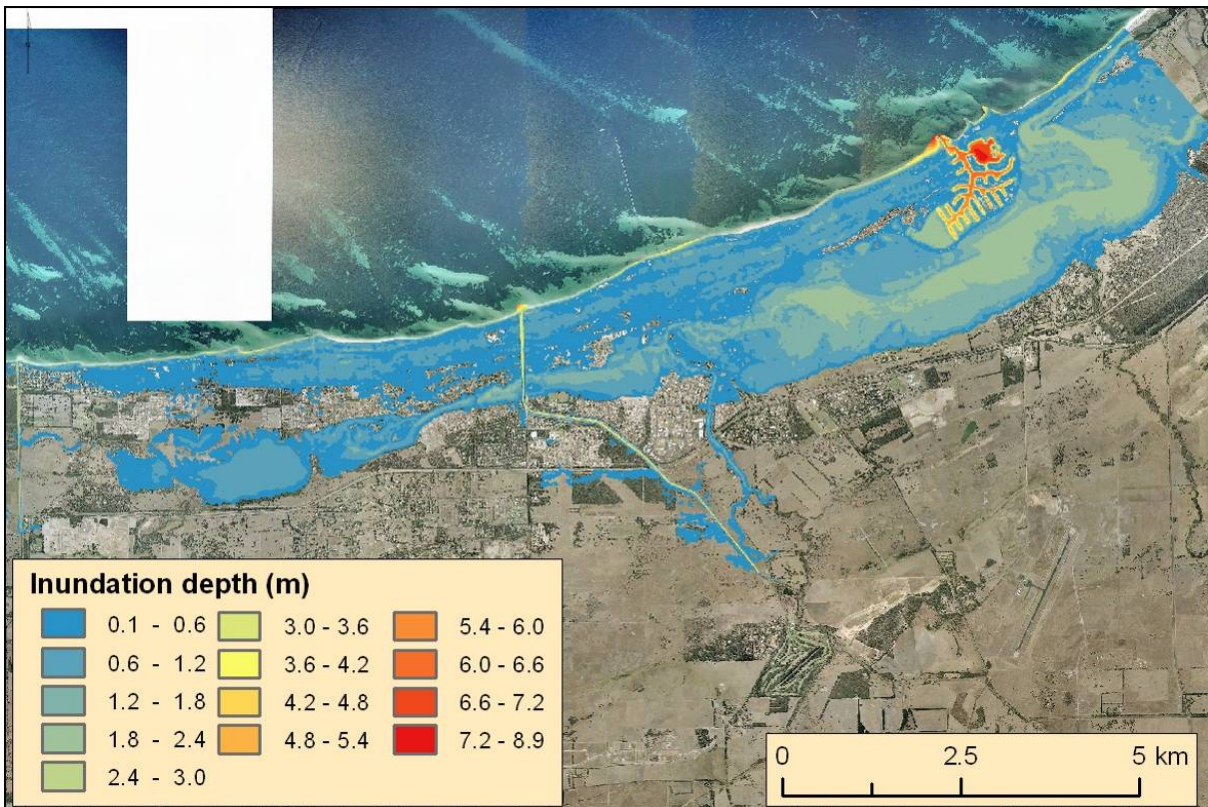


Figure 32. B5 inundation depth (TC Alby Worst case + 25 year ARI flood).

Compared with the same storm-tide scenario but without riverine flooding (B1), differences in inundation extent in the B5 scenario include the presence of water in the Vasse Diversion Drain and the subsequent spill outs close to the diversion point to the Vasse River and on the western side of the drain (Figure 33). The spill out on the western side of the drain can be seen to flow north until it encounters the Busselton Bypass, at which point it can be seen flowing west, parallel to the road. This damming effect of the Busselton Bypass becomes more pronounced with the 100 year ARI flood scenarios (B6, B8, B9 and B10).

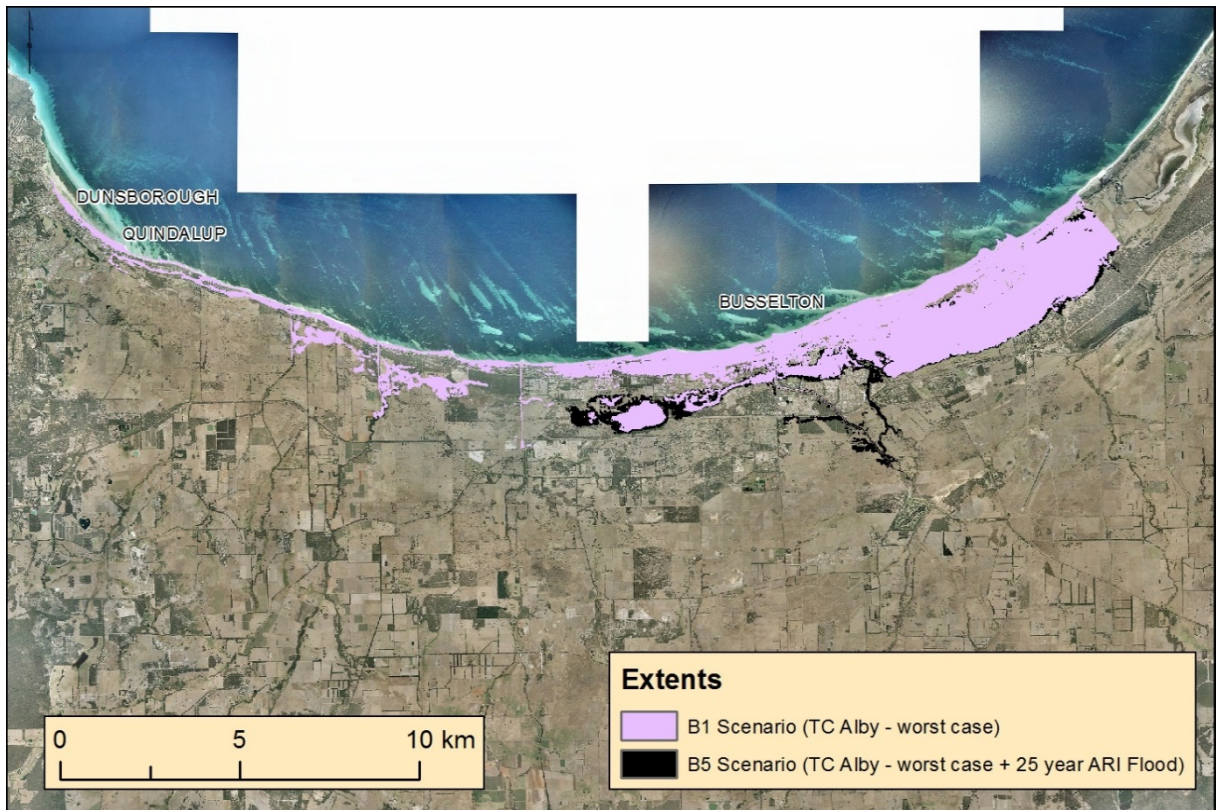


Figure 33. B5 and B1 inundation extents.

The effect of introducing a 25 year ARI flood on the inundation extent is shown in Figure 33 above. The riverine flood waters can be seen to spill out of the Vasse Diversion Drain near its junction with the Vasse River causing small extent increases in the New River Estuary and also a build-up along the Busseton Bypass west of the Vasse Diversion Drain.

The flood waters were also seen to flow over the Moore St. floodgates and into the Broadwater where the inundation extent was also increased.

To examine the effects of adding a 25 year ARI flood to the B1 scenario, a difference raster similar to Figure 27 was produced (Figure 34). Riverine flooding into the Vasse Estuary produces up to 50 cm more inundation depth during the scenario. The flooding down the Vasse Diversion Drain flows over the Moore St. flood gates, contributing to the up to 80 cm of inundation recorded in the Broadwater and the New River Estuary.

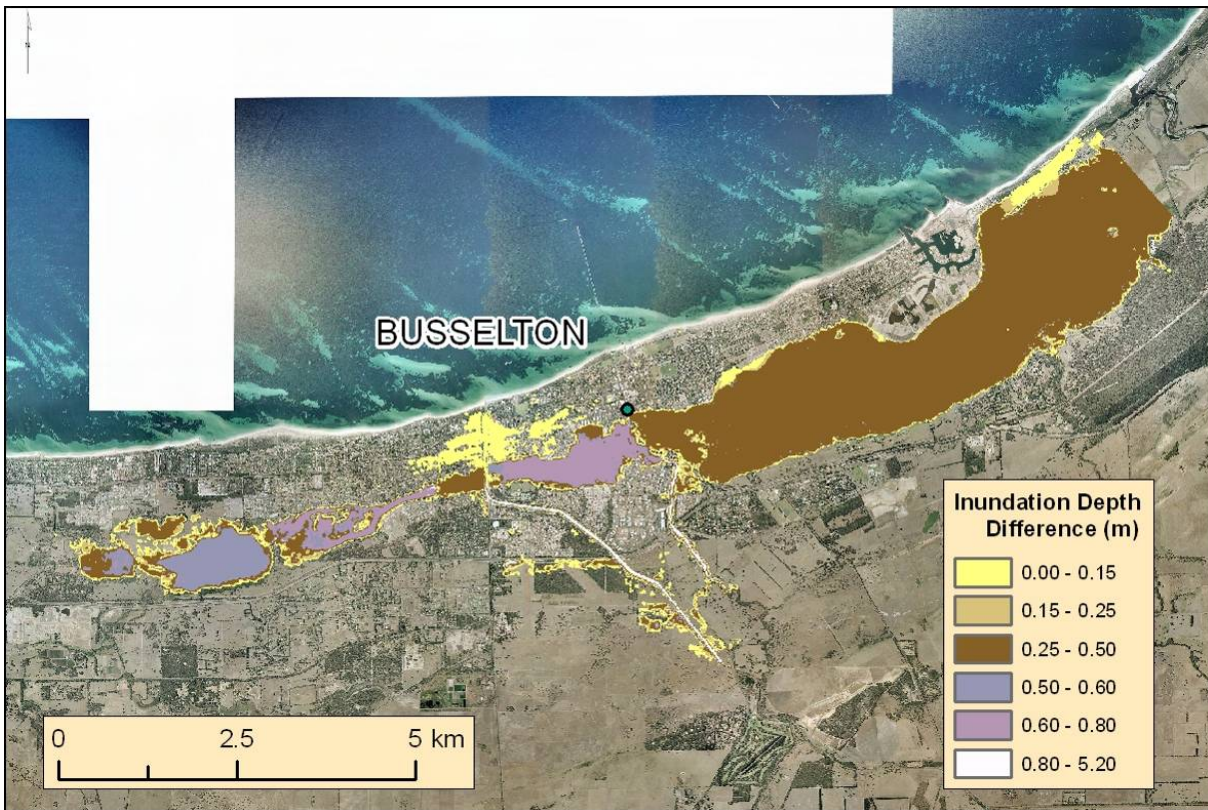


Figure 34. Difference in the inundation depth; B5 - B1 where greater than 0.1 m.

The 25 year ARI flood in this area has begun to overtop Queen Elizabeth Av. on the east side of the Vasse Diversion Drain opposite the Moore St. floodgates and is responsible for the extra maximum depth recorded in the New River Estuary. In later scenarios, with larger floods and increased SLR, this becomes more pronounced.

The general effect that the coincident riverine flooding event has on the Busseton side of the modelling domain discussed here forms a template for each subsequent coincident flooding scenario. Where either sea-level or flood severity has been increased the corresponding increase in inundation extents can be seen. This is evident in the next section showing the effects of adding a 100 year ARI flood to the B1 scenario of a worse track TC Alby storm over the current sea-level.

3.2.1.4. B6 - Worst-case TC Alby + 100 year ARI flood

Figure 35 presents the peak inundation depth for the TC Alby worst case plus 100 year ARI flood scenario.

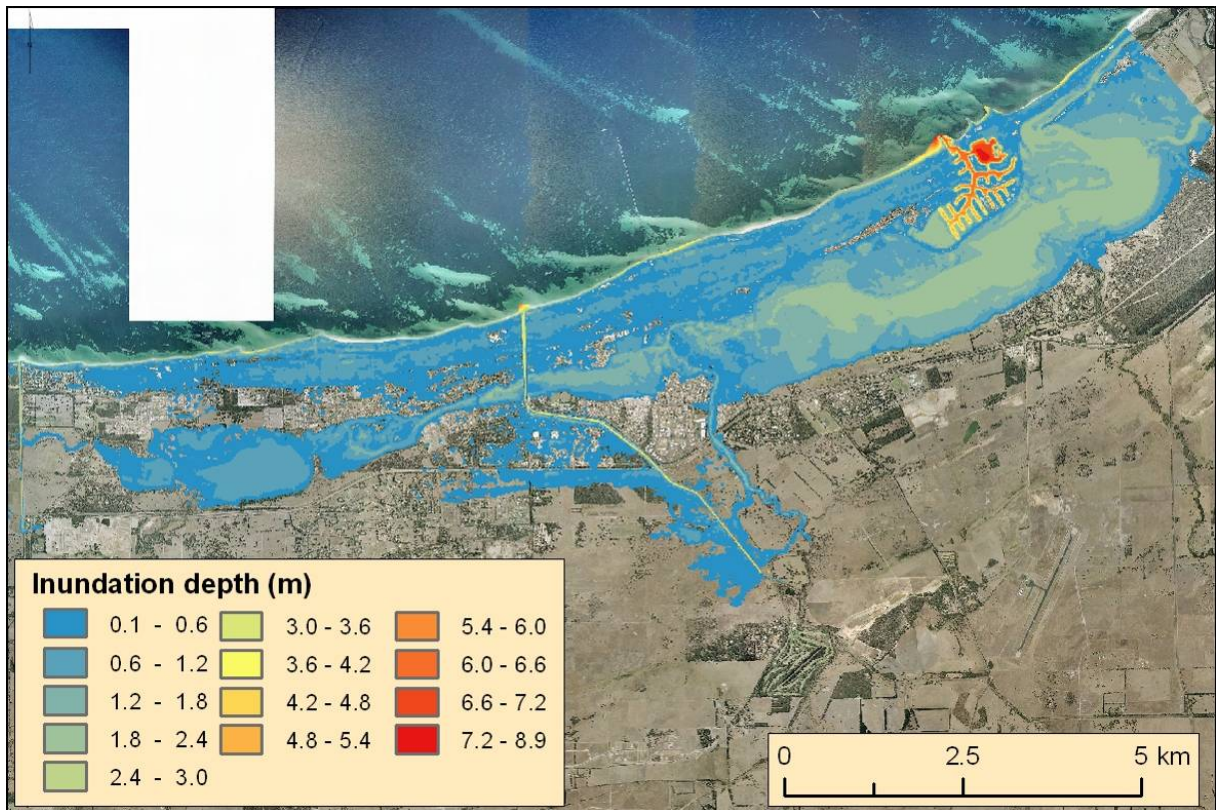


Figure 35. B6 inundation depth (TC Alby Worst case + 100 year ARI flood).

Beyond the clear addition of more inundation due to the Vasse Diversion Drain spill out near the Vasse River junction it is not immediately clear what additional effect the increase of riverine flooding severity has had. The inundation extents shown in Figure 36 show the effect of a 100 year ARI flood coincident with the Worst-case TC Alby and the effect of increasing the flooding from a 25 year ARI to a 100 year ARI scenario.

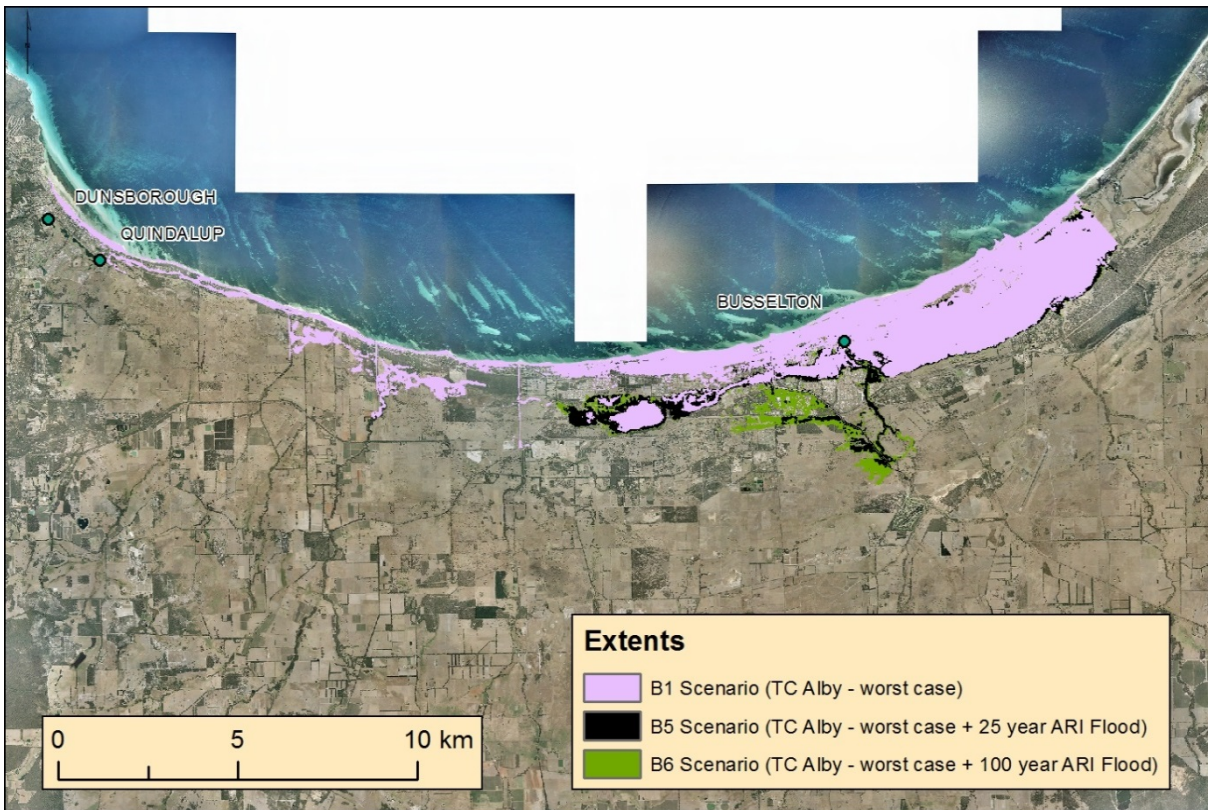


Figure 36. B1, B5 and B6 inundation extents.

Figure 36 builds on Figure 33 to display the effect of increasing the severity of the riverine flood event to a 100 year ARI event. There is a small increase in extent visible around the Broadwater but the greatest increase in extent can be seen in the area around the Busselton Bypass. It is worthwhile to note here that if the Vasse Diversion Drain could be prevented from spilling out the extent of inundation in the area would be unlikely to change significantly.



Figure 37. Difference in the inundation depth; B6 - B1 where the difference is greater than 0.1 m.

Figure 37 shows generally the same areas were affected in the 100 year ARI flood as in the 25 year ARI flood (Figure 34). The exception is more inundation related to the Vasse Diversion Drain breakouts and a general increase in depth as illustrated in Figure 38.

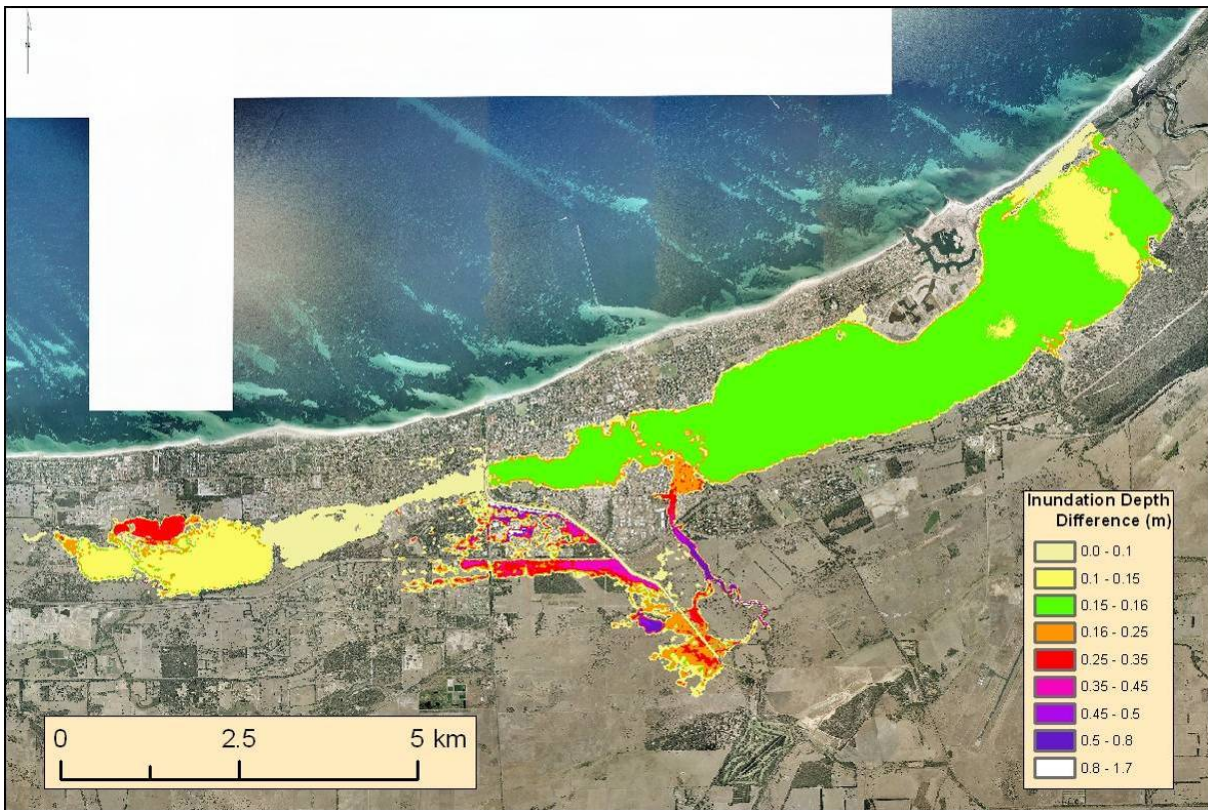


Figure 38. Inundation depth difference - B6 - B5.

Figure 38 shows the effect of increasing the flood severity to a 100 year ARI flood. There is an increase of up to 16 cm across both the Vasse and New River Estuaries while the Broadwater experiences up to a 15 cm increase. The highest areas represented were new areas of inundation not present in the 25 year ARI flooding scenario and occur along the Busselton Bypass. The presence of any culverts or other structures to prevent the build-up of these flood waters on the south side of the bypass were not included in the model setup. If they exist, they are likely to alter the resultant inundation.

3.2.2. 0.4 m SLR scenarios

3.2.2.1. B2 - Worst-case TC Alby + 0.4 m SLR

The B2 scenario inundation depth is shown in [Figure 39](#).

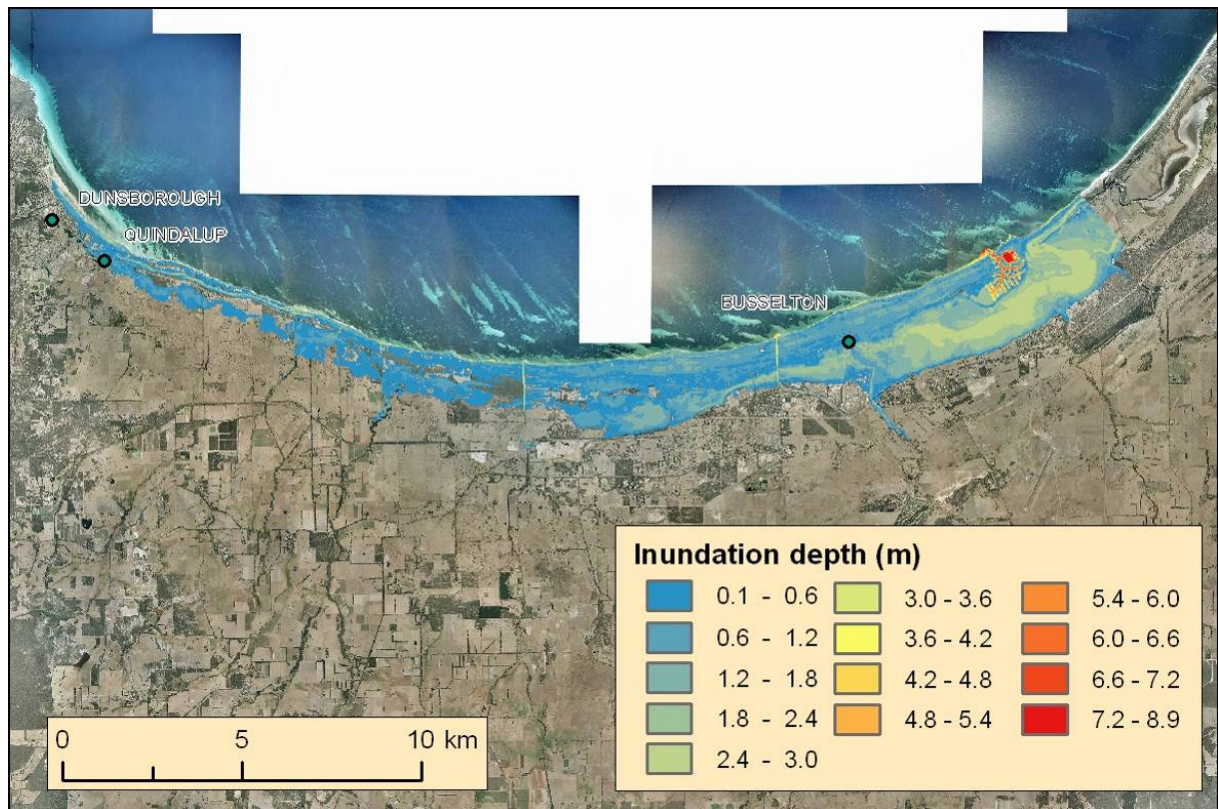


Figure 39. B2 inundation depth (TC Alby - Worst case + 0.4 m SLR).

The SLR in this scenario has increased the general extent of the inundation and has increased the effects of the early levee breakouts in Dunsborough; however it is still distinguishable from the overland storm-tide inundation.

[Figure 40](#) shows the inundation extents of both B1 and B2 in order to highlight the increased inundation extent caused by the SLR. [Figure 41](#) presents a difference raster between B2 and B1 highlighting the increased inundation depth caused by the 0.4 m SLR in the simulations. Note that [Figure 41](#) contains a different depth scale to the other difference rasters to highlight the changes.

In terms of inundation extents, it can be seen from [Figure 40](#) that the greatest change with the inclusion of 0.4 m SLR is west of the Vasse Diversion Drain ([Figure 8](#)). As well as the increase in watercourse breakout extents, compared to [Figure 30](#), there is an increase in the inundation through Toby Inlet and also the area between the Broadwater ([Figure 19](#)) and the coast. The scenario now shows the overland storm-tide inundation is reaching the Broadwater with a 0.4 m SLR.

[Figure 41](#) shows the full modelling domain and presents a broad view of how the 0.4 m SLR affects the inundation depths modelled in addition to the worst case scenario. West of the Broadwater the increase is generally less than 1 m.

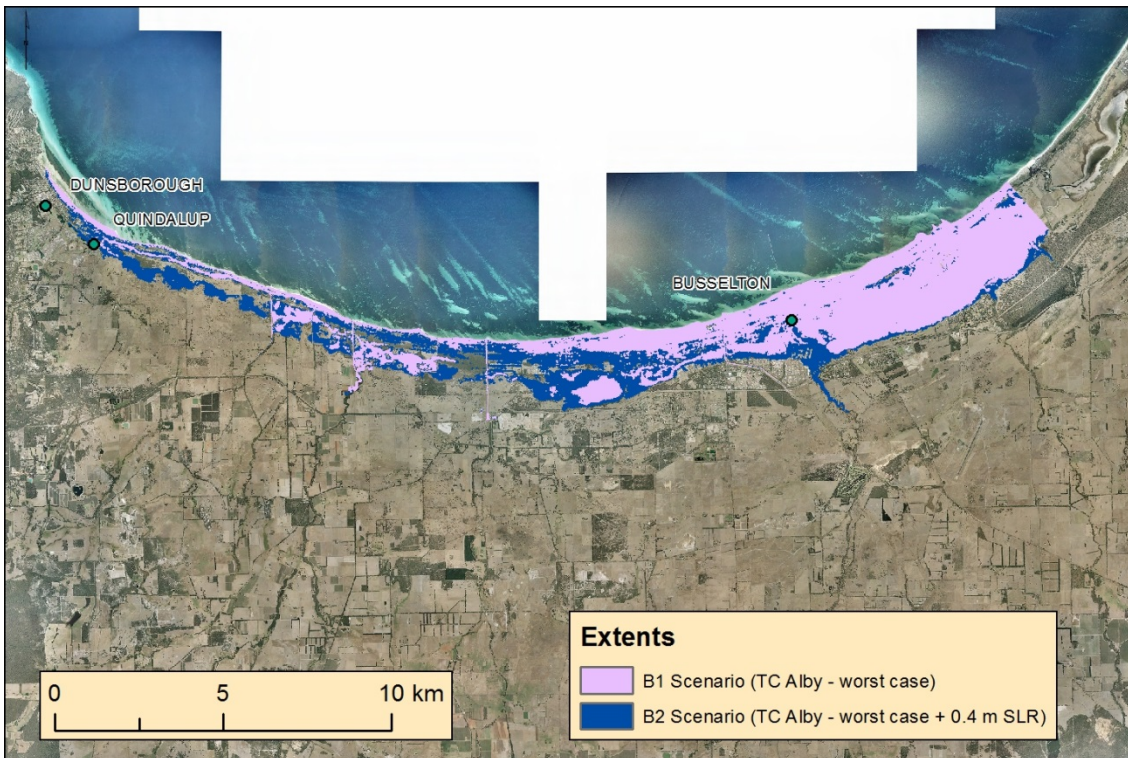


Figure 40. B1 and B2 inundation extents.

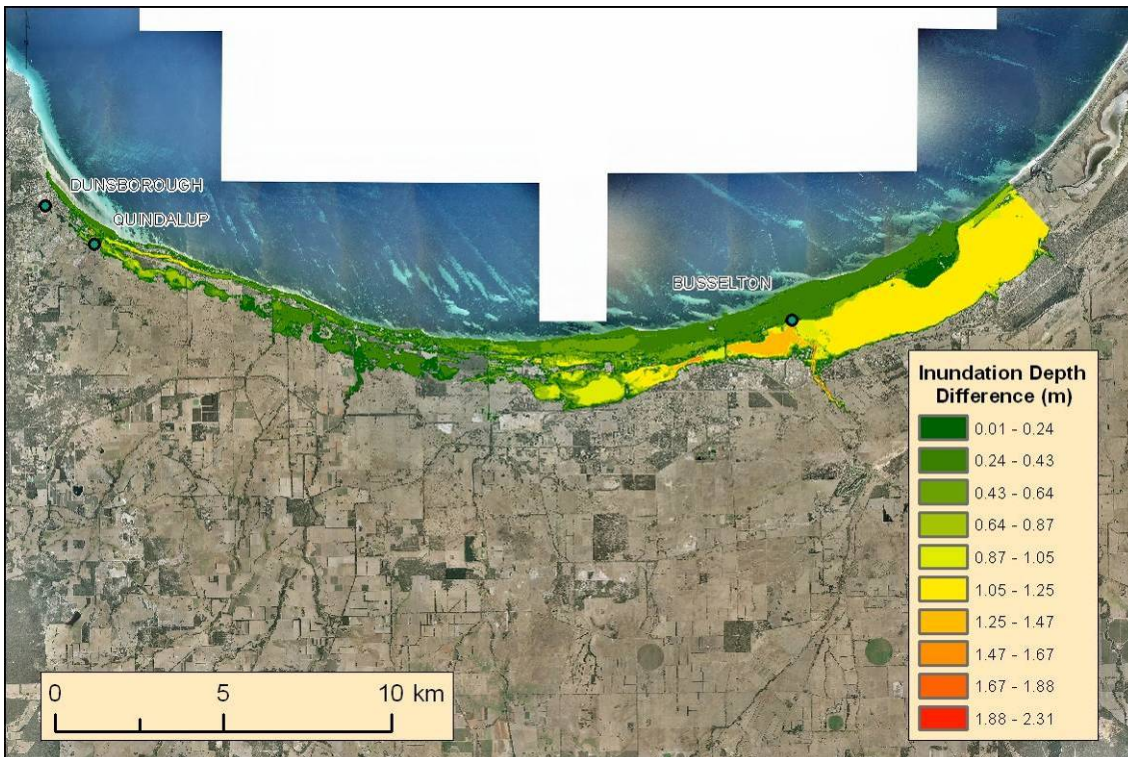


Figure 41. Difference in the inundation depth; B2 - B1.

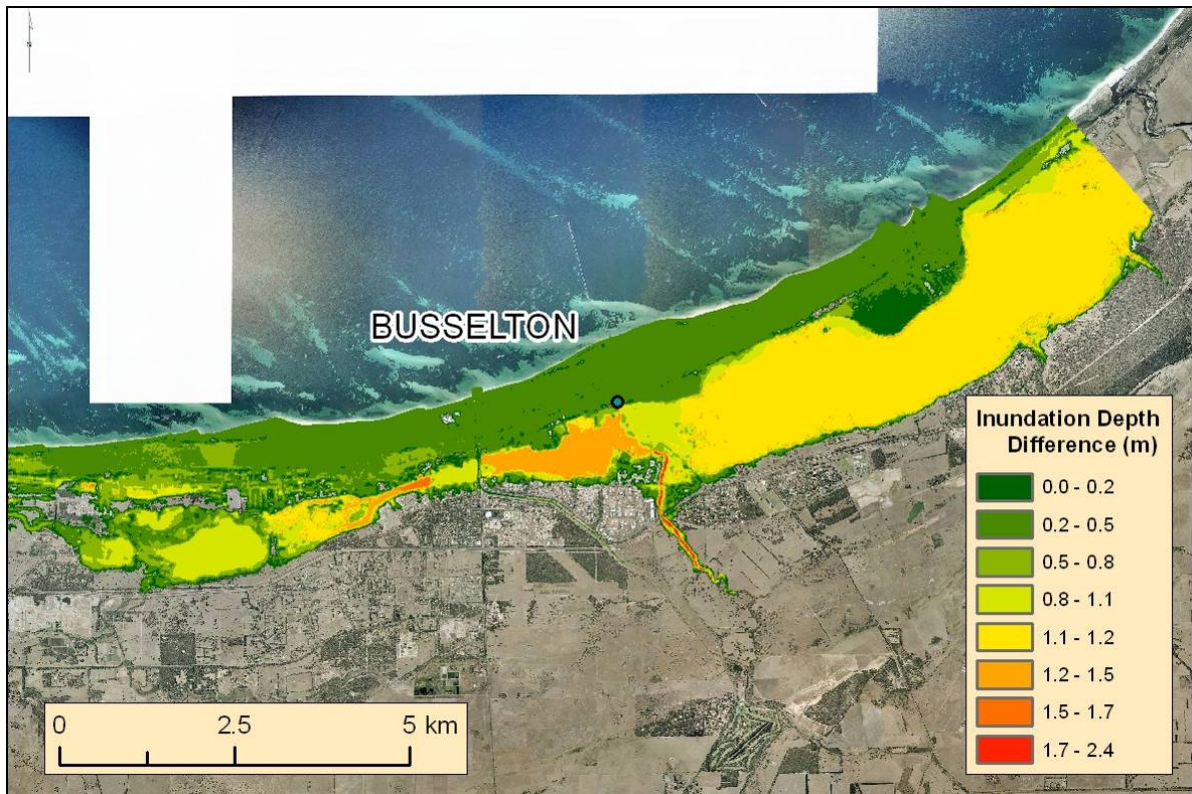


Figure 42. Difference in the inundation depth; B2 - B1 (revised symbol range).

The largest new area of inundation east of the Vasse Diversion Drain can be seen around the Vasse River – New River Estuary junction (Figure 42). In the absence of any detention basins in this area it would be the most susceptible to SLR related inundation during a storm of TC Alby’s magnitude. Figure 42 shows that the greatest increase due to the SLR occurs within the New River, Vasse Estuary and the Broadwater. The maximum inundation depth experienced in the Vasse Estuary during the scenario has increased by up to 1.2 m higher than indicated with no SLR: up to 1.5 m in the New River Estuary and up to 1.7 m in the Broadwater.

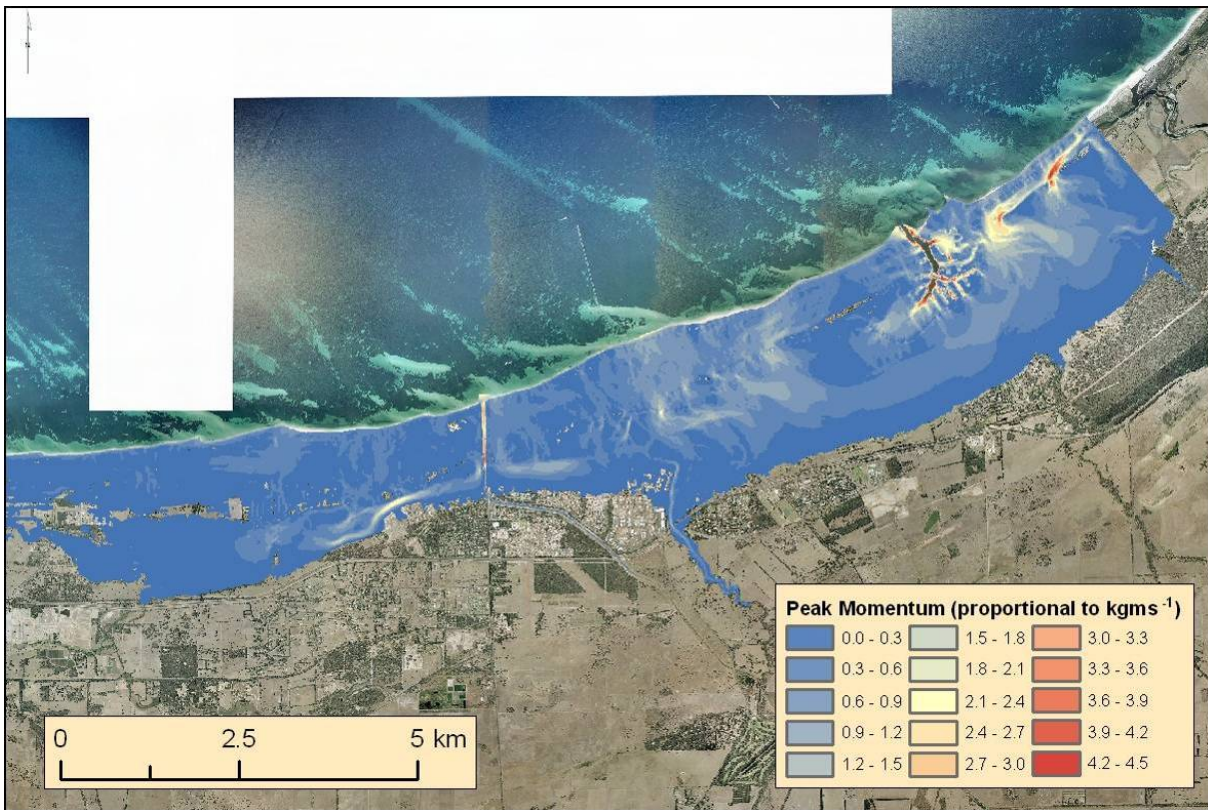


Figure 43. B2 peak momentum.

Figure 43 shows that the majority of the water causing the increased inundation originated from overland flow directly related to the storm tide and with no significant momentum flows adding water from the Vasse Estuary, which seems to be containing most of the water flowing into it from the east.

3.2.2.2. B8 - Worst-case TC Alby + 0.4 m SLR + 100 year ARI flood

The maximum inundation depth for the B8 scenario in Busselton is shown in [Figure 44](#). The Dunsborough area, as not modelled for flood, is identical to that of the B2 scenario and therefore not shown or discussed here. However, the Dunsborough inundation is shown in the B8 map series (see Map series section on [p31](#)).

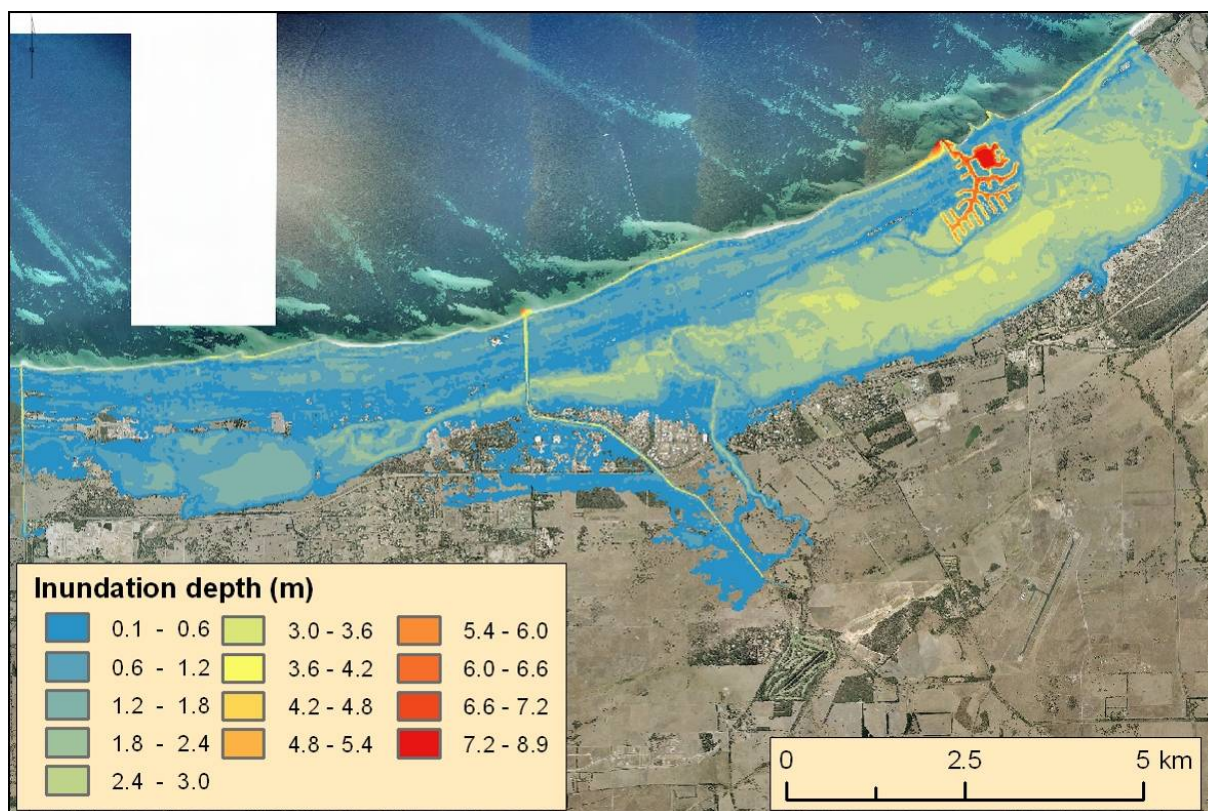


Figure 44. B8 inundation depth (TC Alby - Worst case + 0.4 m SLR + 100 year ARI flood).

Any differences resulting in the coincident 100 year ARI event are not immediately apparent from [Figure 44](#). In order to highlight the changes, as before, visualisations of the differences in extent between scenarios B8 and B2 are shown in [Figure 45](#).

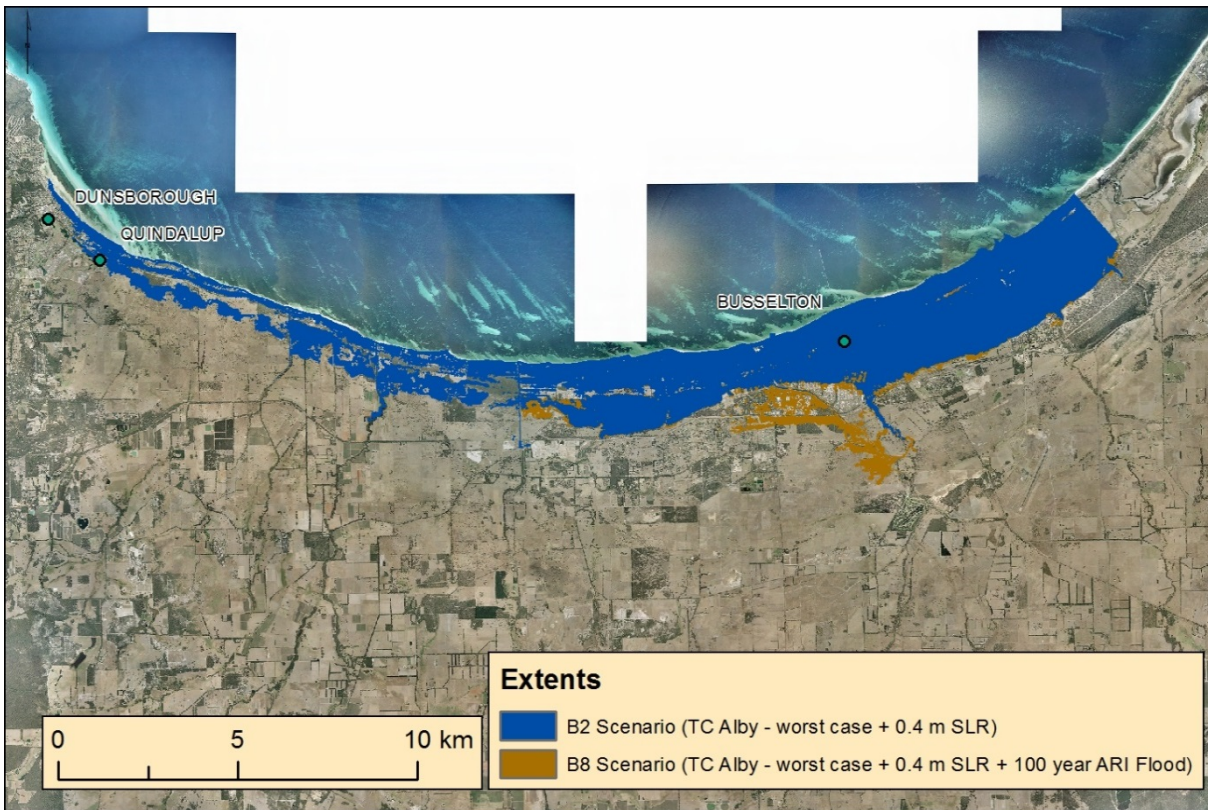


Figure 45. B8 and B2 inundation extents.

As in [Figure 33](#) and [Figure 36](#), the effects of adding riverine flooding to the storm tide is most clearly seen in the spillout of the Vasse Diversion Drain recorded in the modelling and its subsequent flow down to the Busselton Bypass ([Figure 45](#)). With the inclusion of 0.4 m SLR the riverine flood waters do not increase the extent of the inundation around the Broadwater suggesting that the dominant factor is the storm tide. This can also be seen in the Vasse River with storm-tide pushing much further up river than compared to B1 where no SLR was included ([Figure 33](#)).



Figure 46. Difference in the inundation depth; B8 - B2.

Figure 46 demonstrates that the addition of the 100 year ARI flood to the 0.4 m SLR scenario increases the inundation depth in the Vasse and New River estuaries by up to 0.4 m. This inundation depth is less to the east of the Vasse Diversion Drain, up to 0.3 m, which is consistent with water flowing into the Broadwater and settling in the western most part where the increase in depth is again up to 0.4 m.

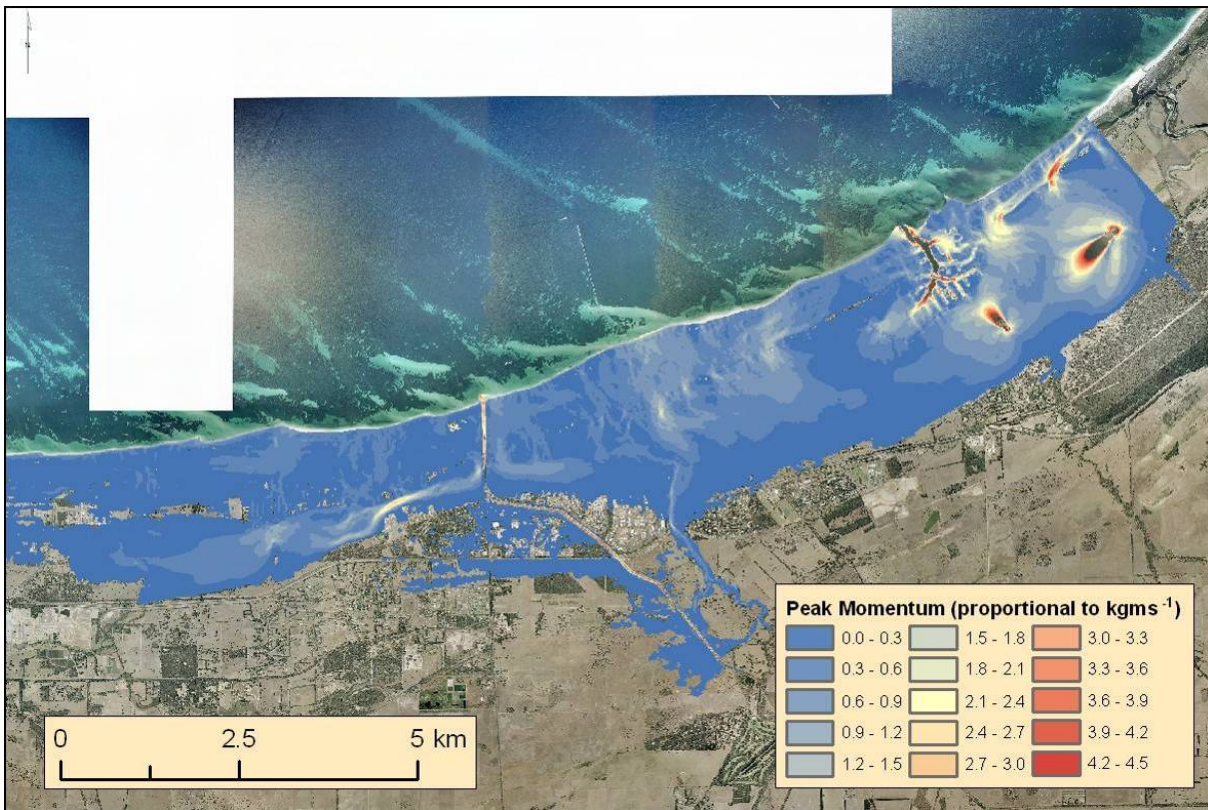


Figure 47. B8 peak momentum.

Figure 47 presents the maximum momentum within the B8 scenario and this does not vary significantly from that of the B2 (Figure 43). This suggests that the Worst-case TC Alby combined with 0.4 m SLR is overwhelmingly the cause of the overland inundation extent whereas the riverine flooding adds only to inundation depths within the estuaries and areas related to spill out of the Vasse Diversion Drain. The input hydrographs can be clearly seen feeding the 100 year ARI flood into the Vasse Estuary (Abba and Sabina Rivers).

3.2.3. 0.9 m SLR scenarios

3.2.3.1. B3 - Worst-case TC Alby + 0.9 m SLR

Figure 48 presents the peak inundation depth for the B3 scenario.

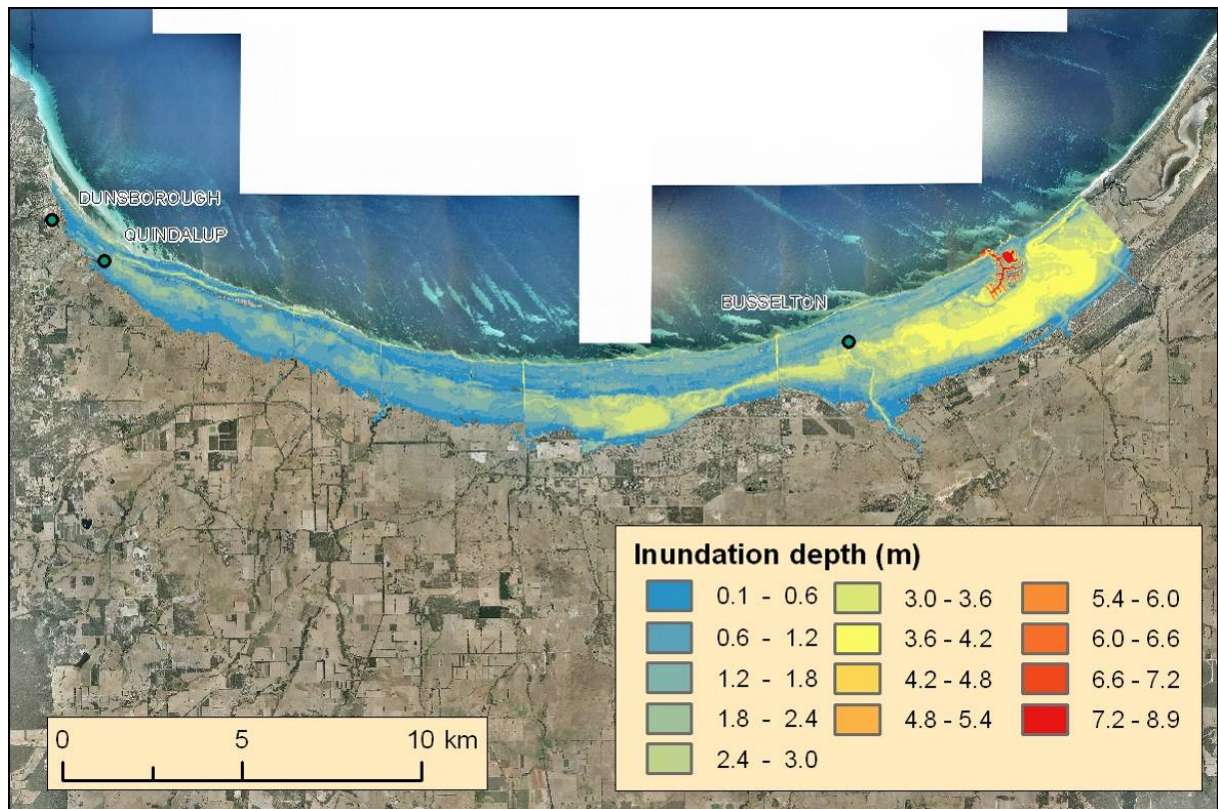


Figure 48. B3 inundation depth (TC Alby - Worst case + 0.9 m SLR).

Figure 49 shows that the inundation extent is increased significantly with the addition of 0.9 m SLR in areas west of Busselton. Figure 50 shows that in simulating the Worst-case TC Alby storm with 0.9 m SLR the majority of the extra inundation depth created around Busselton is in the watercourses and estuaries. The Vasse and New River Estuaries experience increased depths of 2.5 – 2.8 m. The coastal area in front of the Vasse Estuary experiences increased depths of up to 1 m. West of Busselton, although the inundation extent has expanded, the effects of the SLR were not as severe. The majority of extra inundation is below 1.5 m and the largest increases, over 2.4 m, were confined to Toby Inlet.

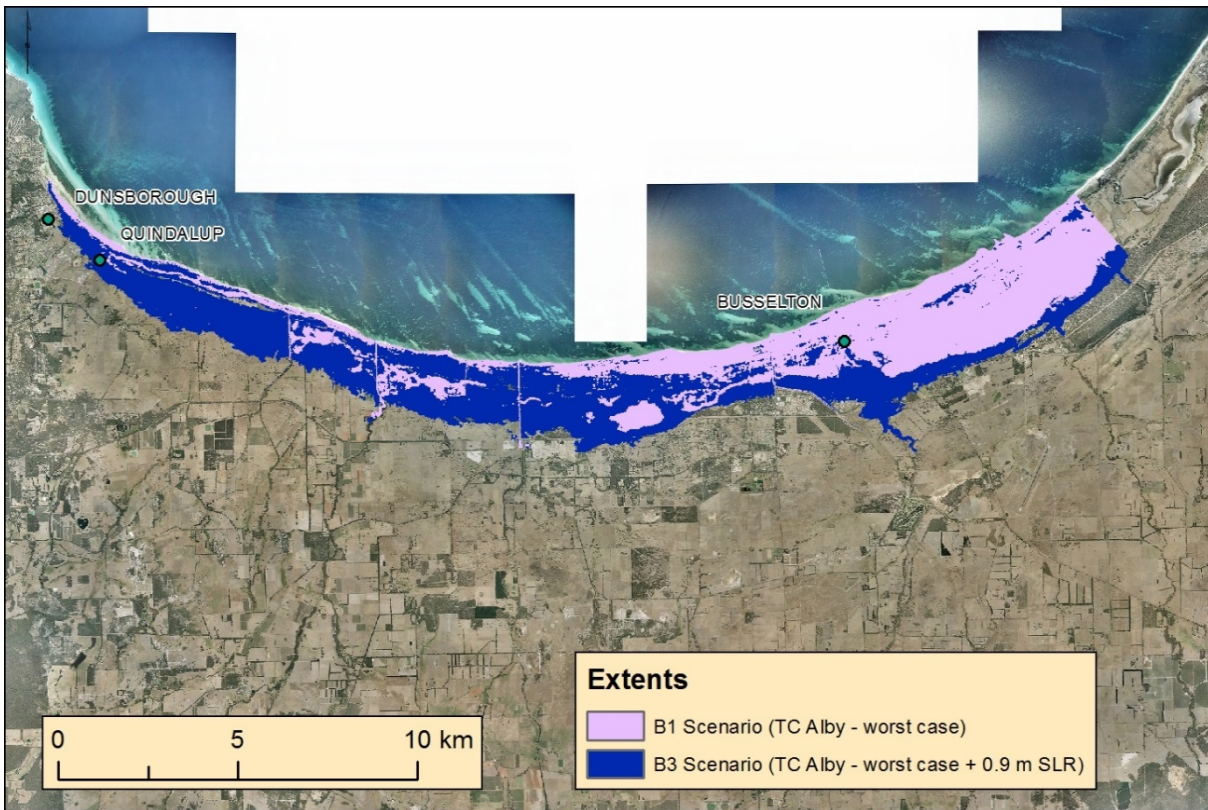


Figure 49. B1 and B3 inundation extents.

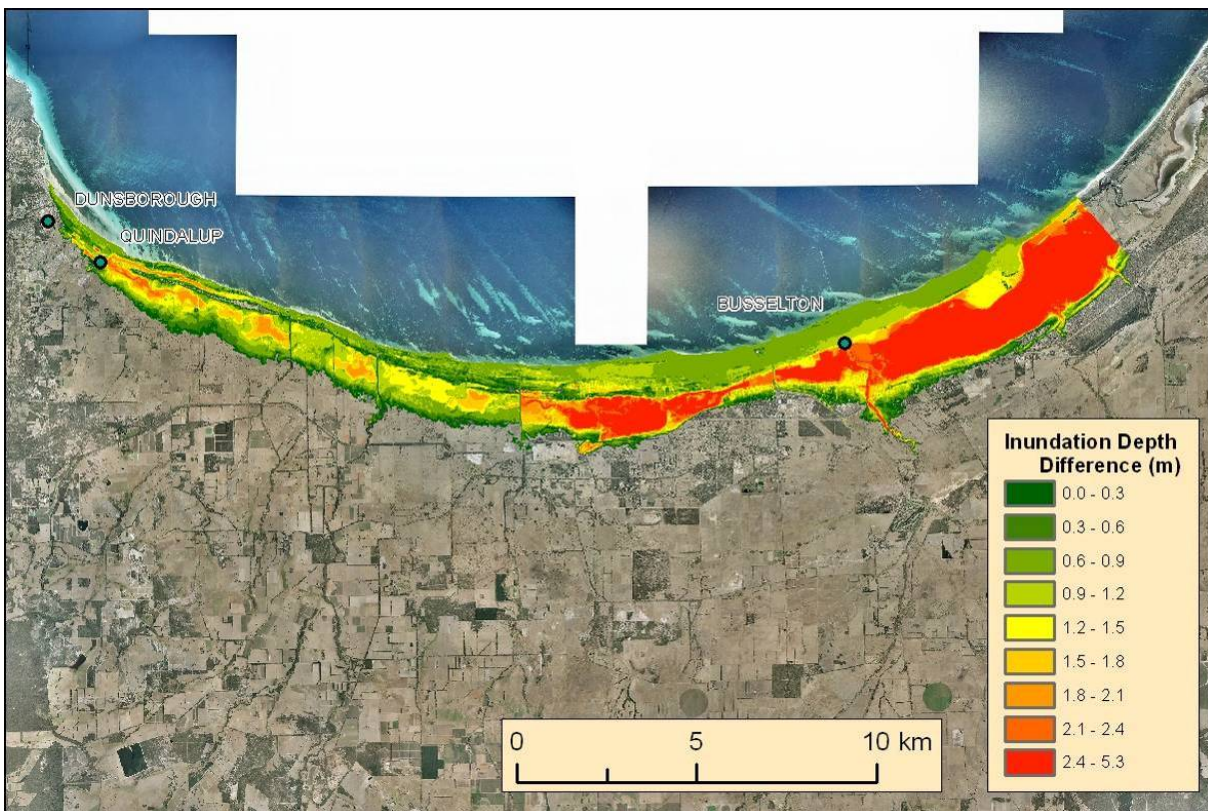


Figure 50. Difference in the inundation depth; B1 - B3.

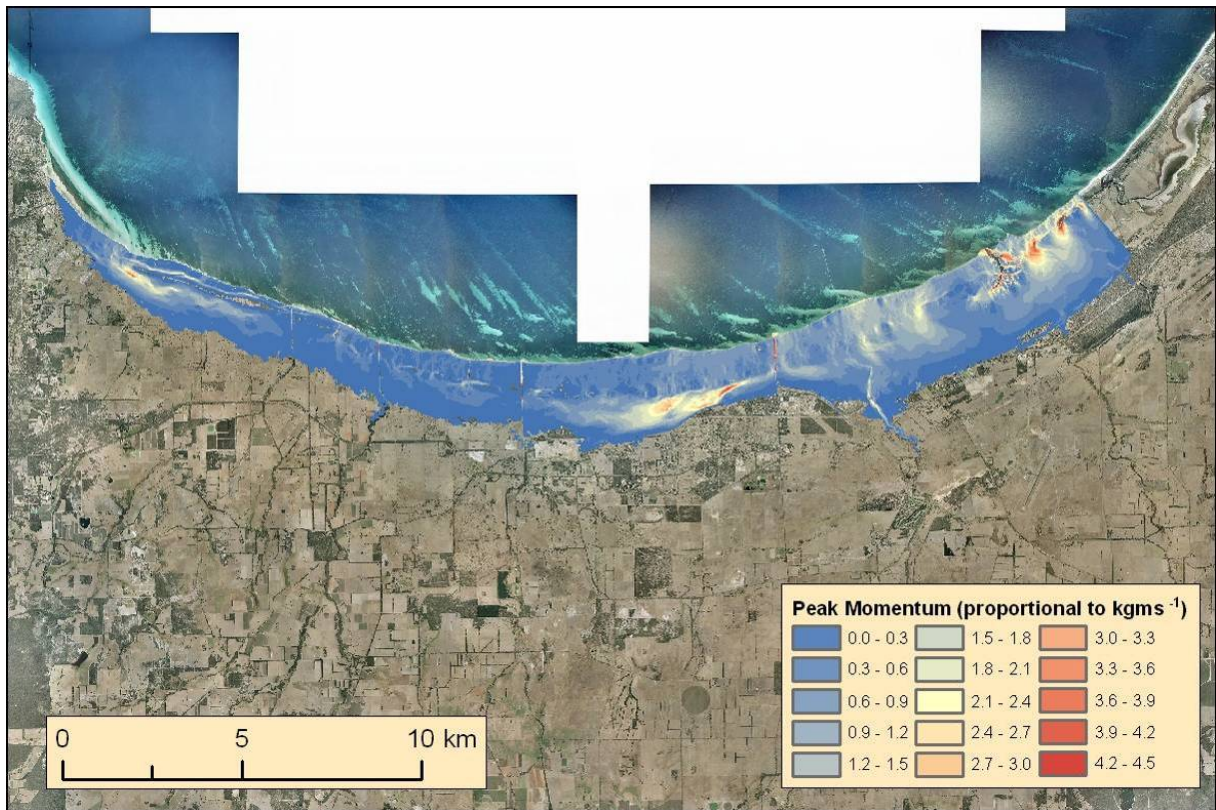


Figure 51. B3 peak momentum.

The momentum structure of this scenario (Figure 51) is similar to previous lesser SLR scenarios. This indicates that regardless of the severity of the inundation caused by storm tide the area responds in a similar way. The storm-tide inundation in the Busselton area is seen to flow overland both west and east of the Busselton Jetty to the New River and Vasse Estuaries respectively where it pushes mainly up the Vasse River. It is worth noting that these scenarios still show a separation between the storm-tide inundation from east of the Marina and that previously mentioned overland flow into the Vasse Estuary. A notable increase in east-west flow into the Broadwater is also present.

3.2.3.2. B7 - Worst-case TC Alby + 0.9 m SLR + 25 year ARI flood

Figure 52 presents the maximum inundation recorded when a 25 year ARI flood was simulated coincidentally with scenario B3, figure centred on Busselton.

The inundation extent differences are illustrated between B7 and B3 in Figure 53. The addition of a 25 year ARI flood to the 0.9 m SLR scenario is seen in Figure 53 to have the largest effect on the inundation extents around the Vasse Diversion Drain and a minor effect to extend the estuary inundation further inland.

The addition of the 25 year ARI flood does not significantly affect the momentum seen in Figure 51. With the 0.9 m SLR the storm-tide pushes further up the Vasse River, and interacts with the Vasse Diversion Drains eastern spill out. The only area remaining solely affected by riverine flooding is due to the drains westerly spill out as previously mentioned (Figure 33).

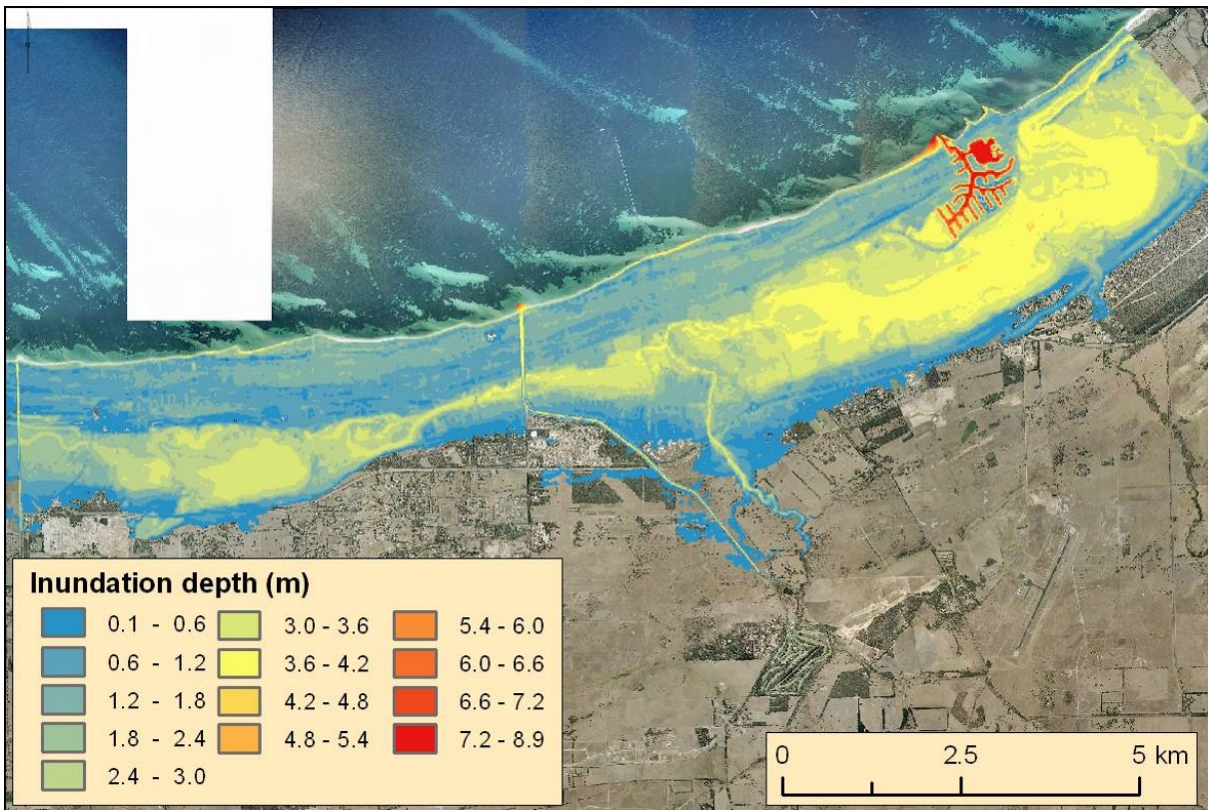


Figure 52. B7 inundation depth (TC Alby - Worst case + 0.9 m SLR + 25 year ARI Flood).

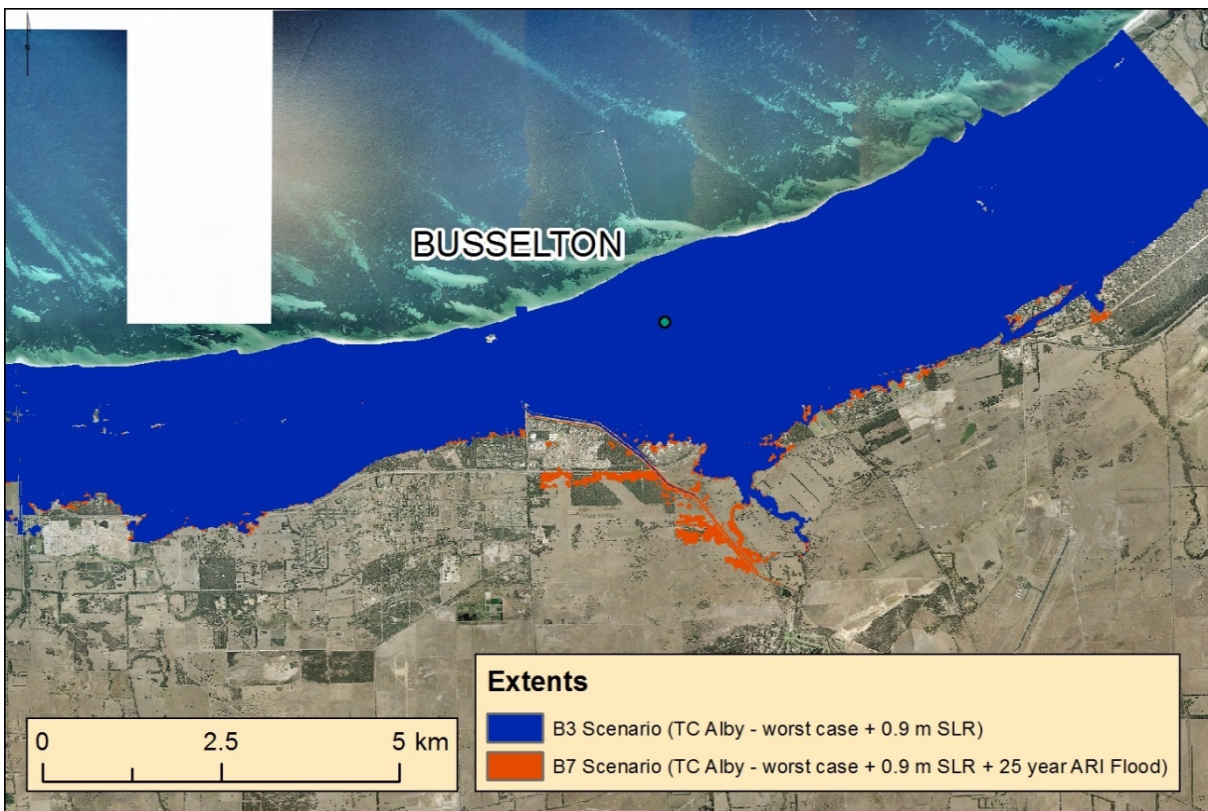


Figure 53. B3 and B7 inundation extents.

3.2.3.3. B9 - Worst-case TC Alby + 0.9 m SLR + 100 year ARI flood

The maximum inundation depth results for scenario B9 are shown, [Figure 54](#). The difference in inundation extent caused by adding a 100 year ARI flood to the B3 scenario is shown in [Figure 55](#).

Features from riverine flooding scenarios already discussed are present in [Figure 55](#) and similarly it is clear that there is little effect on the extent of the inundation due to riverine flooding. The dominant factor is clearly the storm tide.

There is also little to comment on in terms of the effects the riverine flooding has on the maximum momentum recorded in the scenario ([Figure 56](#)). The scale for the maximum class in this figure has been increased to 6.4 to maintain a distance from the inlet flood operator where the values were not realistic (most clearly seen at the Abba and Sabina River hydrograph locations).

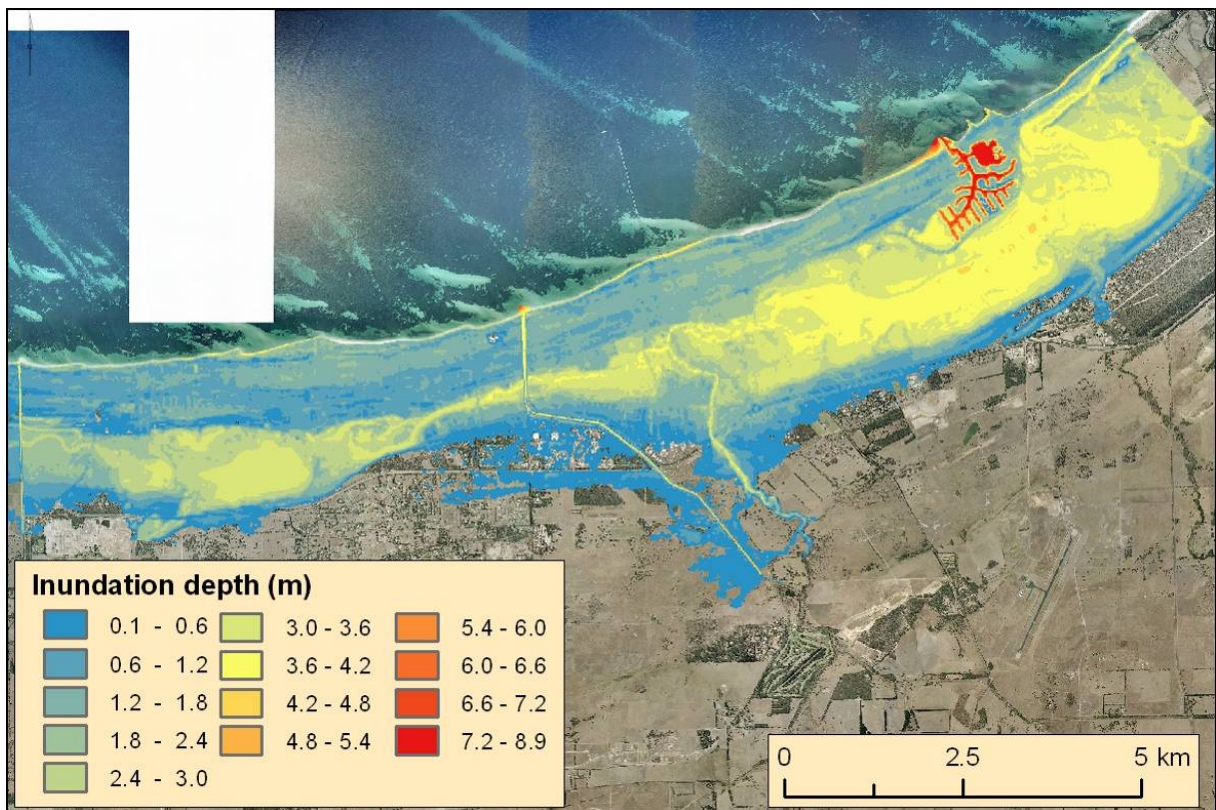


Figure 54. B9 inundation depth (TC Alby – worst case + 0.9 m SLR + 100 year ARI Flood).

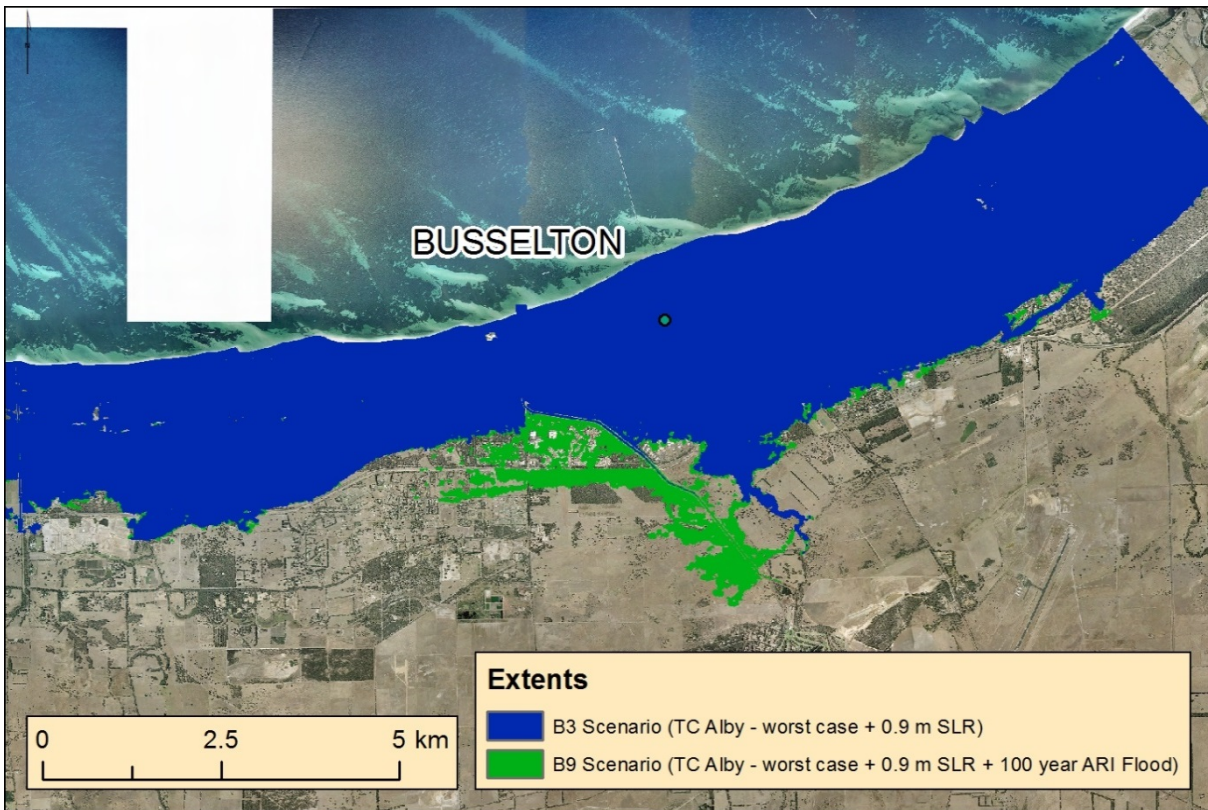


Figure 55. B3 and B9 inundation extents.

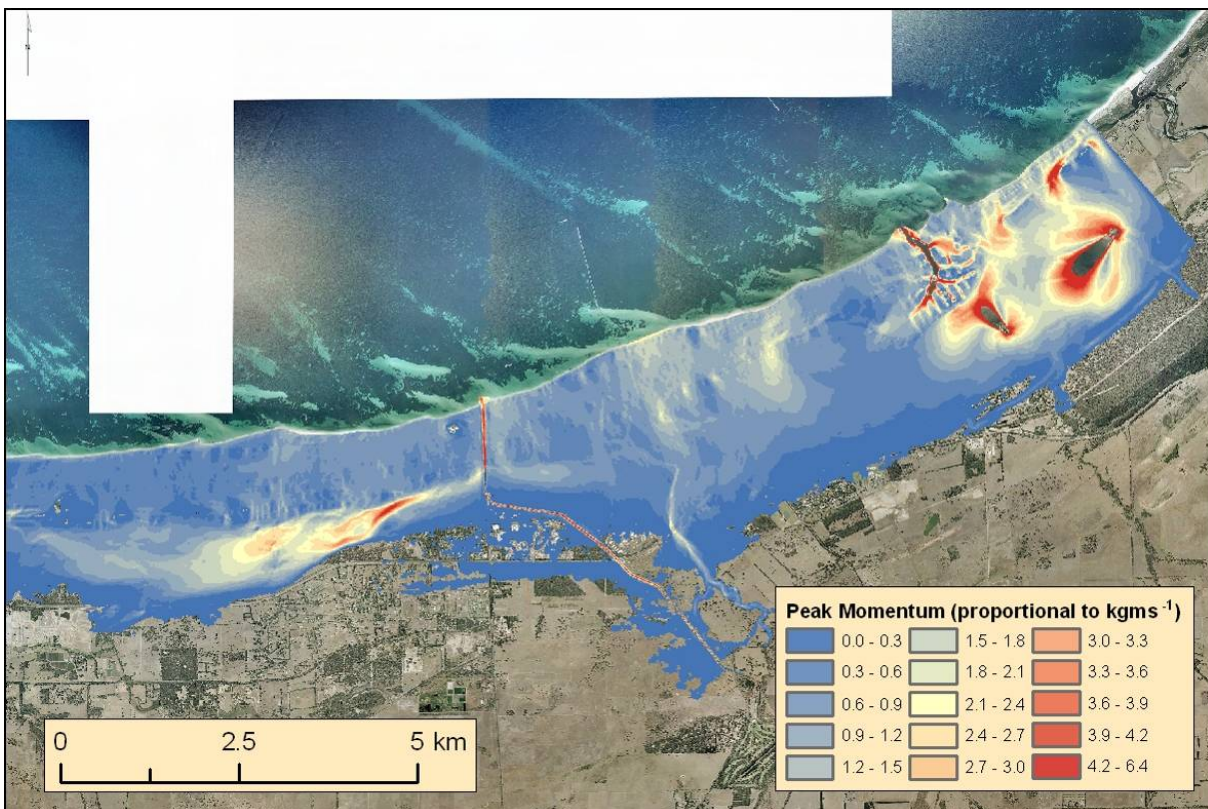


Figure 56. B9 peak momentum.

3.2.4. 1.1 m SLR scenarios

Most of the results for the 1.1 m SLR rise are logical extensions of the previous scenarios with inundation extents increasing further inland and coincident riverine flooding having similar effects.

3.2.4.1. B4 - Worst-case TC Alby + 1.1 m SLR

The overall view of the maximum inundation recorded over the full domain is shown in [Figure 57](#) and can be confirmed as generally an increase in extents from scenario B3 where a 0.9 m SLR was considered.

The inundation extent and difference raster are shown in [Figure 58](#) and [Figure 59](#).

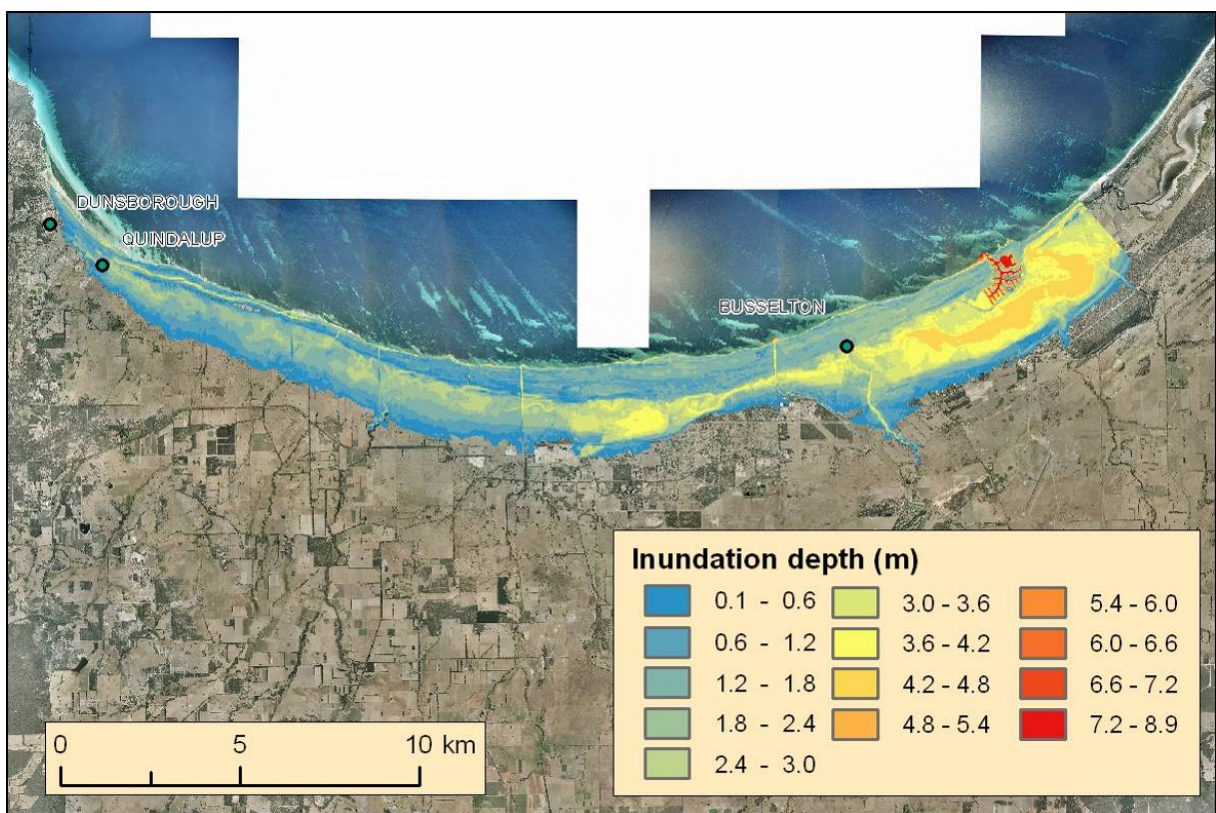


Figure 57. B4 inundation depth (TC Alby - worst case + 1.1 m SLR).

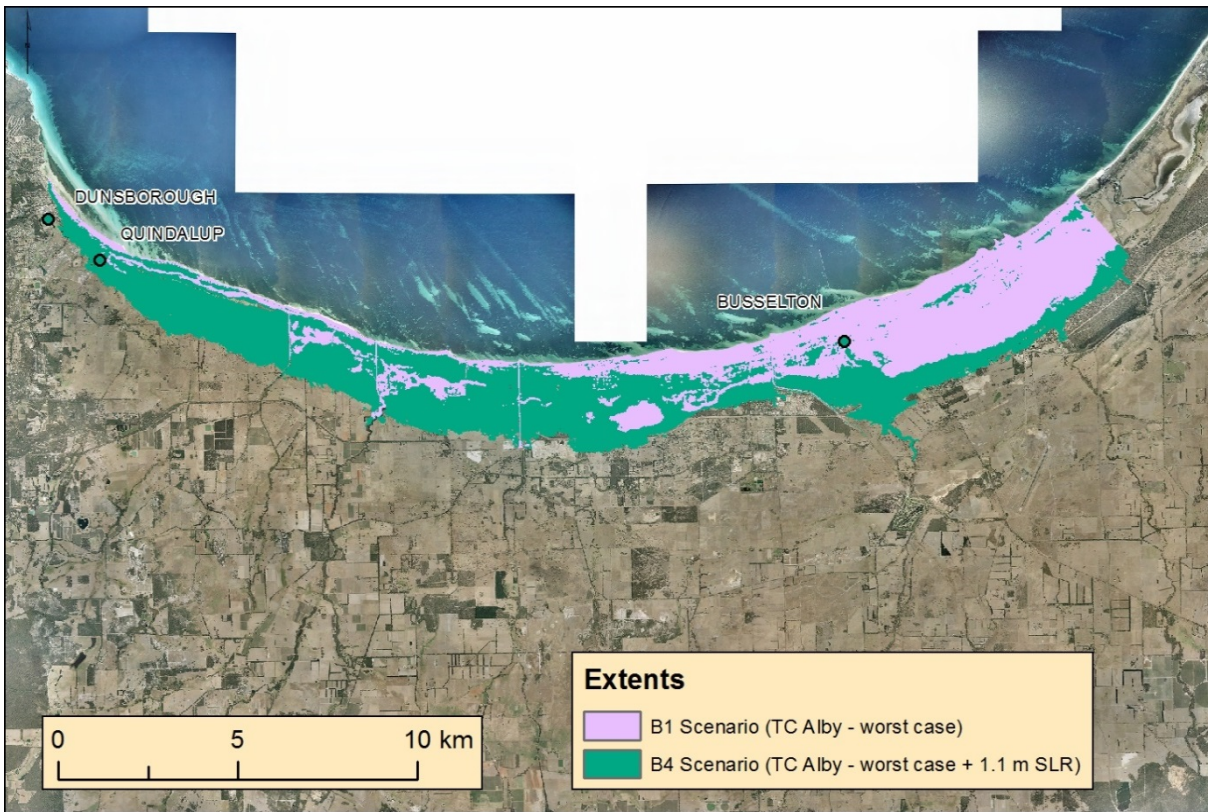


Figure 58. B4 and B1 inundation extents.

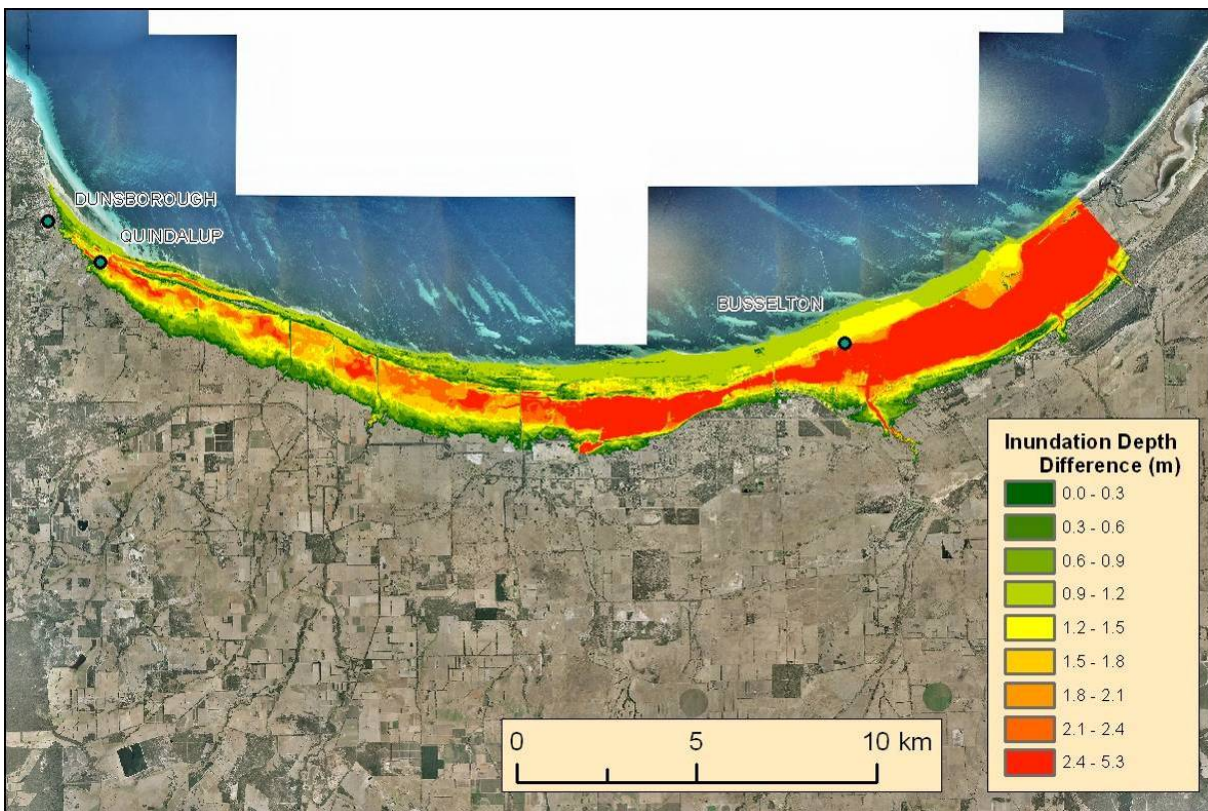


Figure 59. Difference in the inundation depth; B4 - B1.

It is clear, and not unexpected in light of [Figure 57](#), that the 1.1 m SLR has a dramatic effect on both the inundation extents ([Figure 58](#)) and the depth ([Figure 59](#)) as compared with the worst case scenario (B1). The Vasse Estuary experiences depths over 2.9 m and the New River and the Broadwater up to 3.4 m above that simulated for the B1 scenario. Some areas in the Broadwater were up to 4 m above the B1 inundation depths.

The majority of the extra inundation depth caused by the 1.1 m SLR west of the Buayanyup drain is less than 2.0 m, with patches up to 3.4 m in the Toby Inlet.

The maximum momentum rasters are shown in [Figure 60](#).

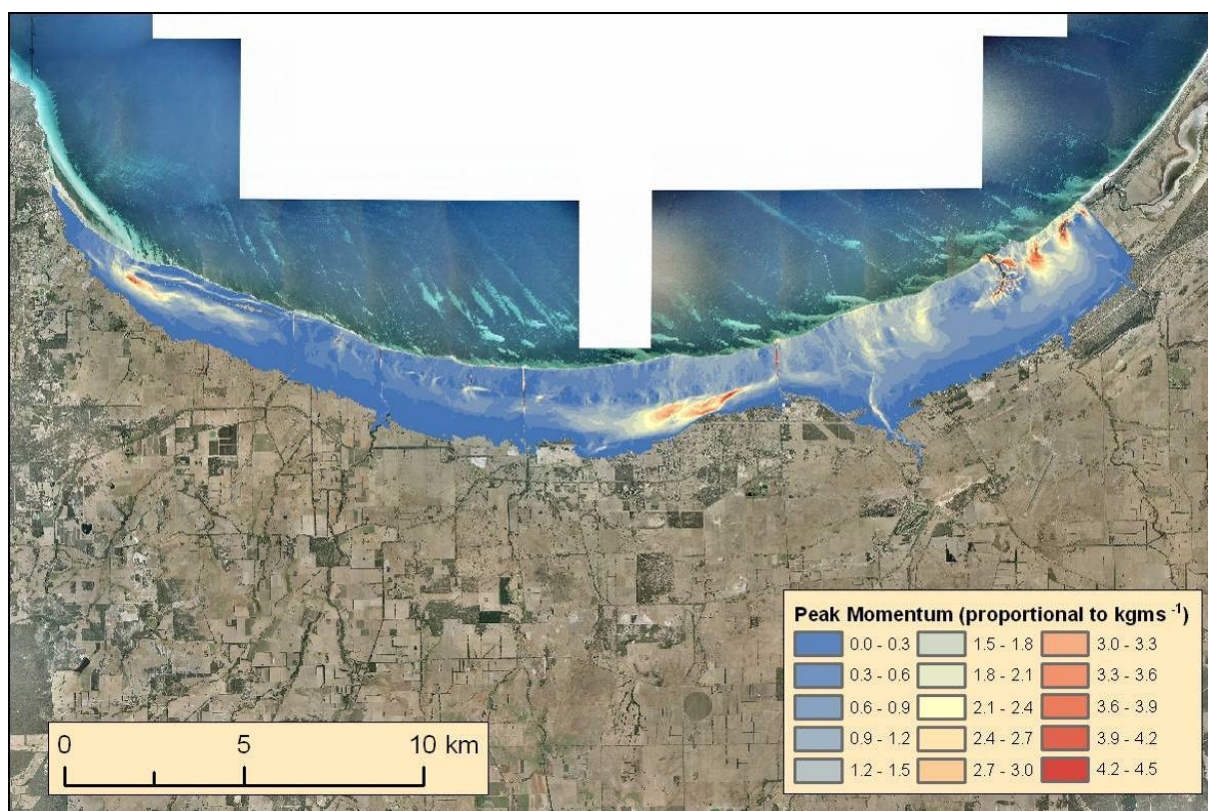


Figure 60. B4 peak momentum.

[Figure 60](#) tells a similar story to the analogous figures for B1, B2 and B3 with the rise in sea level producing only increases in momentum rather than changes in direction.

3.2.4.2. B10 - Worst-case TC Alby + 1.1 m SLR + 100 year ARI flood

As B10 includes riverine flooding, as for all previous scenarios including flooding, only the Busselton area results are commented on here as the area west of the Broadwater remains unchanged to that described in the previous section. The maximum inundation depths recorded during the scenarios are shown in [Figure 61](#).

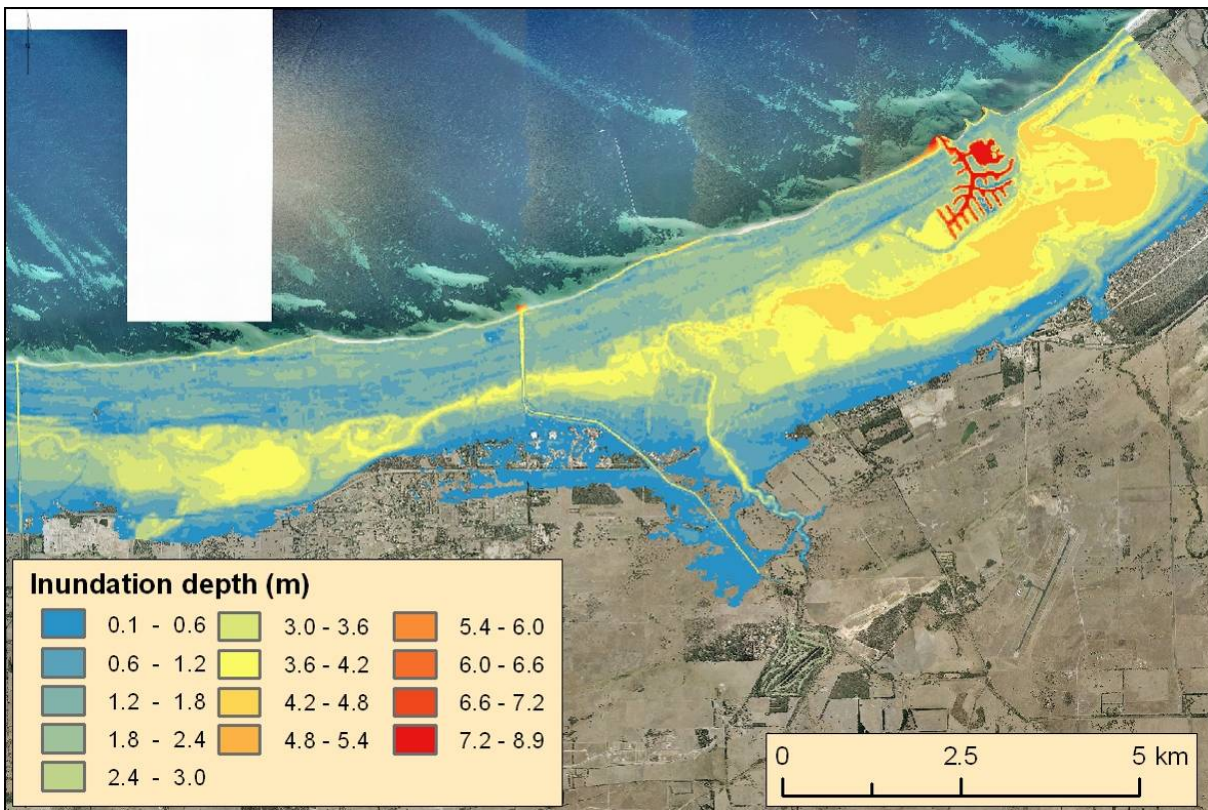


Figure 61. B10 inundation depth (TC Alby - worst case + 1.1 m SLR + 100 year ARI Flood).

When the 100 year ARI flood was combined with the 1.1 m SLR scenario, [Figure 62](#) shows the resulting changes to the inundation extents.

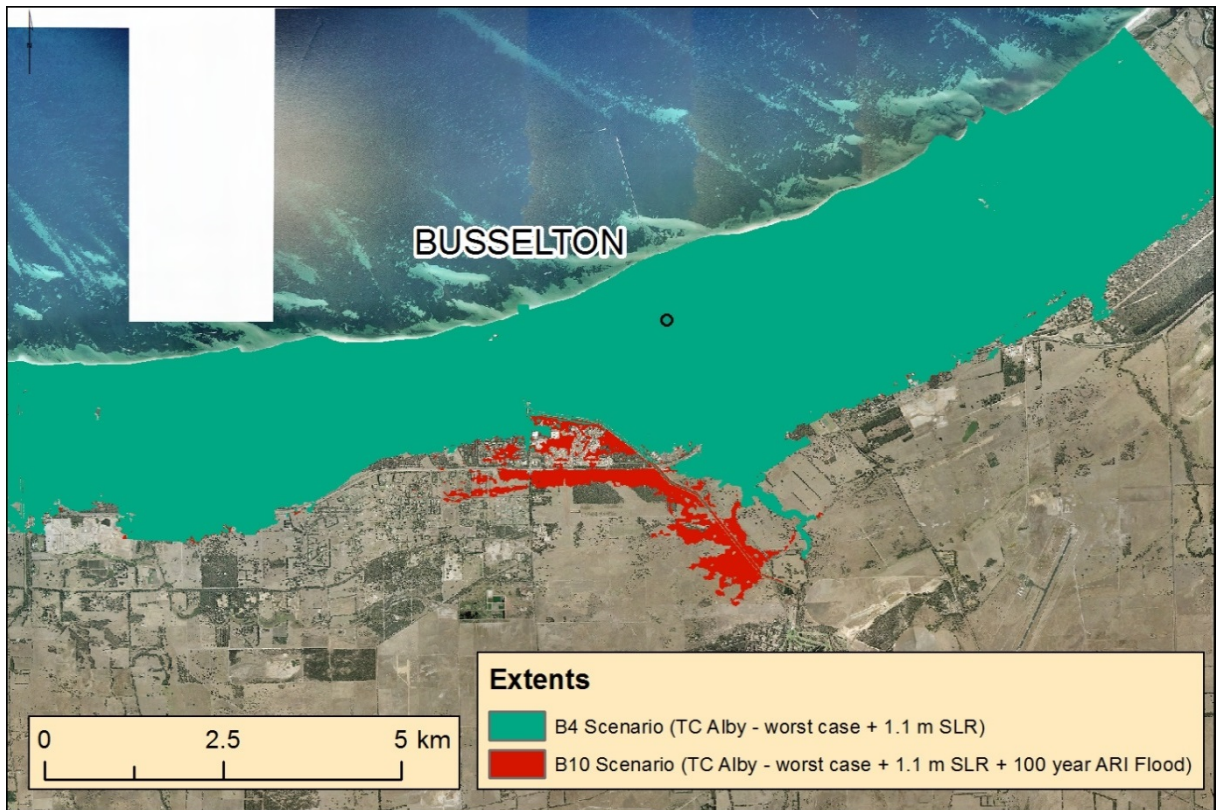


Figure 62. B10 and B4 inundation extents.

At the extremes represented in scenario B10 it seems that the coincident nature of the modelling setup, i.e. storm-tide meeting riverine inundation, is still only showing an impact to the extent of inundation around the Vasse Diversion Drain and associated spill out. A further investigation of the depth differences between the two scenarios is presented in [Figure 63](#) and suggests that the riverine flooding is beginning to affect areas outside of the Vasse Diversion Drain spill out and the Estuaries.

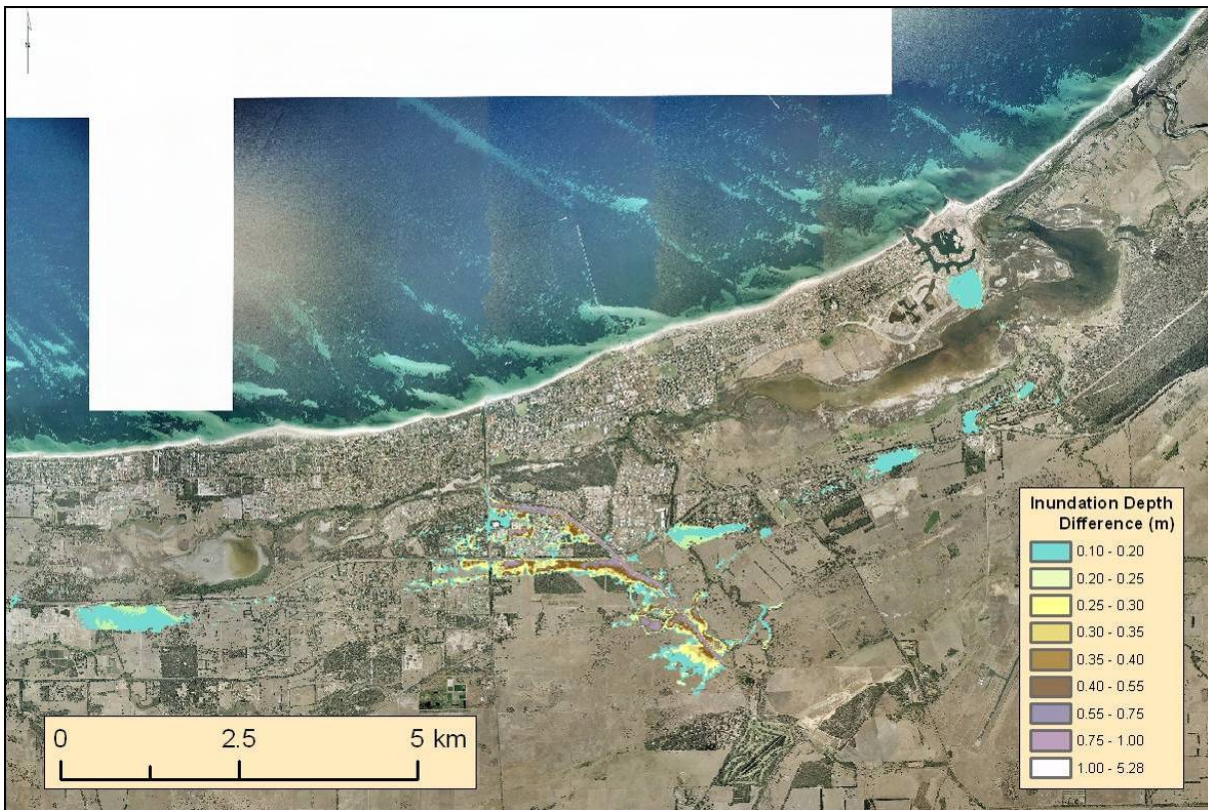


Figure 63. Difference in the inundation depth; B10 - B4 where greater than 0.1 m.

All areas in Figure 63, excluding those due to Vasse Diversion Drain spill out, show that the riverine flood waters have caused the inundation extent to increase. This suggests that the estuaries have reached capacity with the additional riverine flood waters responsible for increasing the extent of inundation beyond the B4 scenario extent.

This highlights the immense capacity that the Vasse Estuary, where initially set at 0.4 m AHD, has to retain water in these inundation scenarios. It also leads to the question of what the results of a scenario, or real event of similar magnitude, would be were the estuaries already full from a preceding inundation event.

3.3. Coastal erosion

The STM spatial outputs represent future coastlines with associated exceedance probabilities for a range of scenarios. These coastlines represent the probability that the beach will erode landward by, or greater than, the distances defined by the future coastline. These lines have been processed to create a series of zones of probability that are presented in [Figure 64](#), [Figure 65](#) and [Figure 66](#).

However, due to the mismatch in spatial and temporal scales at which the coastal erosion modelling was undertaken these spatial outputs could not be used within ANUGA to model the storm tide and riverine flood inundation over a receded shoreline/future elevation surface (DEM). This is discussed further within the Summary and discussion Coastal erosion modelling section ([p78](#)).

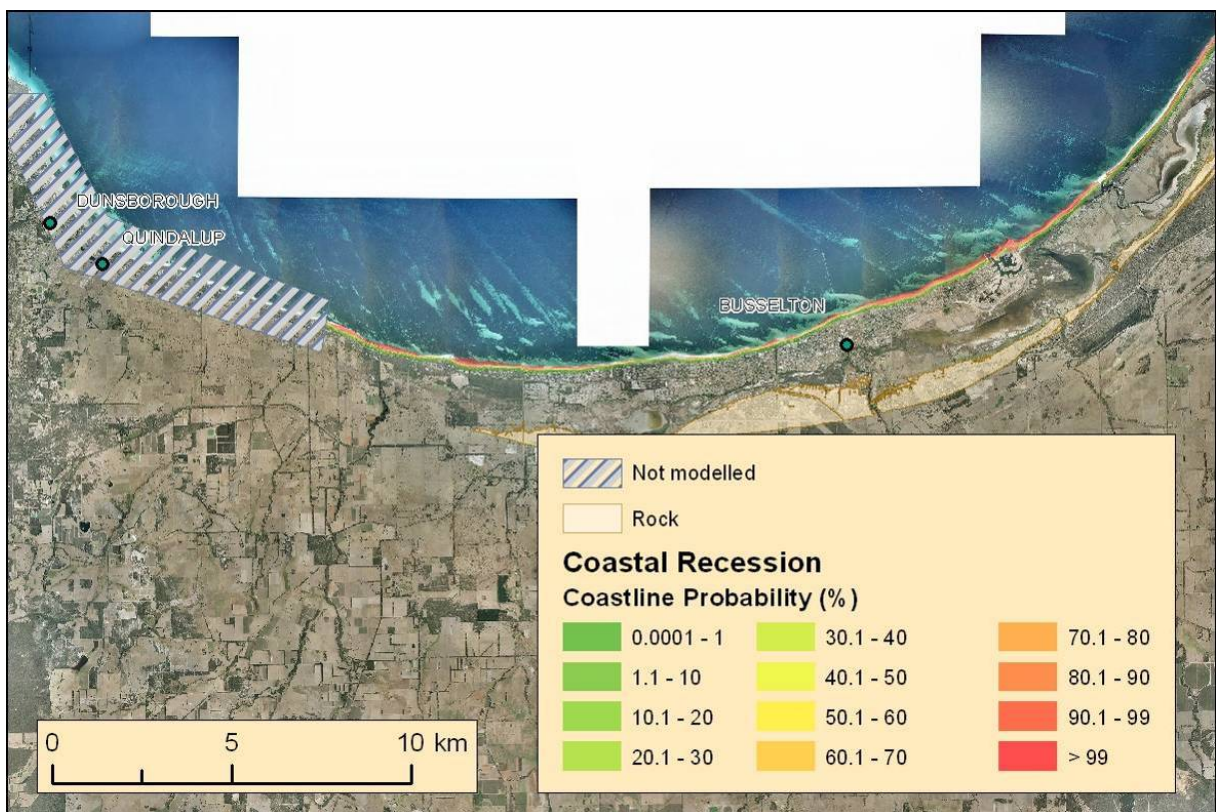


Figure 64. Spatial extent of coastal erosion forecast by the STM for 2030.

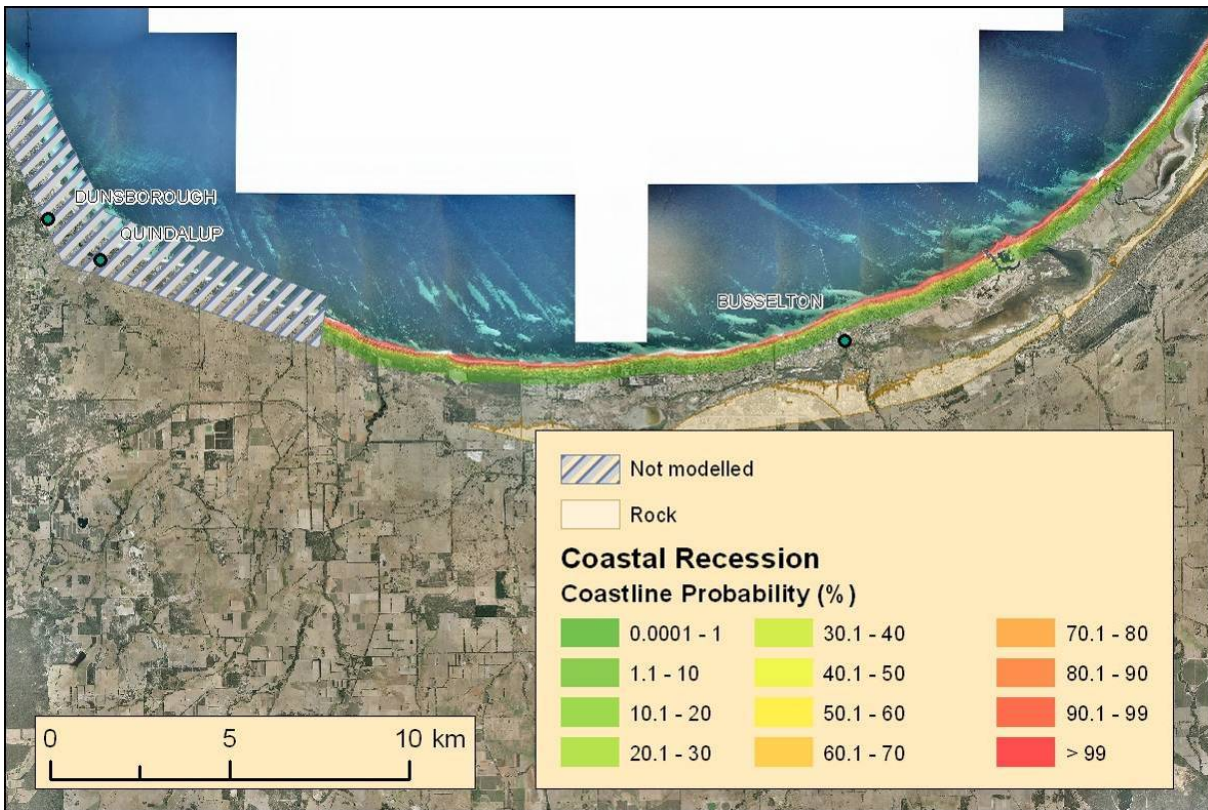


Figure 65. Spatial extent of coastal erosion forecast by the STM for 2070.

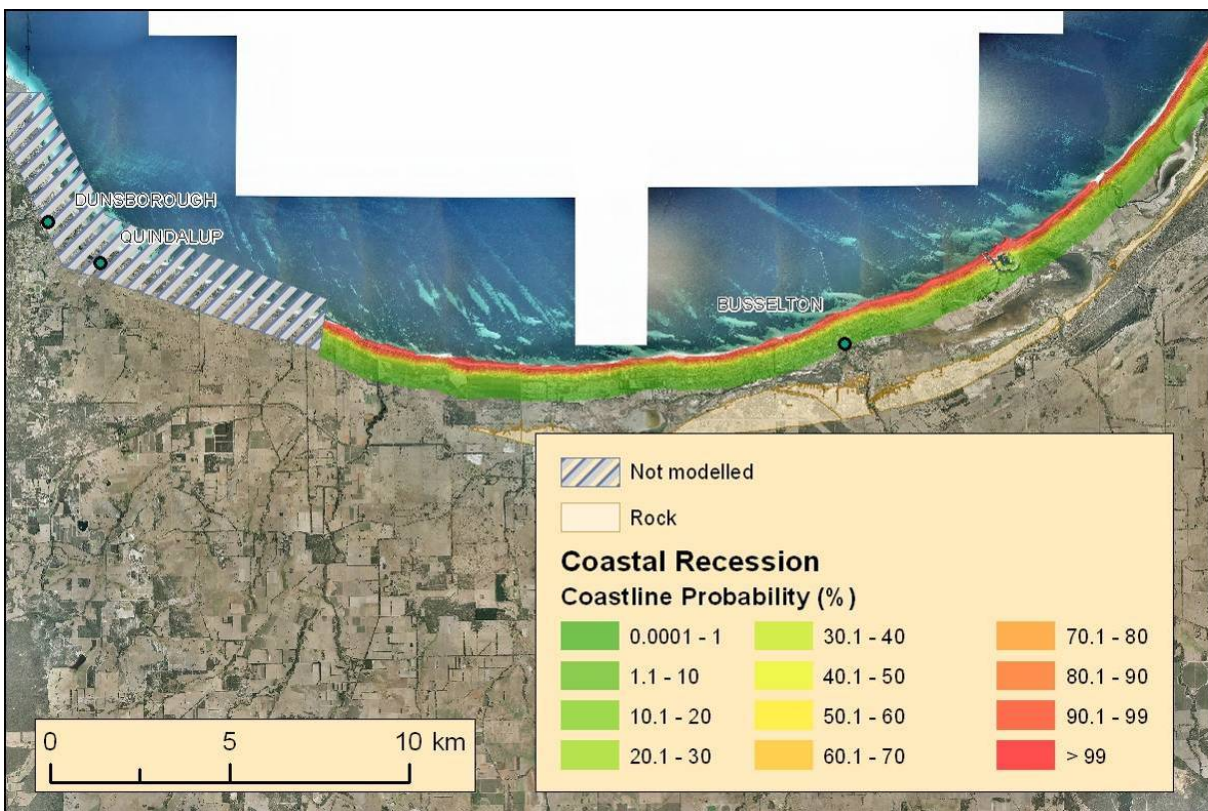


Figure 66. Spatial extent of coastal erosion forecast by the STM for 2100.

4. Summary and discussion

This section:

- summarises the results for the SLR and riverine flooding scenarios modelled by ANUGA
- discusses the implications from the modelling
- suggests areas for further development and enhanceent.

4.1. Results summary

All references in the following summary and discussion of the Vasse and New River Estuaries and the Broadwater refer to those water bodies as they are shown in [Figure 67](#).

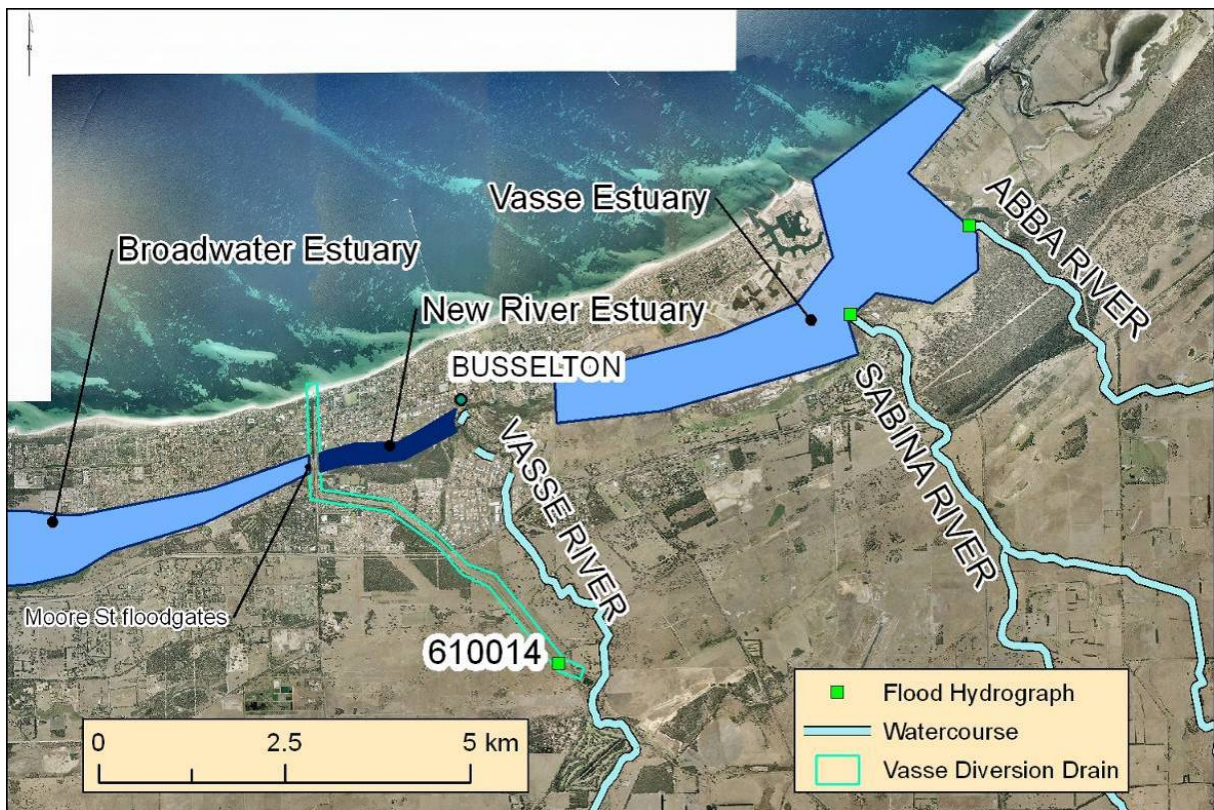


Figure 67. Busselton, including rivers, diversion drain, estuaries and the Moore St floodgate.

4.1.1. SLR scenarios

4.1.1.1. Scenario B2 – TC Alby worst case + 0.4 m SLR

The inundation extent is shown in Figure 68 for the 0.4 m SLR scenario. This SLR has increased the general extent of the inundation from the *worst-case TC Alby scenario*. In particular there has been an increase in inundation caused by levee breakouts west of the Buayanyup drain.

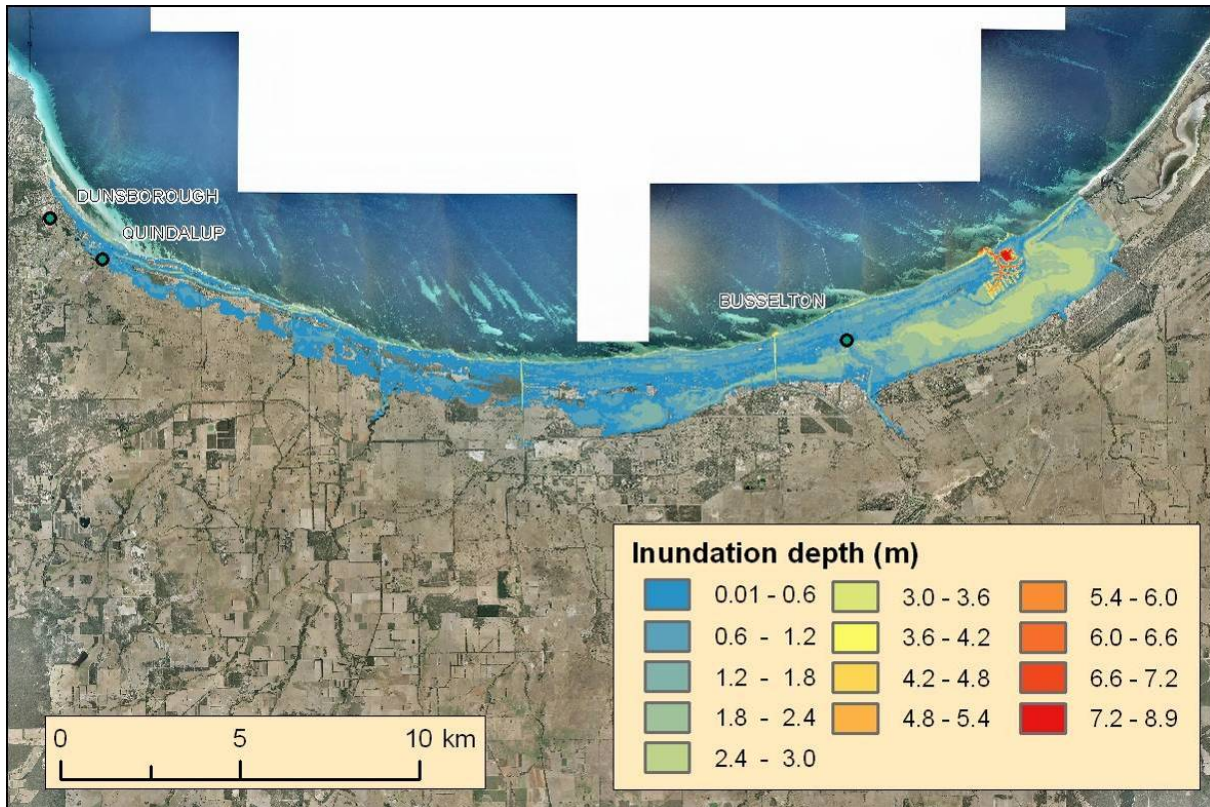


Figure 68. B2 inundation (TC Alby worst case + 0.4 m SLR).

4.1.1.2. Scenario B3 – TC Alby worst case + 0.9 m of SLR

As shown in Figure 69 the 0.9 m SLR has significantly increased the extent of the inundation west of the Buayanyup drain. Around Busselton and to the east, the majority of the extra inundation occurs along the Vasse River and southern boundaries of the Vasse and New River Estuaries. The areas of inundation due to levee breakouts in the west are now indistinguishable from the overland storm-tide inundation.

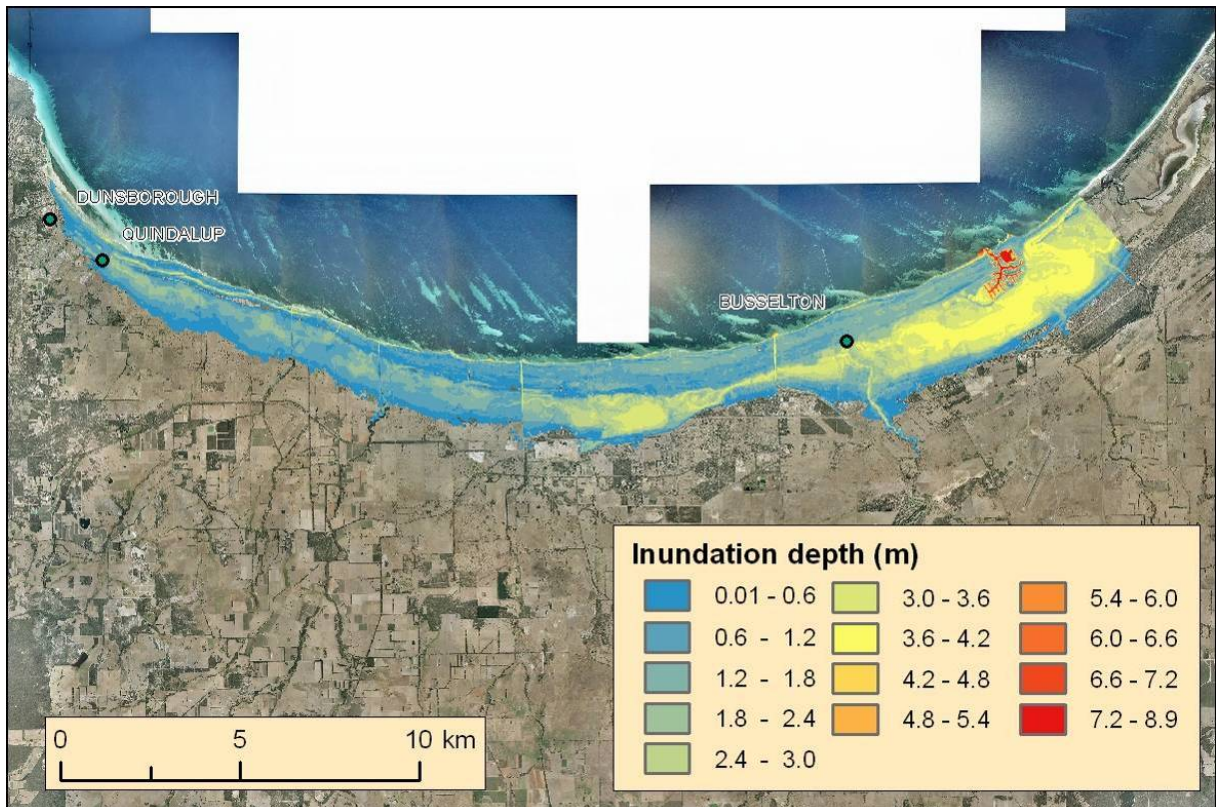


Figure 69. B3 inundation (TC Alby worst case + 0.9 m SLR).

4.1.1.3. Scenario B4 – TC Alby worst case + 1.1 m SLR

The majority of the additional inundation around Busselton for the 1.1 m SLR scenario (Figure 70) is located along the watercourses and southern boundaries of the Vasse and New River Estuaries.

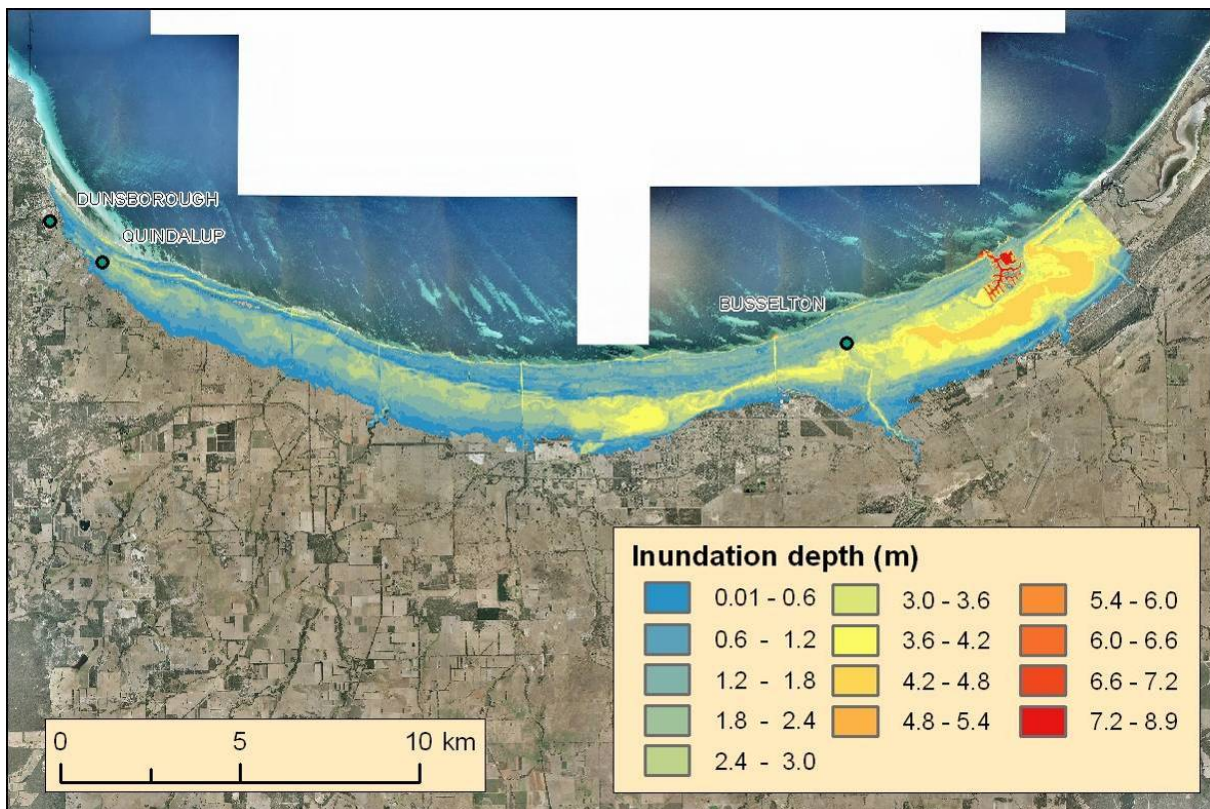


Figure 70. B4 inundation (TC Alby worst case + 1.1 m SLR).

A summary of the change in the inundation extents for each SLR scenario is presented in Figure 71. The prominent green areas west of Busselton indicate that the 0.9 m SLR scenario results in the most significant increase in inundation extent of all the SLR scenarios modelled. Around Busselton and the Vasse Estuary the effect of rising sea levels is a more predictable steady increase in inundation extents caused by a worst-case TC Alby.

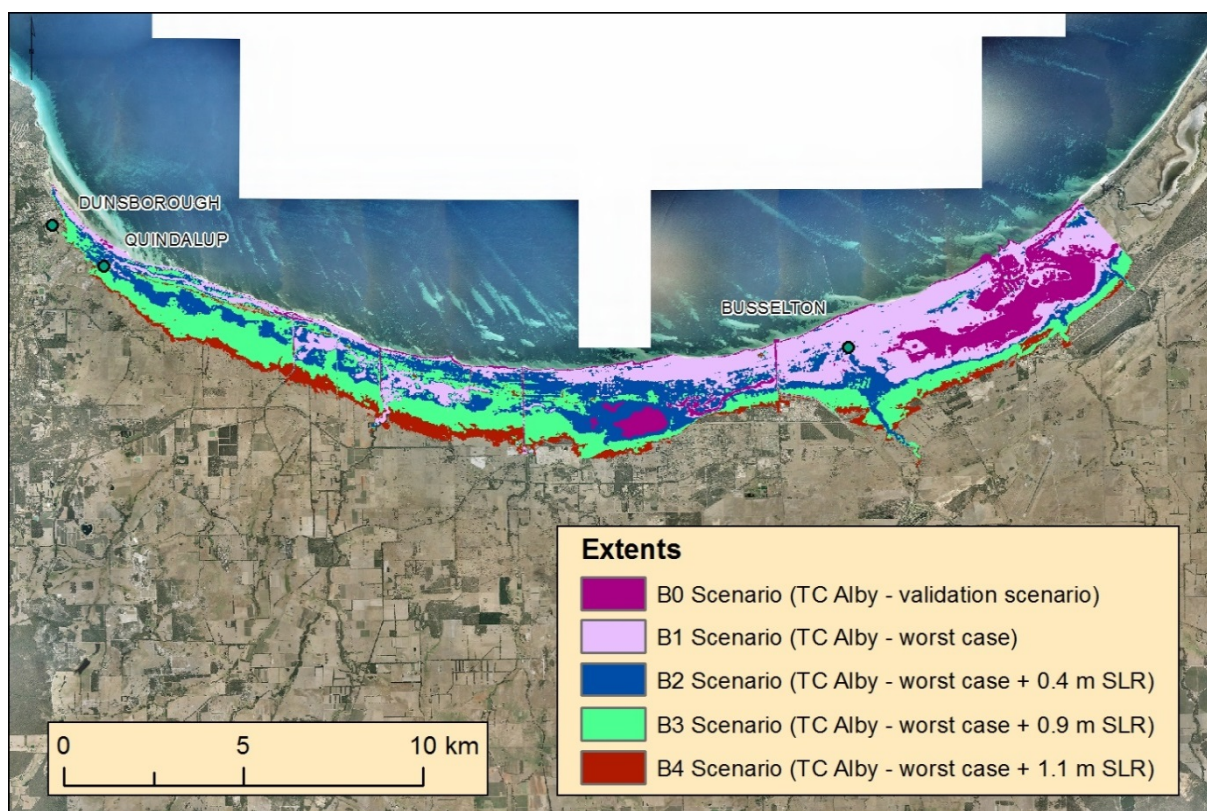


Figure 71. Comparison of the inundation extents for all SLR scenarios with the TC Alby validation (B0) and worst case (B1) scenarios.

4.1.2. Riverine flooding scenarios

The detailed riverine flooding analysis has been discussed in the previous section alongside the results. Following is a summary of the important conclusions found in the analysis of the riverine flooding scenarios.

The addition of riverine flooding, either 25 or 100 year ARI, to the SLR scenarios makes little appreciable difference to the resulting inundation extents as compared with the equivalent base SLR scenario. This seems to be the result of the relatively small volume of flood water, compared to storm tide, and the holding capacity of the Vasse Estuary (with an initial height of 0.4 m AHD).

The 100 year ARI flood plus 1.1 m SLR scenario (B10) suggests that under these circumstances the Vasse Estuary has reached its capacity. The riverine flooding is beginning to increase the depth of the inundation considerably in areas behind the estuary (Figure 63) although the extra inundation depth is not seen to increase inundation extent (Figure 62). These results imply a possible sensitivity of serious riverine flood inundation to the initial water depth in the Vasse Estuary. In summary, as the track change in TC Alby resulted in the most significant change in inundation for the SLR only scenarios, this study suggests the initial water depth of the estuaries may result in the greatest change in inundation depth for coincident flooding and storm-tide scenarios.

4.1.3. Coastal erosion modelling

4.1.3.1. Coastal erosion estimates for Busselton

Table 4 shows the differences in the erosion setback lines calculated by Andrews (2003) and Damara (2007), and coastal erosion forecast by the STM (Cowell and Barry, 2012). Despite using an updated methodology and utilising cross-shore erosion modelling, there is very little difference between the values for erosion setback line calculated by Damara (2007) and those derived from the Coastal Planning Policy by Andrews (2003). As shown by Table 4, there is a significant difference between these values and the coastal erosion forecast by the STM in 2012.

Table 4. Comparison of the setback allowances and coastal erosion distance (in metres) for Busselton.

| SPP 2.6 Allowance | Description | Andrews (2003) | Damara (2007) | Cowell and Barry (2012) 50% probability | Cowell and Barry (2012) 10% probability |
|--|---------------------------------------|----------------|---------------|---|---|
| S1 | Acute erosion - severe storm sequence | 25 m | 9 m | - | - |
| S2 | Historical Trend | 20 m | 11 m | - | - |
| S3 | SLR ¹⁷ | 38 m | 59 m | - | - |
| Setback minimum from HSD / Coastal Recession distance | | 83 m | 79 m | 263 m | 537 m |

The Cowell and Barry (2012) study found that the coastal erosion risk varied along the coast between Busselton and Rockingham due to differences in the sediment transfer rates between sources and sinks. Moreover, they found that their modelling validation results for 1950 - 2000 were consistent with previous investigation by the WA State Government. Estimates of the underlying recession trend for Geographe Bay from 1950 to 2000 range between 20 m (50% probability) of accretion to 11 m (10% probability) of recession. However, from 2030 towards 2100 coastal erosion throughout the entire sediment cell was forecast to be in the order of hundreds of metres (Table 4; Cowell and Barry, 2012), compared to the 80 m calculated by both Andrews (2003) and Damara (2007).

Investigating the difference between these coastal erosion hazard estimates was outside the scope of this study, but these differences present a challenge when attempting to incorporate the coastal erosion estimates into the assessment of inundation by 2100. A recent climate-change impact modelling study was undertaken at Mandurah, WA (Hazelwood and Moore, 2012) which considered these challenges.

One of the objectives of the Mandurah study (Hazelwood and Moore, 2012) was to assess the feasibility of integrating coastal erosion (STM) and hydrodynamic storm-tide modelling in order to assess the vulnerability within the Mandurah LGA to a change in environmental conditions under a range of future climate scenarios. This was to be accomplished by using the outputs of the STM to modify the bathymetry and topography of the area, to be used as an input surface for the storm-tide

¹⁷ Rates of SLR varying for each of the studies reported – Andrews (2003) is based on 0.38 m for the 100 year planning period; Damara (2007) used 0.9 m (medium) and 1.1 m (high) by 2100 and Cowell and Barry (2012) used 1.1 m by 2100.

modelling. However, the resulting future elevation surfaces were not physically credible. Based on the outcomes of the Mandurah study, no further attempt was undertaken to incorporate the STM results into the storm-tide or coincident flood modelling for Busselton.

The WA DoT, WA DoP and the Australian Government commissioned an independent review (Damara, unpublished) of the Busselton to Rockingham STM study (Cowell and Barry, 2012). The results of this are expected to be publicly available shortly, however the review concluded that:

‘The probabilities of future recession distances provided by the STM are not actual probabilities because they are dictated by the range and weightings of the variables within the Monte Carlo simulations. The ranges and weightings of these variables are limited by the amount of scientific knowledge about the underlying coastal processes. Where knowledge is limited, the ranges tend to be wider to accommodate all possible, although sometimes highly unlikely, values. Moreover, there are some fundamental aspects to the modelling that lead to a conservative bias in the outputs. Specifically, the extent and rate of offshore sediment transport across a wide offshore environment of up to 50 metres depth. On this basis the STM outputs should not be interpreted literally as probabilities, and the results should be seen as a demonstration of the uncertainty in modelling the rate of future erosion, rather than actual projections. Any application of the STM outputs requires full knowledge of these underlying issues and limitations.’

4.2. Modelling issues and limitations

Due to the nature of the modelling process, in particular the new research aspects of this study, a number of qualifications must be placed on all the results produced. The following points apply to all modelled scenarios and any interpretation of the results should always be informed by them.

4.2.1. Surface roughness coefficient

Surface roughness affects the flow of water across land and is an important parameter that is often fine-tuned in the validation of flood modelling. It is important, especially where overland riverine flooding is included, to have a realistic value representing the area.

A single surface roughness coefficient, Mannings “n”, of 0.03, was used over the modelling domain in each scenario. This is in line with the range of values (0.03-0.06) used in the JDA review (Davie *et al.*, 1998). ANUGA currently has the ability to implement spatially varying friction values and this is an area of the modelling that can be explored further in future work.

4.2.2. Treatment of estuary storm-tide gates

Infrastructure is in place to divert water flows around the area which is driven by human decision-making processes or reliance on guidelines. Hydrologically important questions for the area include:

- Under what circumstances do the floodgates operate?
- How much, if any, and under what circumstances is, water diverted down the Vasse River?
- When is the Sabina River diverted to the Vasse Diversion Drain?
- When is the Broadwater used to store incoming surge? Etc.

Attempts to seek, or assume answers to such questions and then implementing them in the modelling methodology, although possible, was beyond the scope of this present work. This could form the basis of future, more detailed flood work using ANUGA.

This study assumed the following:

- The floodgates at the Vasse and Wonnerup estuaries are always open.
- The Vasse River is not used to route water from the Vasse Diversion Drain to the Vasse Estuary.¹⁸
- The Sabina River diversion to the Vasse Diversion Drain is not used.
- The floodgates joining the Vasse Diversion Drain and the Broadwater are not used.
- The detention basins in the lower part of the Vasse River are not used.

4.2.3. Wave setup and wind shear

ANUGA does not incorporate wave setup. Wave setup is a super-elevation of the mean water surface over normal 'still' water level due to wave action alone. GCOM2D incorporates this feature and thus the wave dynamics have been propagated close to the coast. Continued development of ANUGA will require wave setup to be incorporated. Neglecting wave setup within the ANUGA domain will likely cause a slight under-prediction of inundation.

ANUGA does not model the storm itself and the resultant wind shear effect on inundation. Currently, ANUGA must be integrated with an open ocean storm-tide model as shown in [Figure 4](#). It is expected that there will be little impact to the estimated inundation as modelled here by not incorporating wind in ANUGA. Wind shear stress is usually very small but its integrated effect over a large body of water can be large (Dean and Dalrymple 1991).

Neglecting the effects of wave setup and wind shear will typically tend to underestimate the inundation extent. By 'forcing' ANUGA at approximately the 10 m depth contour with the GCOM2D outputs the integrated effect of ANUGA not modelling wave setup and wind shear is likely to be small.

4.2.4. Recorded hydrographs

This study used hydrographs from two sources: observations (Vasse Diversion Drain) and model outputs (Abba and Sabina Rivers). While the Vasse Diversion Drain 25 year ARI hydrograph was the August 1997 flood event, that was deemed to be a 25 year ARI event (see Riverine hydrographs section, [p16](#)), the 100 year ARI hydrograph was approximated from the recommended 100 year ARI interim design peak flow and the shape of the 25 year ARI hydrograph. The interim nature of the design peak flow plus estimation of its shape creates uncertainty in these results. For consistency with the other 100 year ARI hydrographs used in this study (Abba and Sabina Rivers) a 100 year ARI hydrograph derived from observations and hydrological modelling is required for the Vasse Diversion Drain.

¹⁸ The modelling shows some water flowing down the Vasse River but this is due to the overtopping of the Vasse Diversion Drain as opposed to the diversion of water at the junction point of the Vasse Diversion Drain and the Vasse River.

4.3. Further work

Possible further work is categorised into improving and expanding on the current modelling. Further work could take on aspects of either or both of these categories.

4.3.1. Improvements to this study

4.3.1.1. Validation

To comprehensively validate ANUGA a more recent storm, to more closely match the current elevation data, with recorded depth observations could be modelled and the results compared with the observations.

4.3.1.2. Flood modelling

This study considered the combined hazards of coincident storm tide and flood events with the result that the storm tide was overwhelmingly the cause of the inundation extent. Flood events were not solely considered. It is possible to re-run the scenarios solely with the flood events to determine the flow of water and compare with the results from this study. This may help to identify where flood inundation is changing when combined with a storm-tide event, e.g. the riverine flood waters may break out of the Vasse Diversion Drain closer to the hydrograph location due to the interactions of combined riverine flood and storm tide.

Also, adjusting the start time of the riverine hydrographs in order to analyse the relationship between the timing of the catchment flood hydrographs with peak storm-tide was not considered. This could be the basis for further work

4.3.1.3. Include flood management measures

This study assumed the estuary management procedures. It is possible to include the estuary management procedures, e.g. flood gate actuation, and re-run the scenarios and compare the results to those of this study.

4.3.1.4. Undertake sensitivity testing

Sensitivity testing could be carried out to identify the inundation extent and depth sensitivity resulting from varying the initial estuary depth and the points at which the ANUGA model is 'forced' by the GCOM2D model. Sensitivity on the orientation of offshore sand bars and the effect this has on the inundation extent is also a possible series sensitivity tests.

Within this study the water holding capacity of the estuaries was identified as a major factor in reducing the inundation extent. However, only one initial level of 0.4 m AHD was considered. Sensitivity testing could be carried out on the initial estuary water levels to determine the variation in resulting inundation. Sensitivity testing could be extended to include a range of other variables of interest, e.g. varying the shape of the simulated riverine hydrographs.

A single series of points, approximating the 10 m depth contour was used where the outputs of the GCOM2D model 'forced' the ANUGA model. These points could be varied, either closer or further from the coastline, to identify the optimum location where the greatest inundation results. i.e. the wave setup and wind shear forces are least diminished.

4.3.2. Expansion of this study

As the combined modified track change and tide identified the greatest change to inundation, a range of storm tracks could be modelled to further investigate the inundation sensitivity.

The current hydrodynamically modelled inundation could be compared to a simple 'bath tub' (Eastman, 1993) method where storm-tide peak heights are identified on the DEM and all lower areas considered inundated. In some cases the local currents, direction of the storm and the bathymetry/topography may be well suited to this form of analysis. As a simple and relatively quick method, identifying where this method works well allows confidence in carrying out this method in the event of current climate hazards, such as emergency response planning, and future climate change scenarios. The caveat still applies with the consideration of the geomorphological changes being difficult to model with confidence within the time frames considered for climate change planning.

The inclusion of infrastructure within the elevation surface will more accurately model the flow of water overland. A DEM that includes surface structures could be created from LiDAR data where 'all returns' are available. Where this data is not available infrastructure could be digitised, such as building footprints, and given elevation values in the DEM. The inundation extents and depths of these scenarios could then be compared to the current results to identify the change in inundation. Further to this, the inundation at the building location can be captured and reported, either for specific buildings or statistically across areas such as suburbs.

Following from the last point, a risk assessment could be completed. Geoscience Australia has broad experience in determining the impact of natural disasters, i.e. risk, by way of combining hazard, exposure and vulnerability (e.g. Cechet *et al.*, 2011, Middelman-Fernandes, 2010, Jones *et al.*, 2005). A broad example of a risk assessment is identifying the probability of building failure as a function of hazard magnitude at the location of the building. Risk can then be quantified in terms of the numbers of buildings damaged to varying degrees and an estimate of replacement cost calculated. Demographic analysis can augment these studies to identify the vulnerability of the population.

5. Conclusions

Geoscience Australia has modelled coincident storm-tide and riverine flooding using a high resolution LiDAR derived DEM. In Busselton, a high-resolution DEM was required to accurately model the flow of water through the sharp-relief drainage channels, e.g. the Vasse Diversion Drain.

The simulated inundation has been compared with TC Alby inundation observations and the tide gauge recordings of this event although, due to bathymetric and topographic changes since 1978, this validation was indicative only.

The key findings were:

- In light of such a large storm as TC Alby, coincident riverine flooding has relatively little effect on the extents of the resulting inundation as compared to the storm-tide inundation.
- The greatest change to resulting inundation observed in this study was that of the track and tide change applied to TC Alby to produce the *worst case scenario* (B1, [Figure 71](#)). This highlights the important effect a storm trajectory has in these scenarios for Busselton.
- Increases in sea-level rise increases the extent of overland inundation ([Figure 71](#)). Following the *worst case scenario* (B1), the *worst case + 0.9 m SLR scenario* (B3) was the next significant increase with larger areas west of the Buayanyup drain being inundated.
- Densely populated areas in Busselton are inundated in all scenarios, but increases in sea-level rise have the effect of increasing the water velocity and depth and therefore the events destructive potential.

The STM produces the greatest recession distances of any coastal erosion modelling completed to date. Within the context of SLR, Andrews (2003) and Damara (2007) predict 38 m and 59 m recession distance respectively for the response to SLR over the next 100 years; although they use differing SLR scenarios, 0.38 m and 0.9 m respectively. Cowell and Barry (2012) identify coastal erosion to be within the range of 263 m and 537 m respectively for a 50% and 10% probability of exceedance under a 1.1 m SLR scenario. Although the STM coastal erosion modified DEMs were considered for inclusion within the ANUGA SLR scenarios, the modified DEMs did not reflect a realistic future surface and therefore these were not included in the ANUGA modelling.

Further work is needed to increase the level of accuracy at which these scenarios represent a real event. Inclusion of hydraulic defences not currently represented in this modelling surface (e.g. detention basins, floodgate operating procedures, river diversions further upstream) are required before any modelling results are used beyond a qualitative assessment. It is worthwhile noting that such modelling is likely to focus on a significantly smaller modelling domain due the computationally intense nature of these models.

This page is intentionally blank

6. References

- Baldock, T., Barnes, M., Guard, P., Hie, T., Hanslow, D., Ranasinghe, R., Gray, D., Nielsen, O., 2007 - Modelling Tsunami Inundation on Coastlines with Characteristic Form. *16th Australasian Fluid Mechanics Conference*. 939-942.
- Bicknell, C., 2010. Sea Level Change in Western Australia, Application to Coastal Planning. *Western Australian Department of Transport*. Web Available: http://www.planning.wa.gov.au/dop_pub_pdf/sea_level_change_in_wa_rev0_final.pdf
- BOM. 2012 TC Alby summary report. Web Available: <http://www.bom.gov.au/cyclone/history/alby.shtml>
- Brunn, P., 1962. Sea-level rise as a cause of shore erosion. *Journal Waterways and Harbours Division*, 88 (1-3), 117-130.
- Bello-Pineda, J. and Hernandez-Stefanoni, J. L., 2007. Comparing the performance of two spatial interpolation methods for creating a digital bathymetric model of the Yucatan submerged platform. *Pan-American Journal of Aquatic Sciences* 2(3), 247-254
- Cechet, R., Sanabria, A., Yang, T., Arthur, W. C., Wang, C. H., and Wang, X., 2011. An Assessment of severe wind hazard and risk for Queensland's Sunshine Coast Region. *19th International Congress on Modelling and Simulation*, Perth, Australia, 12-16 December 2011. Web Available: <http://www.mssanz.org.au/modsim2011/F7/cechet.pdf>
- Cowell, P.J. and Barry, S., 2012. Coastal Recession Risk Due to Climate Change in South-Western Australia. University of Sydney.
- Damara, 2011. Shire of Busselton Coastal Erosion Study – Assessment of Climate Change Impacts, Draft report 96-00-01-B.
- Damara. Unpublished. 2012. Technical Review of “Coastal recession risk in the Busselton-Rockingham coastal cell due to climate change” (Cowell & Barry 2012).
- Davies, J., Ng, R., Robinson, J., Yan, M., 1998. Busselton Regional flood Study Review. JDA Consultant Hydrologists. Report No J375an.doc
- Dean, R.G. and Dalrymple, R.A. 1991. Water wave mechanics for engineers and scientists. World Scientific Publishing Co. Pty. Ltd. Singapore.
- Department of Climate Change. 2009. Climate Change Risks to Australia's Coast. Available online: <http://www.climatechange.gov.au/publications/coastline/climate-change-risks-to-australias-coasts.aspx>
- Eastman, J. R., Kyem, P. A. K., Toledano, J., and Jin, W., 1993. GIS and decision making. *Explorations in Geographic Information Systems Technology*, Vol. 4. Geneva: United Nations Institute for Training and Research (UNITAR).
- Fountain, L., Sexton, J., Habili, N., Hazelwood, M., and Anderson, H., 2010. Storm tide modelling for Bunbury, Western Australia, *Professional Opinion*. No.2010/04
- Geoscience Australia., 1 second SRTM Derived Hydrological Digital Elevation Model (DEM-H) version 1.0, ANZLIC ID: ANZCW0703014615 Metadata: <http://www.ga.gov.au/meta/ANZCW0703014615.html>
- Hazelwood, M., Moore, D., 2012. Regional climate change Impact Modelling for Mandurah, Western Australia. *Geoscience Australia Record*. 2012/062
- Holland, G. J., 1980. An analytic model of the wind and pressure profiles in hurricanes. *Monthly Weather Review*, 108, 1212-1218.
- Holland, G., 2008. A Revised Hurricane Pressure–Wind Model. *Monthly Weather Review*, 136, 3432–3445.
- Hubbert, G., Blake, S., Oliver, S., 2012. Busselton Storm tide Study – Climate Change Scenarios Based On Tropical Cyclone Alby.
- Jakeman, J. D., 2006. On Numerical Solutions of the Shallow Water Wave Equations, Thesis.

- Jakeman, J. D., Nielsen, O.M., Van Putten, K., Mleczeko, R., Burbidge, D. & Horspool, N., 2010. Towards spatially distributed quantitative assessment of tsunami inundation models, *Ocean Dynamics*, 60, 1115-1138. DOI 10.1007/s10236-010-0312-4.
- Jones, T., Middelmann, M., and Corby, N., 2005. Natural Hazard Risk in Perth, Western Australia. *Geoscience Australia*: Canberra.
- Middelmann-Fernandes, M. H., 2010. Flood damage estimation beyond stage–damage functions: an Australian example. *Journal of Flood Risk Management*, 3, 88–96. doi: 10.1111/j.1753-318X.2009.01058.x. Available online: <http://onlinelibrary.wiley.com/doi/10.1111/j.1753-318X.2009.01058.x/full>
- Rodgers, S., 2012. Pers Comms. Busselton Storm Surge/Flood Modelling Project – Data Request. TRIM D2013-64288.
- Rodriguez, E., Morris, C. S., and Belz, J. E. (2006) A global assessment of the SRTM performance. *Photogrammetric Engineering and Remote Sensing* 72 (3), 249-260.
- Van Drie, R., Milevski, P. and Simon, M., 2010. Assessment of Sea-level rise and Climate Change Impacts using ANUGA. *19th NSW Coastal Conference*, 10-12 November 2010, Batemans Bay. Web Available: <http://www.coastalconference.com/2010/papers2010/Rudy%20Van%20Drie%20full%20paper.pdf>
- Vasse River Diversion Drain Flood Hydrology (Unpublished Report). Surface Water Hydrology Series. Obtained by personal correspondence with Department of Water in July 2012.
- Western Australian Planning Commission, 2006. State Coastal Planning Policy. Statement of Planning Policy No. 26. Web Available: http://www.planning.wa.gov.au/dop_pub_pdf/SPP_2_6.pdf